博士論文

Pathological studies on canine histiocytic tumors

（犬の組織球性腫瘍に関する病理学的研究）

Thongtharb Atigan

トンターブ　アティガン

Contents

Contents

GENERAL INTRODUCTION

Histiocytes, a subtype of white blood cells, originate from CD34^{+} precursor stem cells in the bone marrow through the control of granulocyte-macrophage stimulating factor (GM-CSF), macrophage stimulating factor (M-CSF), interleukin (IL)-4 and tumor necrosis factor-α (TNF-α) [17, 32, 57]. Histiocytes are commonly found in the ubiquitous tissues, including the lymph nodes, spleen, liver (as Kupffer cell) and lung (as alveolar macrophages). These immune cells play important roles in the antigen presentation and phagocytosis in the reticuloendothelial system (also known as the mononuclear phagocytic system), which is closely associated with both the innate and adaptive immune responses of the eukaryote. Generally, histiocytes can be divided into 2 main cell types; myeloid dendritic cells (DC) and macrophages based on cytokines released, cell-surface markers and their primary functions [29].

DCs belong to antigen presenting cells (APCs) that play a critical role in the adaptive immune system. Two main functions of DCs are antigen presentation to CD4^{+} T-cells in the initial stage of immune response and naïve T-cell stimulation. Furthermore, the cells also maintain the survival of B-cells resulting in prolonged immune memory. On the basis of immunophenotypic and ultrastructural characterization along with cellular location, in human, DCs can be classified into follicular DC (FDC), Langerhans cells, interstitial DCs (iDC), veiled cells (also known as indeterminate cell) and interdigitating DCs [4, 70]. In dog, these cells are subdivided into epidermal DC (also known as Langerhans cell), iDC and interdigitating DC in T-cell domain of lymphoid organs [32, 57, 60].

For macrophage differentiation, circulating monocytes migrate into tissues and subsequently develop into tissue or resident macrophages, which are important for the innate immune system. Macrophages predominantly have phagocytic capability to

destroy or against invading pathogens as well as foreign bodies to the host. In addition, they also maintain the tissue homeostasis [37]. Currently, macrophages can be classified into classical activated M1 macrophages and alternatively activated M2 macrophages based on producing cytokines and their functions [26, 99]. Furthermore, M2 macrophages are subclassified into M2a, M2b and M2c macrophages based on stimulating cytokines [37, 91]. Functionally, M1 macrophages mainly phagocytize and destroy many pathogens, and have an important role against tumor growth. These cells secrete various types of bioactive factors consisting of reactive oxygen species (ROS), inducible nitric oxide synthase (iNOS; also known as nitric oxide synthase 2 (NOS2)) and pro-inflammatory cytokines such as IL-6, IL-12 and tumor necrotic factor (TNF) that lead tumor cells to destruction. Conversely, M2 macrophages normally release a variety of growth factors such as epidermal growth factor (EGF), fibroblast growth factor (FGF), ascular endothelial growth factor (VEGF), transforming growth factor beta 1 (TGFβ1) and matrix metallopeptidase (MMP) leading to wound healing and tissue remodeling in normal tissues. These factors, moreover, promote tumor cell survival, tumor proliferation, tumor invasion and metastasis [82, 99].

Histiocytic disorders or histiocytic proliferative disorders (HPDs) are included in a group of histiocytic diseases characterized by a variety of clinical presentations and pathological characterizations. Other than human, the HPDs are also documented in various animal species, for instance, dogs, cats, horse, cattle, pig and exotic pets [10, 15, 40, 43, 54, 64, 75]. Nowadays, although there are a lot of reports regarding HPDs, their etiology as well as pathogenesis are still unclear [1, 4, 40, 87]. In canine literatures, HPDs were first described in a Bernese mountain dog in 1970s [4, 32]. Recently, canine HPDs are categorized into 1) non-neoplastic histiocytic (reactive histiocytosis (RH)) and 2)

neoplastic histiocytic diseases (cutaneous histiocytoma and histiocytic sarcoma) based on the clinical behaviors and pathological characterizations [18, 32, 57].

RH, a proliferative form of HPDs, is well documented that originates from mature/dermal DCs (also known as interstitial DCs). RH was first described in 9 dogs in 1986 [55, 65]. Generally, RH can be subclassified into cutaneous and systemic RH based on the number of organs involved, and on the patterns and distribution of lesions [3]. In cutaneous RH, grossly, the lesions are normally confined to the dermis of the head, neck, extremities, scrotum and trunk [65]. Conversely, the lesions of systemic RH are usually observed in the lymph nodes, eyes, liver, spleen, bone marrow and lung [58, 65, 72]. Immunophenotypically, these tumors commonly exhibit CD1a, CD4, CD11c and CD90 (Thy-1) and the immunohistochemical expression pattern of the tumor cells is consistent with the characteristics of dermal DC [3, 20, 57].

In normal tissues, epidermal or immature DCs, namely Langerhans cells generally reside in the basal and the suprabasal layer of the epidermis, and stratified squamous epithelium of the urogenital system [22]. Like in other types of DCs, Langerhans cells play an important role in presenting antigen to T lymphocytes in the adaptive immune system. They will migrate to adjacent draining lymph nodes through lymphatic vessels and subsequently differentiate into mature DCs within these lymphoid tissues [21, 74, 90]. "Histiocytoma" and "canine cutaneous histiocytoma (CCH)" are benign forms of HPDs that arise from Langerhans cells. Normally, CCH is predominantly found in young animals, particularly less than 2 years of age [24]. The typical gross lesion is a solitary mass with or without ulceration and alopecia at the epidermis, particularly in the ear pinna and extremities. Furthermore, multiple skin masses of CCH are also demonstrated with the term of "*Langerhans cell histiocytosis*" [57, 62]. As mentioned before, gross lesions

as well as the cellular morphological features of both RH and CCH are similar. However, the distribution patterns of proliferative/neoplastic histiocytes among the layers of the skin; top-heavy and bottom-heavy lesions, can be used as a basic histological criterion to define CCH and RH, respectively [57, 65]. Although said so, immunohistochemistry (IHC) is highly recommended in order to discriminate tumor cell origins. Far from immunophenotype of RH, the tumor cells of CCH usually express CD1a, CD1b, CD1c, major histocompatibility complex class II (MHCII), CD11c, CD18, intracellular adhesion molecule 1 (ICAM-1 or CD54) and E-cadherin [19, 32, 57, 61, 66]. Puff *et al* [71], moreover, mentioned that CCH expressed matrix metalloproteinases (MMPs).

Histiocytic sarcoma (HS), a malignant form of HPDs, is a fatal and aggressive hematopoietic neoplasm with a worsen prognosis in both human and animals. The lesions commonly found in the skin and visceral organs, particularly lymphoid organs. In dogs, most of the HS cases originate from DCs. However, cases that arise from the macrophage lineage have been illustrated in the term of *"hemophagocytic histiocytic sarcoma"*. Histologically, neoplastic histiocytes are notably pleomorphic and atypical with various number of mitotic figures. Distant metastases are very common. Immunohistochemical studies demonstrated that these HS cells exhibit CD1, CD11c, CD18, ICAM-1 and MHCII [19, 57], which are consistent with the IHC results of DCs. Conversely, hemophagocytic HS cells express CD11d instead of CD11c, supporting that these cells originate from the macrophage lineage [57, 60].

In the Chapter 1, a comparative pathological study on HSs deriving from the neural and extraneural tissues are conducted. In this chapter, proliferative parameters (mitotic index, Ki67 and PCNA proliferative indices) between the 2 primary origins are also described. In accordance with the cell origins, most of canine HS cases of extraneural

origin arise from the DC lineage, whilst hemophagocytic HS belongs to the macrophage lineage. In Chapter 2, therefore, clinicopathological, histological and immunohistochemical features of primary intracranial HSs are described. In addition, inducible nitric oxide synthase (iNOS), an M1 macrophage marker, was employed. In Chapter 3, the two HS cell lines, PWC-HS01 and FCR-HS02 isolated from brain and synovial tumors, respectively, are established newly and examined morphologically and immunocytochemically. In this chapter, the expression of DC and macrophage markers together with molecular characterization are also examined in order to identify cellular phenotype of these 2 established cell lines. Tumorigenicity and metastasis activities of the cell lines are also described. Finally, in the reference article, histological and IHC comparative studies on histiocytic tumor in domestic ferrets are conducted. Because domestic ferrets (*Mustela putorius furo*) become a popular companion animal and accordingly, tumors in ferrets have been increasing.

CHAPTER 1

A comparison of pathological characteristics of

canine histiocytic sarcoma between primary neural

and extraneural origins

INTRODUCTION

In veterinary literatures, histiocytic sarcoma (HS), a histiocytic malignancy, has been well documented in dogs and cats [1, 27, 31, 43, 58, 63, 75, 96]. However, other animal species including cattle, horses and exotic pets were reported sporadically [7, 10, 15, 48, 64]. Lymphoid organs (i.e. spleen and lymph nodes), liver, lung and skin are recognized as the primary lesion of HS in the animals mentioned above.

In the dog, HS occurs most frequently in middle-aged to older purebred dogs, predominantly in the Bernese mountain dog, Retriever and Rottweiler [1, 18, 32, 57, 77]. Moreover, the Pembroke Welsh corgi, Shetland sheep dog and other purebreds are also described sporadically [4, 41, 43, 88, 89, 101]. On the other hand, the occurrence of HS in young animals is also illustrated in the Perro de Presa Canario dog [25] and Great Dane [53]. The clinical presentations vary depending upon the tumor distribution. Recently, several studies have well documented that canine HS mainly originates form myeloid dendritic cells (DC), whereas another type, macrophage origin, is very rare [60, 81]. In accordance with the latter type, unlike dendritic cell origin, all the lesions are specifically confined to the splenic red pulp and bone marrow resulting in splenomegaly or hepatosplenomegaly without grossly visible masses. These neoplastic histiocytes show marked hemophagocytosis and express major histocompatibility complex class II (MHCII), CD18 and CD11d, which are macrophage phenotypes [60, 81]. HSs, moreover, is classified into localized and disseminated forms in accordance with the distribution pattern, including the numbers of primary organ involvement and the evidence of distant metastasis. The localized form is recognized as a solitary mass that mainly manifests in the skin and subcutis of the extremities with local invasion of sentinel lymph node. In the disseminated form, on the contrary, multiple masses occur preferentially in the spleen,

8

lung and bone marrow with a rapid and widespread metastasis [4]. Despite canine HSs are clearly categorized into 2 different forms, the histological and immunohistochemical (IHC) features between localized and disseminated HS are identical [32, 43].

As mentioned before, the primary lesions of HS are commonly found in the visceral organs and skin, whereas the occurrence in the central nervous system (CNS) is considered to be unusual [87]. The pathological features of HS in the CNS and extraneural organs, moreover, have not been described. Therefore, the aim of this chapter is to elucidate the histological and IHC features of 54 canine HS cases between neural and extraneural organs.

MATERIALS AND METHODS

Animals

Tumor samples from 54 dogs (45 biopsies and 9 necropsies) between 2009 and 2015 were submitted to Department of Veterinary Pathology, Graduate School of Agricultural and Life Sciences, the University of Tokyo for pathological examination. All the tumors were histologically diagnosed as HS. The signalment, clinical presentations, and tumor location and distribution were summarized in **Table 1.1**. In accordance with tumor location, the 54 dogs were divided into 2 groups; 1) HS with the central nervous system involvement (HS-CNS) and 2) HS without the central nervous system involvement (HS-NCNS).

Histological examination

The tissue samples were fixed in 10% neutral buffered formalin solution and then routinely embedded in paraffin. All tissue sections (2 – 4 µm-thick) were stained with hematoxylin and eosin (HE) and then observed under a light microscope. In order to determine the mitotic index (MI), 10 areas with a highest density of mitotic figures were randomly selected and the total number of mitoses was counted per 10 high power fields (hpf; 400X).

Immunohistochemical examination

All the sections, after antigen retrieval, were immersed in 10% hydrogen peroxide (H_2O_2) in methanol at room temperature for 5 min and subsequently incubated in 8% skim milk at 37^oC for 30 min in order to block non-specific reactions. All the tissues were reacted with each primary antibody at 4^oC overnight. The primary antibodies used and antigen retrieval methods are detailed in **Table 1.2**. The horseradish peroxidase (HRP)-labeled polymer reagent (Envision$^+$ system-HRP labeled polymer reagent, Dako, Tokyo, Japan) was applied at 37^oC for 40 min. For the detection of CD208, the sections were reacted with a biotinylated secondary antibody (1:400, anti-rat IgG (H+L) antibody, KPL, MD) at 37^oC for 1 hr, and then incubated with streptavidin/HRP reagent (1:300, Dako, Glostrup, Denmark) at room temperature for 40 min. All the sections were rinsed with Tris-buffered saline (TBS) prior to treating with a 3-3'-diaminobenzidine solution containing 0.03% H_2O_2, and counterstained with Mayer's hematoxylin (Muto Pure Chemicals, Tokyo, Japan). Normal canine tissues, moreover, were used as positive controls, whereas negative controls were performed through applying TBS instead of the

primary antibodies. For immunohistochemical scoring, positive tumor cells were counted in five randomly selected areas (hpf; 400X). Semiquantitative scores were divided into 4 categories as follows: - (negative) = no positive tumor cells, + (weakly positive) = 1 − 25% positive tumor cells, ++ (moderately positive) = 26 − 50% positive tumor cells and +++ (strongly positive) = >50% positive tumor cells. In addition, the Ki67 and PCNA expression was also determined by counting the number of positive nuclei in 10 randomly selected areas (hpf; 400X). The average percentage of positive cells was defined as Ki67- and PCNA-proliferative indices.

Statistical analyses

Chi-square or Fisher's exact test was used to assess the association between tumor distribution and primary tumor origins, as appropriate. Mann-Whitney *U* test was performed to determine the significance of the difference of the mean MI, Ki67 and PCNA indices of proliferative activity and the difference of the expression of immunohistochemical markers between HS-CNS and HS-NCNS groups. The Ki67 and PCNA indices were demonstrated as mean ± standard error (SE). Two-sided significant level was used that $p<0.05$ was considered statistically significant.

RESULTS

Clinicopathological features

The 54 dogs examined included 31 males and 23 females (male: female ratio = 1.35:1) with a range of 3 years to 14 years (median age = 9 years and 4 months). The breeds were comprised of Pembroke Welsh corgis (n = 15), Flat coated retrievers (n = 11), Bernese mountain dogs (n=3), Beagle (n = 3), Mongrels (n = 3), Shetland sheepdogs (n = 3), Golden retrievers (n = 2), Labrador retrievers (n = 2), Miniature dachshunds (n = 2), Miniature schnauzers (n = 2), Basset hound (n = 1), Norfolk terrier (n = 1), Pointer (n = 1), Pomeranian (n = 1), Rottweiler (n = 1), Shiba (n = 1), Siberian husky (n = 1) and unknown breed (n = 1) **(Fig. 1.1)**. Various clinical signs were recorded depending upon the numbers of primary and/or distant organ involvement. On the basis of tumor distribution, the tumors were classified into localized (n = 41) and disseminated (n = 13) **(Table 1.1)**. As mentioned above, all the samples were divided into HS-CNS (n = 23) and HS-NCNS (n = 31), and the latter was detected in the spleen and lymphoid organs (n = 10), limbs (n = 6), lung (n = 5), oral cavity (n = 3), gastrointestinal tracts (n = 2), thoracic wall (n = 2), abdominal cavity (n = 1), and skin and subcutis (n = 1) **(Fig. 1.2)**. We found that there has been strong significant association between the tumor distribution and their origin (*p<0.001*).

Histological examination

Microscopically, all the tumor samples were poorly demarcated. Most of the cases contained numerous round to pleomorphic cells that arranged in a sheet or a solid pattern. These cells had clear eosinophilic cytoplasm with distinct borders. Their nuclei were

eccentric with a round to polygonal shape. The prominent magenta-colored nucleoli (1 – 2 nucleoli/nucleus) were observed. Moderate to marked cellular atypia including anisocytosis, anisokaryosis and anisonucleoliosis was noted. Bizarre mononuclear and multinucleated giant tumor cells interspersing within tumor lesions were commonly found (**Fig. 1.3**). Cytoplasmic vacuolation and hemophagocytosis were occasionally observed, particularly in hemophagocytic histiocytic sarcoma (cases No. 30 – 33; **Fig. 1.4**). In some cases, the shape of tumor cells was predominantly spindle to fusiform and the cells were arranged in an irregular pattern. These cells had a moderate amount of eosinophilic cytoplasm with indistinct borders. The nuclei were concentric and usually ovoid- to spindle-shaped. The nucleoli were occasionally found. Mild atypia was noted (**Fig. 1.5**). Although, various numbers of atypical mitoses were observed in all the cases, the HS-CNS group had higher MIs than those in the HS-NCNS group ($p<0.05$; **Table 1.3 and Fig. 1.6**). Moreover, moderate to large numbers of small lymphocytes often admixing with plasma cells were commonly found in the lesions of all 54 cases (**Fig. 1.7**). Tumor necrosis were occasionally observed.

Immunohistochemical examination

Moderate to strong cytoplasmic or membrane staining for HLA-DR, Iba-1 and CD204 was found in all the cases. Cytoplasmic and membrane immunoreactivities to CD163 were variably distributed in 42 cases. Twenty-two cases had moderate to strong cytoplasmic staining for lysozyme. Variable or weak cytoplasmic and/or nuclear immunoreactivity to S100 were noted in 17 cases. In addition, a patchy dot-like cytoplasmic immunoreactivity to CD208 was observed in 25 cases (**Table 1.3 and Fig.**

1.8). Tumor cells were negative for myeloid/histiocyte antigen (MAC387) in all the cases. There was a significant difference in CD204 immunoreaction between HS-CNS and HS-NCNS groups ($p<0.05$), whereas the immunoreactivities of other markers showed no significant differences between them **(Fig. 1.9)**. Ki67 and PCNA proliferative indices ranged $0.5 - 67.9\%$ (average $31.1\pm2.4\%$) and $19.1 - 95.1\%$ (average $62.6\pm1.9\%$), respectively **(Table 1.3 and Fig. 1.9)**.

DISCUSSION

In this chapter, histopathological and immunohistochemical features of 54 canine HS cases were examined. Based on tumor locations, all the tumors were divided in to HS with CNS involvement (HS-CNS; n = 23) and HS without CNS involvement (HS-NCNS; n = 31). The occurrence of canine HS was higher in male than in female as demonstrated previously [4, 60, 80, 88]. The Pembroke Welsh corgi and Flat coated retriever were most frequently affected in HS-CNS and HS-NCNS, respectively. These occurrence tendency was consistent with that described previously [18, 43, 51]. Other purebreds such as the Shetland sheepdog, Bernese mountain dog and Golden retriever were affected sporadically. This observation suggests that a genetic factor possibly contributes the occurrence of canine HS. All the HS cases presented various types and degrees of clinical signs **(Table 1.1)**. This suggests that symptoms in dogs with HS is relatively non-specific and seems to depend upon organs involved. Among the 54 cases, 41 were the localized HS and 13 were disseminated. Interestingly, only the localized form was observed in HS-CNS group, showing that distant metastases from primary CNS tumors may be an unusual phenomenon and that localized HS is a common form of HS with CNS involvement. Although cellular morphology of HS-CNS and HS-NCNS were not different, MI in the former was significantly higher than the latter. This suggests that HS derived from CNS may have a more aggressive biological behavior than HS of extraneural origin.

The present results revealed that mitotic index in HS derived from CNS was higher than that arose from the extraneural organs. This observation suggests that biological behaviors of HS with CNS involvement is relatively more aggressive than HS occurring in other organs.

In general, pathological diagnosis of HS is often challenging. The cellular morphology of HS cases varied from round to pleomorphic-shaped with marked atypia, which mimics histological features of other hematopoietic tumors, malignant melanoma and undifferentiated carcinoma. Therefore, immunohistochemistry is highly recommended in order to identify the tumor types. The present results showed that all the tumor cases (n=54) had an intense IHC staining for major histocompatibility complex class II (MHCII), Iba-1 and CD204. These molecules are comprehensive markers for the diagnosis of histiocytic diseases in both human and animals. These results strongly suggest that all the present cases had a histiocytic differentiation.

Tumor cells of the majority of the present HS cases were positive also for CD163 (hemoglobin scavenger receptor) that is specific for the monocyte/macrophage lineage [13, 46]. This marker is usually used for detecting tumor associated macrophages (TAMs) within tumor lesions [26, 99]. Therefore, the present neoplastic histiocytes derived from both neural and extraneural organs might be part of macrophage phenotype. Lysozyme (also known as muramidase) is also widely used as one of markers for histiocytes [59]. Herein, although all the cases were confirmed as HS, tumor cells in only 22 cases exhibited lysozyme, supporting that these cases appeared histiocytic phenotype. Conversely, negative immunostaining for lysozyme was observed in 32 cases despite positive immunoreactivity to HLA-DR, Iba-1 and CD204. These observations suggest that HS cells can dedifferentiate to the stem-like stage or differentiate to another cell lineage, which may lead to the lack of lysozyme/muramidase expression [59].

Recently, S100 protein is widely used for the diagnosis of human histiocytic diseases [5, 28, 36, 42, 70, 94, 98] as well as for the detection of human dendritic cells [47, 67]. On the other hand, CD208 (also known as dendritic cell-lysosomal associated

membrane protein; DC-LAMP), a new DC marker in human, is closely associated with DC differentiation and maturation [23]. However, pneumocytes of human, mouse, sheep and cattle also exhibit this molecule [76, 79]. Among the 54 present HS cases, 17 were positive for S100 and 25 for CD208, suggesting the DC origin of these tumor cells. MAC387 is commonly used as a monocyte/macrophage marker in both medical and veterinary researches [16, 49, 83, 92]. In the current study, all the tumor cells were negative for this molecule. In addition, canine cutaneous histiocytoma and reactive histiocytosis did not react for MAC387 (data not shown).

There were no significant differences in the expression of the markers between HS-CNS and HS-NCNS, reflecting that the immunophenotype of HS cells arising from both neural and extraneural organs are identical. However, neoplastic histiocytes from CNS tend to exhibit monocyte/macrophage markers than those from extraneural organs. Conversely, HS with DC differentiation was frequently found in extraneural organs, which is consistent with those described previously [18, 32].

In this chapter, although histological and IHC features between the 2 HS categories, HS-CNS and HS-NCNS are identical, the former is relatively more aggressive than the latter based on data of mitotic index.

Table 1.1 Fifty four cases of canine histiocytic sarcoma

Group [a]	No.	Breeds	Age [b]	Sex [c]	Clinical presentations [d]	Tumor location	Tumor distribution	Sample collection
HS-CNS	1	Pembroke Welsh corgi	11Y	FX	Gait abnormalities, depression, worsening respiratory status MRI: Central nervous system tumor	Central nervous system	Localized	Tissue biopsy
	2	Pembroke Welsh corgi	11Y5M	F	Right hemiplegia, seizure MRI: Brain tumor	Central nervous system	Localized	Tissue biopsy
	3	Labrador retriever	8Y	M	Seizure, progressive depress MRI: Brain tumor	Central nervous system	Localized	Tissue biopsy
	4	Pembroke Welsh corgi	7Y2M	M	Seizure, subconscious, circling, aimless pacing, somnolence, torticollis, left eye vision loss MRI: Brain tumor	Central nervous system	Localized	Tissue biopsy
	5	Labrador retriever	8Y6M	M	Seizure, circling, head pressing, proprioceptive deficit, head tilt, slow blink reflex	Central nervous system	Location	Tissue biopsy
	6	Pembroke Welsh corgi	11Y5M	MX	Seizure, stupor MRI: Brain tumor	Central nervous system	Localized	Tissue biopsy
	7	Mongrel	9Y	F	Circling, proprioceptive deficit, head pressing, right eye vision loss MRI: Brain tumor	Central nervous system	Localized	Tissue biopsy
	8	Beagle	14Y	MX	Seizure MRI: Brain tumor	Central nervous system	Localized	Tissue biopsy
	9	Pembroke Welsh corgi	5Y2M	FX	Gait abnormality, lateral recumbence MRI: Brain tumor	Central nervous system	Localized	Necropsy
	10	Siberian husky	11Y	FX	n/d MRI: Brain tumor	Central nervous system	Localized	Necropsy
	11	Shetland sheepdog	11Y	M	Seizure MRI: Brain tumor	Central nervous system	Localized	Tissue biopsy
	12	Shetland sheepdog	9Y	M	Behavioral change (aggressive), gait abnormality (wobble) MRI: Brain tumor	Central nervous system	Localized	Tissue biopsy
	13	Shetland sheepdog	11Y11M	FX	Circling, walking difficulty MRI: Brain tumor	Central nervous system	Localized	Tissue biopsy
	14	Mongrel	4Y	MX	Anorexia, negative blink reflex, mydriasis MRI: Brain tumor	Central nervous system	Localized	Tissue biopsy
	15	Pembroke Welsh corgi	10Y	FX	n/d MRI: Brain tumor	Central nervous system	Localized	Necropsy

Table 1.1 Fifty four cases of canine histiocytic sarcoma (continued)

Group [a]	No.	Breeds	Age [b]	Sex [c]	Clinical presentations [d]	Tumor location	Tumor distribution	Sample collection
HS-CNS	16	Pembroke Welsh corgi	9Y	MX	Seizure, paralysis, tremor, proprioceptive deficit, inactivity CT scan and MRI: Brain tumor	Central nervous system	Localized	Tissue biopsy
	17	Pembroke Welsh corgi	8Y	FX	Proprioceptive deficit MRI: Brain tumor	Central nervous system	Localized	Tissue biopsy
	18	Flat coated retriever	12Y	M	Seizure, confusion, subconscious, lateral recumbence CT scan and MRI: Brain tumor	Central nervous system	Localized	Tissue biopsy
	19	Miniature schnauzer	4Y	M	Seizure, progressive depress CT scan: Brain	Central nervous system	Localized	Tissue biopsy
	20	Pembroke Welsh corgi	8Y	M	n/d MRI: Brain tumor	Central nervous system	Localized	Tissue biopsy
	21	Beagle	10Y11M	M	Seizure, paralysis, circling MRI: Brain tumor	Central nervous system	Localized	Tissue biopsy
	22	Pembroke Welsh corgi	9Y9M	M	Seizure, drooling, tremor MRI: Brain tumor	Central nervous system	Localized	Tissue biopsy
	23	Pembroke Welsh corgi	12Y	F	Brain tumor	Central nervous system	Localized	Tissue biopsy
HS-NCNS	24	Flat coated retriever	7Y10M	M	Difficult to defecation and micturition Radiography and CT scan: Mass at sublumbar lymph node Cytology: Numerous atypical histiocytes	Spleen and other lymphoid organs	Localized	Tissue biopsy
	25	Bernese mountain dog	3Y5M	M	Inappetence Ultrasonography: Hepatic nodules, diffused splenomegaly	Spleen and other lymphoid organs	Disseminated	Tissue biopsy
	26	Flat coated retriever	8Y2M	FX	Pale mucous membrane, exercise intolerance	Spleen and other lymphoid organs	Localized	Tissue biopsy
	27	Beagle	9Y7M	MX	Inappetence, vomiting Ultrasound and CT scan: Splenic mass, multiple nodules at sacral lymph node Blood chemistry: Elevated pancreatic enzyme	Spleen and other lymphoid organs	Localized	Tissue biopsy
	28	Pointer	12Y9M	FX	Inappetence, Splenic and pulmonary masses Hematology: Thrombocytopenia with giant platelets	Spleen and other lymphoid organs	Localized	Tissue biopsy
	29	Golden retriever	11Y	FX	Mandibular and popliteal lymphadenopathy Cytology: Lymphoma was suspected	Spleen and other lymphoid organs	Disseminated	Tissue biopsy

Table 1.1 Fifty four cases of canine histiocytic sarcoma (continued)

Group [a]	No.	Breeds	Age [b]	Sex [c]	Clinical presentations [d]	Tumor location	Tumor distribution	Sample collection
HS-NCNS	30	Flat coated retriever	9Y10M	MX	Inappetence, hepatosplenomegaly Hematology: Regenerative anemia, thrombocytopenia, histiocytosis Cytology: Atypical macrophages with phagocytosis	Spleen and other lymphoid organs	Disseminated	Necropsy
	31	Norfolk terrier	6Y5M	M	Splenomegaly with splenic mass Hematology: Regenerative anemia, thrombocytopenia, hypoalbuminemia Cytology (bone marrow): Myelodysplastic syndrome was suspected	Spleen and other lymphoid organs	Disseminated	Necropsy
	32	Bernese mountain dog	4Y8M	M	Inappetence, anemia, hepatosplenomegaly Cytology: Numerous hemosiderin laden macrophage with extramedullary hematopoiesis	Spleen and other lymphoid organs	Disseminated	Necropsy
	33	Miniature dachshund	8Y4M	FX	Weakness Hematology and blood chemistry: Anemia, thrombocytopenia, hyperbilirubinemia, elevated FDP and TAT	Spleen and other lymphoid tissues	Disseminated	Necropsy
	34	Flat coated retriever	9Y2M	M	Left hindlimb lameness, soft tissue swelling around the pelvis Radiography: Periosteal bone formation and bone lysis at pubic to femoral area CT scan: Mass at pelvic cavity and femur with iliac fossa lymphadenopathy	Limb	Disseminated	Tissue biopsy
	35	Flat coated retriever	8Y6M	MX	Hindlimb stiffness CT scan: Mass at pelvis and right hindlimb, internal iliac lymphadenopathy	Limb	Localized	Tissue biopsy
	36	Mongrel	13Y4M	FX	Skin masses around lower back region Cytology: Histiocytic sarcoma was suspected	Limb	Localized	Tissue biopsy
	37	Flat coated retriever	3Y5M	FX	Swelling of the third phalanx of left hindlimb Radiography: Periosteal bone formation	Limb	Localized	Tissue biopsy

Table 1.1 Fifty four cases of canine histiocytic sarcoma (continued)

Group [a]	No.	Breeds	Age [b]	Sex [c]	Clinical presentations [d]	Tumor location	Tumor distribution	Sample collection
HS-NCNS	38	Rottweiler	9Y8M	MX	Right tarsal area swelling Radiography and CT scan: Bone lysis, splenic and subcutaneous masses at thoracic part Cytology: Anaplastic plasmacytoma was suspected	Limb	Disseminated	Necropsy
	39	Golden retriever	7M10M	MX	Right hindlimb lameness CT scan: Soft tissue tumor at right hip joint Cytology: Histiocytic sarcoma was suspected	Limb	Localized	Tissue biopsy
	40	Basset hound	9Y7M	FX	Left hindlimb non-weight bearing, swelling at the left stifle joint with the presence of excess synovial fluid accumulation Cytology: Neoplastic disease was suspected	Limb	Localized	Tissue biopsy
	41	Flat coated retriever	8Y6M	MX	Right forelimb non-weight bearing Ultrasonography and CT scan: Mass at right shoulder joint, scapula and humerus: bone lysis with periosteal bone formation, right superficial cervical and axillary lymphadenopathy	Limb	Disseminated	Tissue biopsy
	42	Pembroke Welsh corgi	8Y4M	M	Inappetence, body weight loss Radiography: Pulmonary mass was observed	Lung	Localized	Tissue biopsy
	43	Flat coated retriever	6Y2M	FX	Chronic cough CT scan: Mass at left cranial lung lobe, bronchoalveolar lymphadenopathy	Lung	Localized	Tissue biopsy
	44	Pembroke Welsh corgi	11Y	F	Bleeding from external genitalia Radiography: Mass (15x10x10 cm) at left caudal lung lobe	Lung	Localized	Tissue biopsy
	45	Unknown	12Y10M	MX	Inappetence, poor general condition, tachypnea, tachycardia, hypertension Radiography and CT scan: Mass at right middle lung lobe	Lung	Localized	Tissue biopsy
	46	Miniature schnauzer	12Y	M	Epilepsy Radiography: Mass at thoracic cavity and ascites MRI: Brain shrinkage	Lung	Disseminated	Necropsy

21

Table 1.1 Fifty four cases of canine histiocytic sarcoma (continued)

Group [a]	No.	Breeds	Age [b]	Sex [c]	Clinical presentations [d]	Tumor location	Tumor distribution	Sample collection
	47	Flat coated retriever	10Y2M	M	Facial puffiness, soft tissue swelling at buccal region CT scan: Soft tissue mass at right buccal region Cytology: Degenerative neutrophils and clumping epithelial cells	Oral cavity	Localized	Tissue biopsy
	48	Miniature dachshund	13Y6M	M	Masses at left mandibular and right inguinal areas, left mandibular lymphadenopathy (1.5 cm in diameter) Cytology: Histiocytic sarcoma was suspected	Oral cavity	Disseminated	Tissue biopsy
	49	Shiba	12Y7M	FX	Oral mass with left mandibular lymphadenopathy MRI: Bone lysis at mandible, mandibular, retropharyngeal and superficial cervical lymphadenopathy Cytology: Malignant melanoma was suspected	Oral cavity	Disseminated	Tissue biopsy
HS-NCNS	50	Pembroke Welsh corgi	9Y7M	FX	Mucous soft stool, vomiting Ultrasound: Mass at gastrointestinal tract (small intestine)	Gastrointestinal tract	Localized	Tissue biopsy
	51	Pembroke Welsh corgi	10Y10M	FX	Diarrhea Ultrasonography: Small intestinal mucosa thickness Cytology: Numerous lymphocytes and histiocytes were observed Blood chemistry: Hypoalbuminemia	Gastrointestinal tract	Localized	Tissue biopsy
	52	Bernese mountain dog	7Y6M	F	Left forelimb lameness, multiple masses at skin and lung CT scan: Mass at costochondral junction Cytology: Disseminated histiocytic sarcoma was suspected	Thoracic wall	Disseminated	Tissue biopsy
	53	Flat coated retriever	9Y2M	M	Mass at anterior part of thorax	Thoracic wall	Localized	Tissue biopsy
	54	Pomeranian	9Y	FX	Abdominal mass	Abdominal cavity	Localized	Tissue biopsy

[a] HS-CNS = Histiocytic sarcoma with central nervous system involvement; HS-NCNS = Histiocytic sarcoma without central nervous system involvement. [b] Y = Year(s); M = Month(s).
[c] M = Male; F = Female, X = Neutering. [d] CT scan = Computed tomography scan; MRI = Magnetic resonance imaging; n/d = No data; FDP = Fibrin degradation products;
   TAT = Thrombin-antithrombin complex.

Table 1.2 Primary antibodies used for immunohistochemical examination

Antibodies to [a]	Type [b]	Dilution rate [c]	Antigen retrieval for IHC [d]	Expression	Source
Ki67	Mouse, mAb (MIB-1)	RTU	Citrate buffer, pH 6.0 (HIER), 121°C, 10 min	-	Dako, Glostrup, Denmark
PCNA	Mouse, mAb (PC10)	1:250	Citrate buffer, pH 6.0 (HIER), 121°C, 10 min	-	Dako, Glostrup, Denmark
HLA-DR	Mouse, mAb (TAL.1B5)	1:50	Citrate buffer, pH 6.0 (HIER), 121°C, 10 min	Antigen presenting cell	Santa Cruz, CA, USA
Iba-1	Rabbit, pAb	1:250	Citrate buffer, pH 6.0 (HIER), 121°C, 10 min	Microglia, macrophage	Wako, Osaka, Japan
CD204	Mouse, mAb (SRA-E5)	1:100	Tris/EDTA buffer, pH 9.0 (HIER), 121°C, 10 min	Monocyte, macrophage	TransGenic, Kobe, Japan
CD163	Mouse, mAb (AM-3K)	1:100	Citrate buffer, pH 2.0 (HIER), 121°C, 10 min	Histiocyte	TransGenic, Kobe, Japan
Lysozyme	Rabbit, pAb	1:1000	Proteinase K (PIER), room temperature, 30 min	Monocyte, macrophage	Dako, Glostrup, Denmark
S100	Rabbit, pAb	1:1000	Citrate buffer, pH 6.0 (HIER), 121°C, 10 min	Dendritic cell	Dako, Tokyo, Japan
CD208 (DC-LAMP)	Rat, mAb (1010E1.01)	1:100	Citrate buffer, pH 6.0 (HIER), 121°C, 10 min	Dendritic cell	Dendritics, Lyon, France
Myeloid/Histiocyte antigen	Mouse, mAb (MAC387)	1:250	Proteinase K (PIER), room temperature, 30 min	Histiocyte, macrophage	Dako, Glostrup, Denmark

[a] HLA-DR = Human leukocyte antigen-DR; Iba-1 = Ionized calcium-binding adapter molecule-1; CD = Cluster of differentiation; DC-LAMP = Dendritic cell lysosome-associated membrane glycoprotein; PCNA = Proliferating cell nuclear antigen.
[b] pAb = Polyclonal antibody; mAb = Monoclonal antibody.
[c] RTU = Ready-to-use.
[d] HIER = Heat-induced epitope retrieval; PIER = Proteolytic-induced epitope retrieval.

Table 1.3 Mitotic index and immunohistochemical characteristics of 54 dogs with histiocytic sarcomas

Group [a]	No.	MI [b]	Proliferative markers (% positive)		IHC results [c]						
			Ki67	PCNA	HLA-DR	Iba-1	CD204	CD163	Lysozyme	S100	CD208
HS-CNS	1	4	30.1	53.9	+++	+++	+++	-	-	-	+++
	2	33	53.3	57.5	+++	+++	+++	+++	+++	+	+++
	3	39	32.9	75.7	+++	+++	+++	+++	+++	-	++
	4	56	26.0	67.2	+++	+++	+++	++	+++	+	-
	5	37	15.7	36.1	+++	+++	+++	++	-	+	-
	6	58	23.4	54.8	+++	+++	+++	+++	+++	-	-
	7	70	49.1	76.9	+++	+++	+++	+++	-	-	-
	8	4	0.5	55.5	+++	+++	+++	+++	-	+	++
	9	22	29.5	70.0	+++	+++	+++	+++	+++	-	-
	10	0	2.0	74.4	+++	+++	+++	-	+++	-	++
	11	12	2.8	68.7	+++	+++	+++	-	-	+	-
	12	24	38.4	45.6	+++	+++	+++	-	-	-	+
	13	62	6.5	56.7	+++	+++	++	++	-	-	-
	14	44	5.7	46.1	+++	+++	+++	-	-	-	-
	15	8	3.0	55.7	+++	+++	+++	++	+++	-	-
	16	26	33.00	61.8	+++	+++	+++	+++	-	-	-
	17	11	42.4	52.4	+++	+++	+++	-	-	-	-
	18	39	40.8	63.8	+++	+++	+++	++	-	-	-
	19	6	18.4	69.6	+++	+++	+++	+++	-	-	++
	20	10	18.9	74.1	+++	+++	+++	+++	-	-	-
	21	7	26.7	68.6	+++	+++	+++	++	-	-	++
	22	44	48.8	71.7	+++	+++	+++	+++	-	-	-
	23	32	64.3	95.1	+++	+++	++	+++	+++	-	+
Mean ± SE of HS-CNS			**26.6±3.8**	**63.1±2.7**							
HS-NCNS	24	1	29.4	82.4	++	+++	++	+	++	-	+++
	25	13	38.6	55.9	+++	+++	+++	+++	+++	-	++
	26	19	36.8	67.2	+++	+++	+++	++	+++	-	+++
	27	27	35.4	75.4	+++	+++	+++	+	-	-	+++
	28	1	61.1	59.2	+++	++	+++	-	-	+++	+++
	29	0	28.9	53.7	+++	+++	+++	+	-	-	-
	30	17	30.7	61.4	+++	+++	+++	+++	++	+	+++
	31	12	18.7	42.6	+++	+++	+++	+++	-	-	+++

Table 1.3 Mitotic index and immunohistochemical characteristics of 54 dogs with histiocytic sarcoma   (continued)

Group [a]	No.	MI [b]	Proliferative markers (% positive)		IHC results [c]						
			Ki67	PCNA	HLA-DR	Iba-1	CD204	CD163	Lysozyme	S100	CD208
HS-NCNS	32	14	26.6	53.2	++	+++	+++	+++	+++	-	+++
	33	15	46.5	62.2	+++	+++	+++	+++	+++	++	-
	34	2	19.6	46.7	+++	+++	+++	-	-	++	-
	35	1	37.2	45.3	+++	+++	+++	-	-	-	-
	36	10	22.3	80.7	+++	+++	+++	+++	-	+++	-
	37	5	40.2	73.1	+++	+++	+++	-	-	-	++
	38	71	43.3	67.5	+++	+++	+++	+++	-	-	+++
	39	4	61.2	57.2	+++	+++	+++	+++	-	+	-
	40	30	52.8	87.3	+++	+++	+++	+++	+++	+++	-
	41	15	46.9	61.4	+++	+++	+++	++	++	+	+++
	42	23	26.4	65.8	+++	+++	+++	+++	-	-	+++
	43	13	35.6	55.8	+++	+++	+++	-	-	-	+++
	44	59	9.1	59.5	+++	+++	+++	+++	+++	+++	-
	45	1	14.1	57.3	+++	+++	+++	++	-	-	-
	46	44	67.9	79.8	+++	+++	+++	+++	+++	-	-
	47	1	5.0	19.1	+++	+++	++	++	++	-	-
	48	3	10.0	70.0	+++	+++	++	-	+++	-	+++
	49	38	62.8	72.5	+++	+++	+++	+++	++	-	-
	50	5	12.2	34.6	+++	+++	+++	+	+++	+++	-
	51	20	45.7	72.5	+++	+++	+++	++	-	-	+++
	52	8	36.2	60.7	++	+++	+++	++	-	+++	-
	53	1	35.7	66.5	++	+++	+++	+++	-	-	+++
	54	31	30.5	80.1	+++	++	+++	++	-	+++	+
Mean ± SE of HS-NCNS			**34.4±3.0**	**62.1±2.6**							

[a] HS-CNS = Histiocytic sarcoma with central nervous system involvement; HS-NCNS = Histiocytic sarcoma without central nervous system involvement.
[b] MI = Mitotic index.
[c] HLA-DR = Human leukocyte antigen-DR; Iba-1 = Ionized calcium-binding adapter molecule-1; CD = Cluster of differentiation;
 Immunohistochemical scoring: - (Negative) = negative labeled cells; + (Weakly positive) = 1 − 25% labeled cells;   ++ (Moderately positive) = 26 − 50% labeled cells;
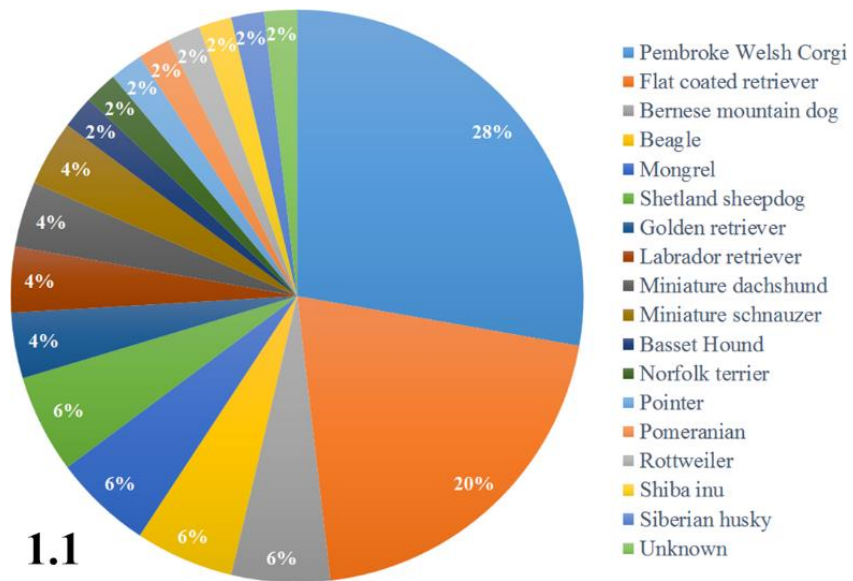 +++ (Strongly positive) = > 50% labeled cells.

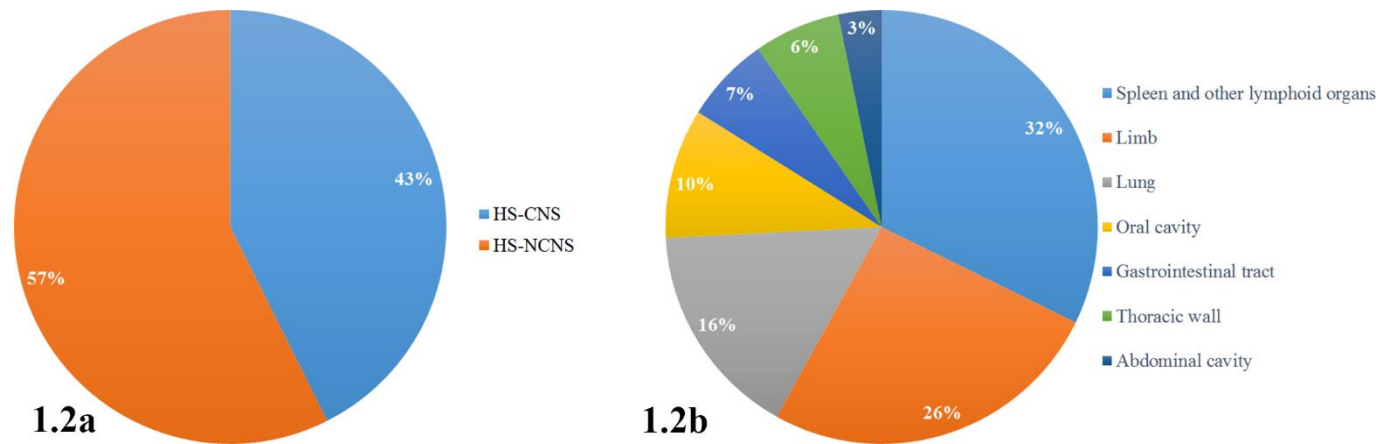**Figure 1.1**. Breeds of dogs affected with HS.

Figure 1.2. The location of 54 HS cases. The cases were divided into HS-CNS and HS-NCNS groups (a) in accordance with tumor location. In HS-NCNS group, the lesions were located in the spleen and other lymphoid organs, limb, lung, oral cavity, gastrointestinal tract, thoracic wall, abdominal cavity, and skin and subcutis (b).
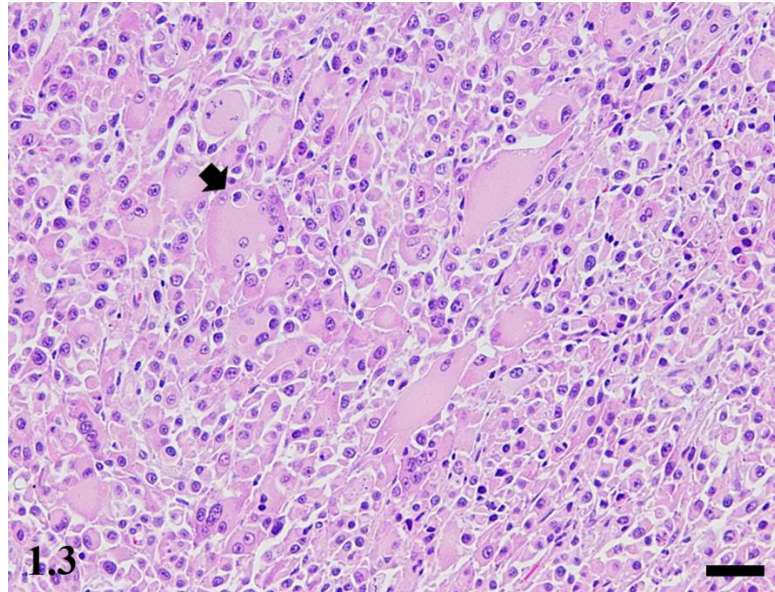
Figure 1.3. Histiocytic sarcoma. Right hindlimb. Dog. Case No. 37. The tumor contains numerous neoplastic histiocytes with severe cellular atypia. These cells have abundant eosinophilic cytoplasm. Their nuclei are eccentric and round to polygonal. Prominent nucleoli are noted in some tumor cells. Multinucleated giant cells are commonly found. The phagocytosis by tumor cells is also observed (arrow). HE. Scale bar = 20 μm.
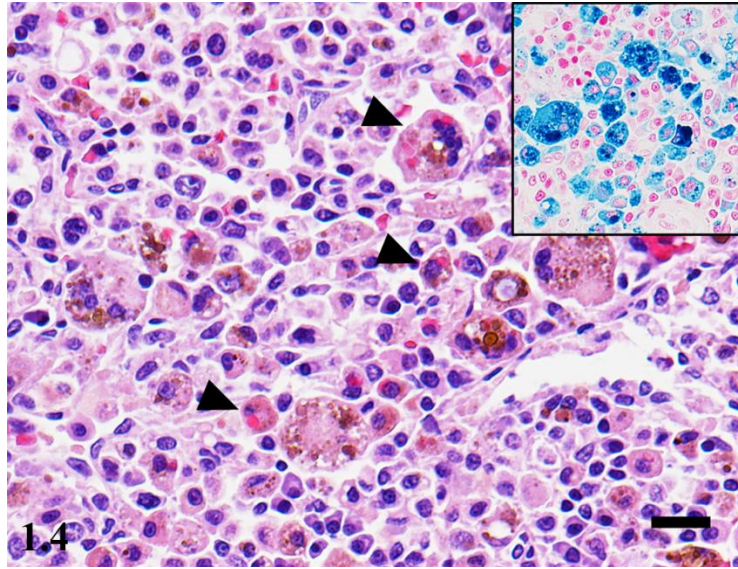
Figure 1.4. Hemophagocytic histiocytic sarcoma. Spleen. Dog. Case No. 30. Numerous neoplastic histiocytes expand to the splenic red pulp. These cells contain red blood cells hemophagocytosis, (arrowheads) and brown pigments. The latter are positive for Berlin blue stain (inset), indicating hemosiderin. The cytoplasmic vacuolation, moreover, is occasionally found. HE. Berlin blue (inset). Scale bar = 20 μm (including inset).
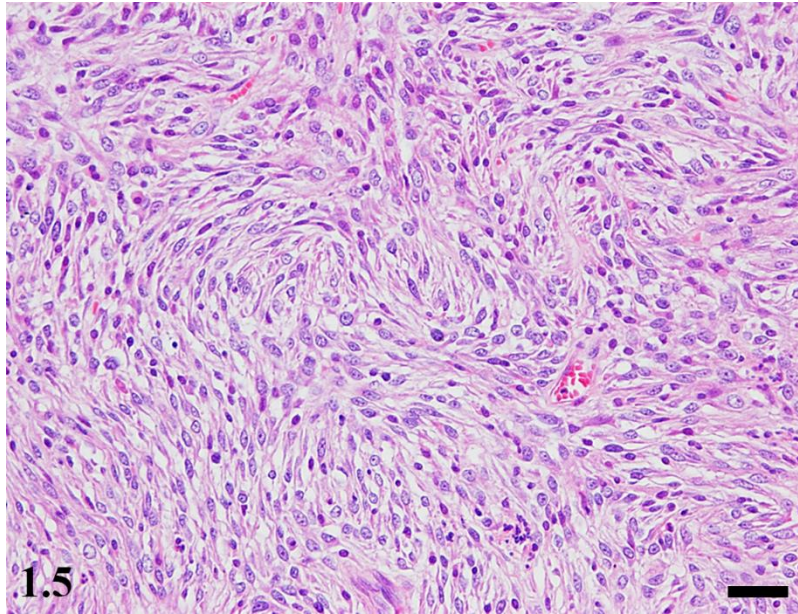
Figure 1.5. Histiocytic sarcoma. Lung. Dog. Case No. 44. The tumor consists of numerous spindle-shaped tumor cells that arrange in a storiform pattern. These cells have the eosinophilic cytoplasm with the indistinct border. Their nuclei are oval-shaped with prominent nucleoli. Mild cellular atypia is noted. Moderate infiltration of small lymphocytes is observed. HE. Scale bar = 20 μm.
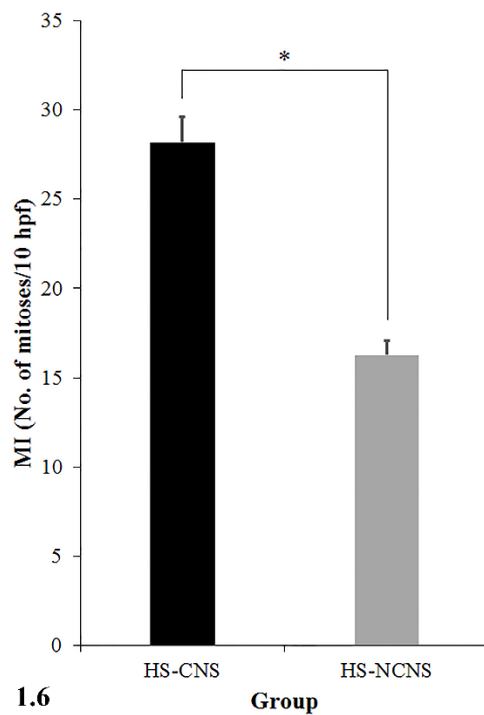
Figure 1.6. Mitotic index of 54 cases with histiocytic sarcoma. MI of HS-CNS group is significantly higher than that of HS-NCNS group. Mann-Whitney U test. *: $p<0.05$.
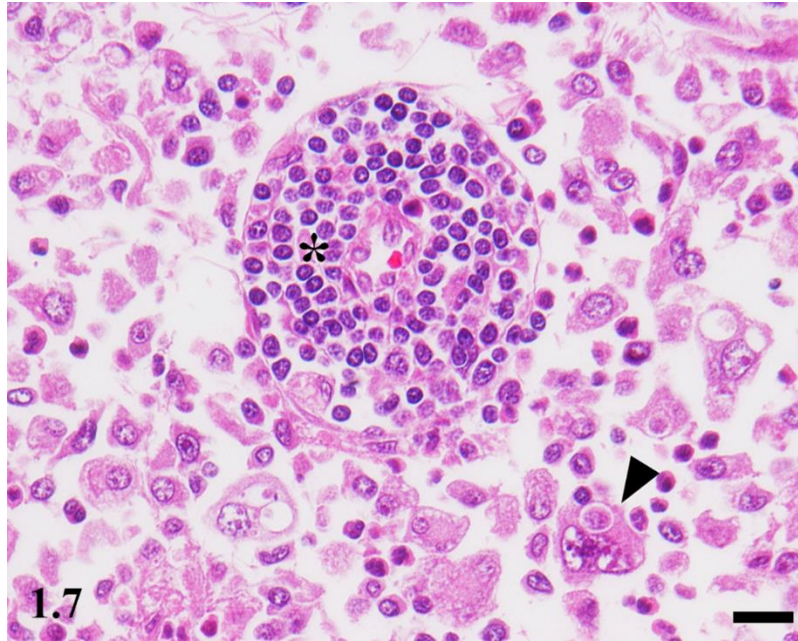
Figure 1.7. Histiocytic sarcoma. Brain. Dog. Case No. 9. Numerous neoplastic histiocytes invade to the brain cortex. The tumor cells are highly pleomorphic and show marked phagocytosis (arrowhead). Perivascular lymphocytic cuffing is notably observed (asterisk). HE. Scale bar = 20 μm.
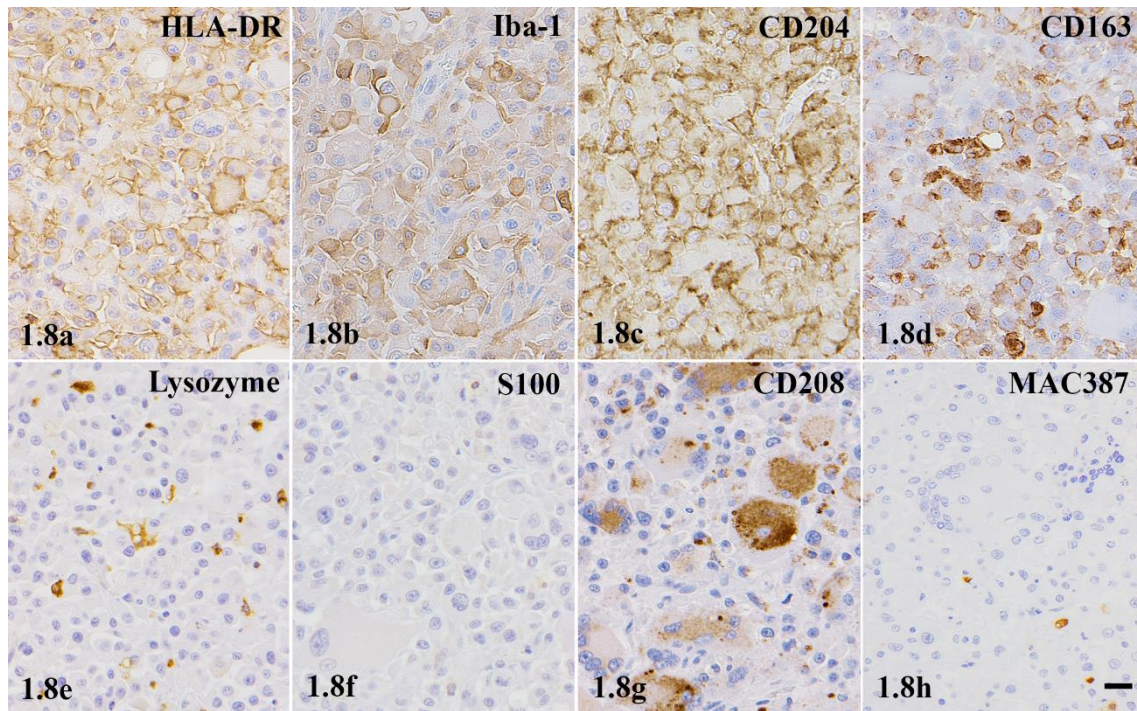
Figure 1.8. Histiocytic sarcoma. Limb. Dog. Case No. 38. Neoplastic histiocytes are strongly positive for HLA-DR (a), Iba-1 (b), CD204 (c), CD163 (d) and CD208 (g), but negative for lysozyme (e), S100 (f) and myeloid/histiocyte antigen (MAC387) (h). Normal macrophages are also positive for lysozyme (e). IHC. Hematoxylin counterstain. Scale bar = 20 μm.
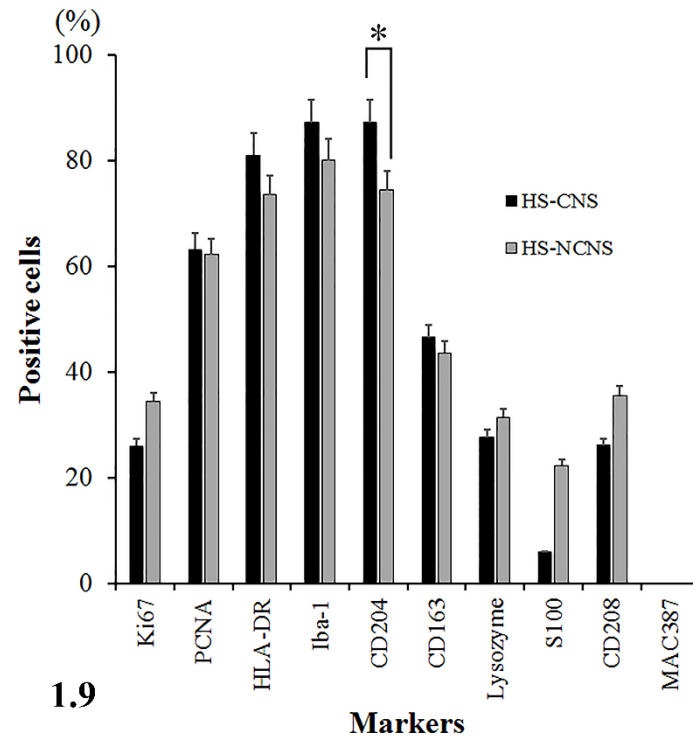
Figure 1.9. The % expression of the markers. The percent of CD204-immunopositive cells in the HS-NCNS group is significantly higher than that in the HS-NCNS group. No significant differences are observed in other markers between the groups. Mann-Whitney *U* test. *: *p<0.05*.

CHAPTER 2

Histopathological and immunohistochemical studies on

canine intracranial histiocytic sarcoma

INTRODUCTION

In accordance with cellular phenotypes, the cell of origin of canine histiocytic sarcoma (HS) encompasses either myeloid dendritic cell (DC) or macrophage. This tumor occurs most frequently in several organ systems including the spleen, lymph node, liver and lung [6, 32, 45, 50, 57, 60]. Moreover, the occurrence of HS in gastrointestinal tract skin and skeletal tissues has also been documented [3, 27, 80]. Most of the canine HS cases consistently express cluster of differentiation (CD) 1, CD11c, CD18, intracellular adhesion molecule-1 (ICAM-1) and major histocompatibility complex class II (MHC II) that are closely associated with immunophenotype of DC [19, 32]. On contrary, canine HS cases originating from macrophage (also known as hemophagocytic histiocytic sarcoma) are very rare and usually exhibit CD11d instead of CD11c [60, 81].

In human and animals, the incidence of HS with the central nervous system (CNS) involvement is very low when compared to HS arising from other organ systems. In veterinary literatures, to our knowledge, there have been only 10 publications describing the occurrence of HS with CNS manifestation [14, 43, 44, 51, 85-89, 101]. Ide *et al* mentioned that the cellular morphologies of both localized and disseminated HSs in the CNS were histologically identical, like in other organ systems [43, 80]. Moreover, immunohistochemical (IHC) expression patterns of those were not associated with the tumor cell origins. HS cases with the CNS involvement exhibited mainly histiocytic markers such as MHC II, lysozyme and CD18. Currently, most of the histiocytic marker provided to confirm cellular origin of HS are only available for frozen tissue samples. Furthermore, the cellular origin and histogenesis of HS in the CNS is still unclear due to the low incidence. In this chapter, therefore, clinicopathological, histological and IHC features of intracranial HS in 23 dogs, the sample data from Chapter 1, by using

36

conventional diagnostic markers are described in details. In addition, the expression of inducible nitric oxide synthase (iNOS; also known as nitric oxide synthase 2 (NOS2)) was examined to identify the macrophage phenotype of HS in the brain.

MATERIALS AND METHODS

Samples

Formalin-fixed canine brain HS samples from 20 biopsies and 3 necropsies between 2009 and 2014 were pathologically examined at Department of Veterinary Pathology, Graduate School of Agricultural and Life Sciences, the University of Tokyo. The signalment, neurological signs, and tumor location of the 23 cases are summarized in **Table 2.1**.

Histology

Two to four-μm thick paraffin tissue sections were stained with hematoxylin and eosin (HE). The tumors were morphologically divided into 2 categories (round/polygonal and spindle cell types) as described previously [18]. In the present study, cases with multinucleated giant cells were included in round/polygonal cell type.

Immunohistochemistry

The procedures of IHC and IHC scoring system were same as described in Chapter 1. Primary antibodies and antigen retrieval methods used in this chapter are detailed in **Table 2.2**.

Statistical analyses

Chi-square or Fisher's exact test was used to assess the association between clinicopathological features together with hemophagocytic activity and necrosis, and morphological difference of tumor cells, as appropriate. In addition, Mann-Whitney U test was performed to determine the significance of difference of mean MI between two cell phenotypes. Two-sided significant level was used that p-value <0.05 was considered statistically significant.

RESULTS

Tumor occurrence

Twenty three dogs examined included 14 males and 9 females with a range of 4 years to 14 years (the median age of 9 years). Breeds were comprised of the Pembroke Welsh corgi (n=11), Shetland sheepdog (n=3), Labrador retriever (n=2), Beagle (n=2), mixed breed (n=2), Flat coated retriever (n=1), Miniature schnauzer (n=1) and Siberian husky (n=1). Various neurological signs were recorded in 19 dogs, which included seizure (n=12), altered level of consciousness (n=5), circling (n=5), abnormal vision (n=4), gait abnormalities (n=4), proprioceptive deficits (n=4), hemiplegia and paralysis (n=3), disorientation (n=2), head pressing (n=2), head tilt (n=2), tremor (n=2), behavioral change (n=1) and somnolence (n=1). Most of the tumors (n=21) were observed in the cerebrum, whereas two cases (Cases No. 4 and 15) were in the cerebellum. Complete postmortem examination was performed only in Cases No. 4, 5 and 15, and as far as examined in the 3 cases, tumor invasions to distant organs were not detected.

Histological examination

Microscopically, brain lesions of all cases were poorly demarcated and invading to the brain parenchyma **(Fig. 2.1)**. Tumor cells were morphologically classified into 2 types. The first type included round- to pleomorphic-shaped cells with eosinophilic cytoplasm and a distinct border. Cytoplasmic vacuolation was occasionally found. These cells had eccentric, round to ovoid nuclei with prominent nucleoli (1 – 2 nucleoli/nucleus). Marked anisocytosis and anisokaryosis were noted with various numbers of atypical mitoses. Multinucleated giant tumor cells were frequently found.

Hemophagocytosis was commonly observed in almost all the cases **(Fig. 2.2 and Table 2.3)**. The second type included spindle-shaped cells with an indistinct border. These cells were arranged in an irregular pattern. Their nuclei were ovoid to spindle and concentrically located. The nucleoli were obscure. Mild anisocytosis and anisokaryosis, and atypical mitoses were noted **(Fig. 2.3)**. Hemophagocytosis was seen in only one case (Case No. 23). In both tumor types, moderate to marked infiltration of small lymphocytes was notably observed around small-sized blood vessels and in the neoplastic lesions. Moderate necrosis was occasionally found. Tumor cells of the round/polygonal type exhibited more active hemophagocytosis than those of the spindle type ($p<0.05$). However, there were no significant differences in other parameters (age, sex and necrosis) and MI between the two cell types **(Table 2.4)**.

Immunohistochemistry

Intense cell membrane and/or cytoplasmic immunoreactivities to HLA-DR, Iba-1 and CD204 were observed in all 23 tumors (100.00%). Strong, diffuse cytoplasmic staining for iNOS was detected in 20 cases (86.96%). Tumor cells in 17 cases (73.91%) were positive for CD163 with strong membrane staining. Nine tumors (39.13%) exhibited focal to diffuse cytoplasmic staining for lysozyme and CD208. Variable or weak cytoplasmic S100 immunoreaction was noted in 5 cases (21.74%) **(Fig. 2.4 and Table 2.3)**.

DISCUSSION

Despite canine histiocytic sarcoma has been well documented over the past several years, there have been only 10 publications demonstrating the occurrence of HS in the CNS. In the present study, HS in the brain was frequently found in the Pembroke Welsh Corgi, which is consistent with the results of previous studies [43, 51, 88]. Seizure is the major neurological sign of the present HS cases in the brain, while other clinical signs were found sporadically. A variety of the clinical signs might be associated with the affected areas of the brain. Based on the clinical histories and diagnostic imaging results, the tumor invasion and metastasis to other distant organs were not detected, supporting that the brains are the primary site of HS in all the present 23 cases. Furthermore, only the localized distribution pattern was observed in all the present cases, supporting that localized lesions might be the main form of intracranial HS in the dog as described previously [14, 43, 88, 101].

Tumor cells were infiltrated to the brain parenchyma in all cases. The term of *primary intracranial canine histiocytic sarcoma*, therefore, applies to the present cases. McMenamin *et al* [56] demonstrated that antigen presenting cells (ACP) were commonly found in the meninges and choroid plexus of the normal rat brain and that the cells have the similar immunophenotype and ultrastructural characteristics to DC. I, therefore, postulate that the cellular origin of canine HS in the brain is possibly resident DC in either the meninges or choroid plexus.

The lesions of canine HS in the brain can be histologically classified into 2 types (round/polygonal and spindle cell types) like those in the spleen and extremities described previously [18]. Interestingly, the present results showed hemophagocytic activity of

round/polygonal cell type was significantly higher than that of spindle cell type, suggesting that the biological behaviors of round/polygonal cells are probably more aggressive than the other. On the contrary, there were no significant differences between the 2 types in sex, age, the presence of necrosis as well as in the expression of markers of tumor cells (data not shown). These results support that the difference of tumor cell morphology cannot be used as a histological predictive parameter for primary intracranial HS in the dog, unlike HS cases in extraneural tissues [18].

Lysozyme is widely used as a histiocytic marker in both human and animals to substantiate a diagnosis of histiocytic disorders. Human histiocytic tumors that originate from the macrophage lineage exhibit a high expression of lysozyme, whereas those arising from DC have a low expression or are devoid of this molecule [11, 36, 52, 59, 98]. In the present study, an intense lysozyme-immunoreactivity was observed in 8 cases, supporting that these tumors have the macrophage phenotype. On the other hands, S100 and CD208 are used as markers for human DCs. The S100 molecule is specifically expressed in the DC lineage cells except for follicular DCs, whereas CD208 is exclusively expressed in human mature DCs and closely associated with DC differentiation and maturation [23, 70]. In the present study, S100 and CD208 immunoreactivities were observed in 5 and 9 cases, respectively, supporting that these tumors had the DC phenotype. HLA-DR, Iba-1 and CD204 immunoreactivity was detected in all the 23 cases, confirming that the tumors originated from histiocytes [32, 46, 69]. iNOS was detected in 20 cases, and CD163 in 17 cases, and the two molecules are widely used as M1 and M2 macrophage markers, respectively [26, 99]. In addition, 15 of 23 cases showed double positive for iNOS and CD163. However, 7 of 23 cases exhibited either M1 or M2 macrophage phenotype, and the remaining one case was negative for both

macrophage and DC markers. These observations suggest that variable immunophenotypic features of the tumor cells might be associated with the differentiation stage.

Primary HS of the CNS is an aggressive malignant neoplasm, and has a worse prognosis. This tumor is the major cause of cancer-related death in both human and animals. Canine HS in the brain may possess the features of both macrophage and DC, but the macrophage type including M1 and M2 is relatively predominant compared to the DC phenotype. This was also found in HS cases in the extraneural tissues, but was uncommon event [57].

Table 2.1 Twenty three cases of primary intracranial canine histiocytic sarcomas

Tumor cell morphology	No.	Breed	Age [a]	Sex [b]	Neurological sign [c]	Tumor localization [d]	Sample collection
Round/polygonal cell type	1	Pembroke Welsh corgi	11Y	FX	Gait abnormalities, depression, worsening respiratory status	Cerebrum (temporal lobe)	Biopsy
	2	Pembroke Welsh corgi	11Y5M	F	Right hemiplegia, seizure	Cerebrum (left frontal to parietal lobe)	Biopsy
	3	Pembroke Welsh corgi	7Y2M	M	Seizure, subconscious, circling, aimless pacing, somnolence, torticollis, left eye vision loss	Cerebrum (right temporal to occipital lobe)	Biopsy
	4	Pembroke Welsh corgi	5Y2M	FX	Gait abnormality, lateral recumbence	Cerebrum (right temporal lobe) and cerebellum	Necropsy
	5	Pembroke Welsh corgi	10Y	FX	n/d	n/d	Necropsy
	6	Pembroke Welsh corgi	12Y	F	n/d	Cerebrum (right temporal lobe)	Biopsy
	7	Labrador retriever	8Y	M	Seizure, progressive depress	Cerebrum (left frontal lobe)	Biopsy
	8	Labrador retriever	8Y6M	M	Seizure, circling, head pressing, proprioceptive deficit, head tilt, slow blink reflex	Cerebrum (right occipital lobe)	Biopsy
	9	Mixed breed	9Y	F	Circling, proprioceptive deficit, head pressing, right eye vision loss	Cerebrum (left parietal lobe)	Biopsy
	10	Mixed breed	4Y	MX	Anorexia, negative blink reflex, mydriasis	Cerebrum (frontal lobe)	Biopsy
	11	Shetland sheepdog	9Y	M	Behavioral change (aggressive), Gait abnormality (wobble)	Cerebrum (frontal lobe)	Biopsy
	12	Shetland sheepdog	11Y11M	FX	Circling, walking difficulty	Cerebrum (occipital lobe)	Biopsy
	13	Beagle	14Y	MX	Seizure	Cerebrum (base of brain to olfactory bulb)	Biopsy
	14	Flat coated retriever	12Y	M	Seizure, confusion, subconscious, lateral recumbence	Cerebrum (right temporal and occipital lobe)	Biopsy
	15	Siberian husky	11Y	FX	n/d	Cerebellum	Necropsy
Spindle cell type	16	Pembroke Welsh corgi	11Y5M	MX	Seizure, stupor	Cerebrum (fornix)	Biopsy
	17	Pembroke Welsh corgi	9Y	MX	Seizure, paralysis, tremor, proprioceptive deficit, inactivity	Cerebrum (right frontal lobe)	Biopsy
	18	Pembroke Welsh corgi	8Y	FX	Proprioceptive deficit	Cerebrum (right frontal and temporal lobe)	Biopsy
	19	Pembroke Welsh corgi	8Y	M	n/d	Cerebrum (right frontal lobe)	Biopsy
	20	Pembroke Welsh corgi	9Y9M	M	Seizure, drooling, tremor	Cerebrum (left temporal lobe)	Biopsy
	21	Beagle	10Y11M	M	Seizure, paralysis, circling	Cerebrum (left frontal lobe)	Biopsy
	22	Miniature schnauzer	4Y	M	Seizure, progressive depress	Cerebrum (left temporal lobe)	Biopsy
	23	Shetland sheepdog	11Y	M	Seizure	Cerebrum	Biopsy

[a] Y = Year (s); M = Month (s). [b] M = Male; F = Female; X = Sterilization. [c] n/d = No data.

[d] Tumor locations were confirmed by magnetic resonance imaging (MRI) and/or computed tomography (CT); n/d = No data.

44

Table 2.2 Primary antibodies used in immunohistochemical examination

Antibody to [a]	Type [b]	Dilution	Antigen retrieval for IHC [c]	Expression	Source
HLA-DR	Mouse, mAb (TAL.1B5)	1:50	Citrate buffer, pH 6.0 (HIER), 121°C, 10 min	Antigen presenting cell	Santa Cruz, CA, USA
Iba-1	Rabbit, pAb	1:250	Citrate buffer, pH 6.0 (HIER), 121°C, 10 min	Microglia, macrophage	Wako, Osaka, Japan
CD204	Mouse, mAb (SRA-E5)	1:100	Tris/EDTA buffer, pH 9.0 (HIER), 121°C, 10 min	Monocyte, macrophage	TransGenic, Kobe, Japan
CD163	Mouse, mAb (AM-3K)	1:100	Citrate buffer, pH 2.0 (HIER), 121°C, 10 min	Histiocyte, M2 macrophage	TransGenic, Kobe, Japan
iNOS	Rabbit, pAb	1:200	Citrate buffer, pH 6.0 (HIER), 121°C, 10 min	M1 macrophage	Abcam, Tokyo, Japan
Lysozyme	Rabbit, pAb	1:1000	Proteinase K (PIER), room temperature, 30 min	Monocyte, macrophage	Dako, Glostrup, Denmark
S100	Rabbit, pAb	1:1000	Citrate buffer, pH 6.0 (HIER), 121°C, 10 min	Dendritic cell	Dako, Tokyo, Japan
CD208 (DC-LAMP)	Rat, mAb (1010E1.01)	1:100	Citrate buffer, pH 6.0 (HIER), 121°C, 10 min	Dendritic cell	Dendritics, Lyon, France

[a] HLA-DR = Human leukocyte antigen-DR; Iba-1 = Ionized calcium-binding adapter molecule; CD = Cluster of differentiation;
  DC-LAMP = Dendritic cell lysosome-associated membrane glycoprotein.
[b] pAb = Polyclonal antibody; mAb = Monoclonal antibody.
[c] IHC = Immunohistochemistry, HIER = Heat-induced epitope retrieval; PIER = Proteolytic-induced epitope retrieval.

Table 2.3 Histological and immunohistochemical features of primary intracranial canine histiocytic sarcomas

No.	Breed	Tumor cell morphology [a]	MI [b]	Hemophagocytosis [c]	Necrosis [d]	IHC results [e]							
						HLA-DR	Iba-1	CD204	CD163	iNOS	Lysozyme	S100	CD208
1	Pembroke Welsh corgi	Round/polygonal cell type	4	+	-	+++	+++	+++	-	+++	-	-	+++
2	Pembroke Welsh corgi	Round/polygonal cell type	33	-	+	+++	+++	+++	+++	+++	+++	+	+++
3	Pembroke Welsh corgi	Round/polygonal cell type	56	+	+	+++	+++	+++	++	+++	+++	+	-
4	Pembroke Welsh corgi	Round/polygonal cell type	22	+	+	+++	+++	+++	+++	+++	+++	-	-
5	Pembroke Welsh corgi	Round/polygonal cell type	8	+	-	+++	+++	+++	++	+	+++	-	-
6	Pembroke Welsh corgi	Round/polygonal cell type	32	-	+	+++	+++	++	+++	+++	+++	-	+
7	Labrador retriever	Round/polygonal cell type	39	+	-	+++	+++	+++	+++	+++	+++	-	++
8	Labrador retriever	Round/polygonal cell type	37	-	+	+++	+++	+++	++	+++	-	+	-
9	Mixed breed	Round/polygonal cell type	70	+	+	+++	+++	+++	+++	+++	-	-	-
10	Mixed breed	Round/polygonal cell type	44	-	+	+++	+++	+++	-	+	-	-	-
11	Shetland sheepdog	Round/polygonal cell type	24	+	-	+++	+++	+++	-	+	-	-	+
12	Shetland sheepdog	Round/polygonal cell type	62	+	+	+++	+++	++	++	-	-	-	-
13	Beagle	Round/polygonal cell type	4	+	+	+++	+++	+++	+++	-	-	+	++
14	Flat coated retriever	Round/polygonal cell type	39	+	-	+++	+++	+++	++	+	-	-	-
15	Siberian Husky	Round/polygonal cell type	0	+	+	+++	+++	+++	-	+++	+++	-	++
16	Pembroke Welsh corgi	Spindle cell type	58	-	+	+++	+++	+++	+++	+++	+++	-	-
17	Pembroke Welsh corgi	Spindle cell type	26	-	-	+++	+++	+++	+++	++	-	-	-
18	Pembroke Welsh corgi	Spindle cell type	11	-	+	+++	+++	+++	-	-	-	-	-
19	Pembroke Welsh corgi	Spindle cell type	10	-	+	+++	+++	+++	+++	+	-	-	-
20	Pembroke Welsh corgi	Spindle cell type	44	-	+	+++	+++	+++	+++	++	-	-	-
21	Beagle	Spindle cell type	7	-	-	+++	+++	+++	++	+	-	-	++
22	Miniature schnauzer	Spindle cell type	6	-	+	+++	+++	+++	+++	+	-	-	++
23	Shetland sheepdog	Spindle cell type	12	+	+	+++	+++	+++	-	++	-	+	-
	Total					**23**	**23**	**23**	**17**	**20**	**8**	**5**	**9**

[a] Round/polygonal cell type = > 50% of tumor cell population are neoplastic histiocytes and multinucleated giant cells; Spindle cell type = > 50% of tumor cell population are spindle-shaped cells.
[b] Mitotic index = Number of mitotic figures per 10 high power fields.
[c] Hemophagocytosis score: + = Hemophagocytosis is present; - = Hemophagocytosis is absent.
[d] Necrosis score: + = Necrotic area is observed; - = No necrotic area is observed.
[e] Immunohistochemical scoring: - (Negative) = Negative tumor cells; + (Weakly positive) = 1 – 25% positive tumor cells;
   ++ (Moderately positive) = 26 – 50% positive tumor cells; +++ (Strongly positive) = > 50% positive tumor cells.

Table 2.4 Factors related to cellular morphology in primary intracranial canine histiocytic sarcoma

Factor	Round/polygonal cell type (n=15)	Spindle cell type (n=8)	*p*-value
Sex			0.086
Male	7	7	
Female	8	1	
Age range			1.000
< 3 years	0	0	
≥ 3 year, < 6 years	2	13	
≥ 6 years	1	7	
Tumor location			0.558
Cerebrum	13	8	
Cerebellum	1	0	
n/d [a]	1	0	
Hemophagocytosis (Presence)	11	1	0.009
Necrosis (Presence)	10	6	1.000

[a] n/d = No data.
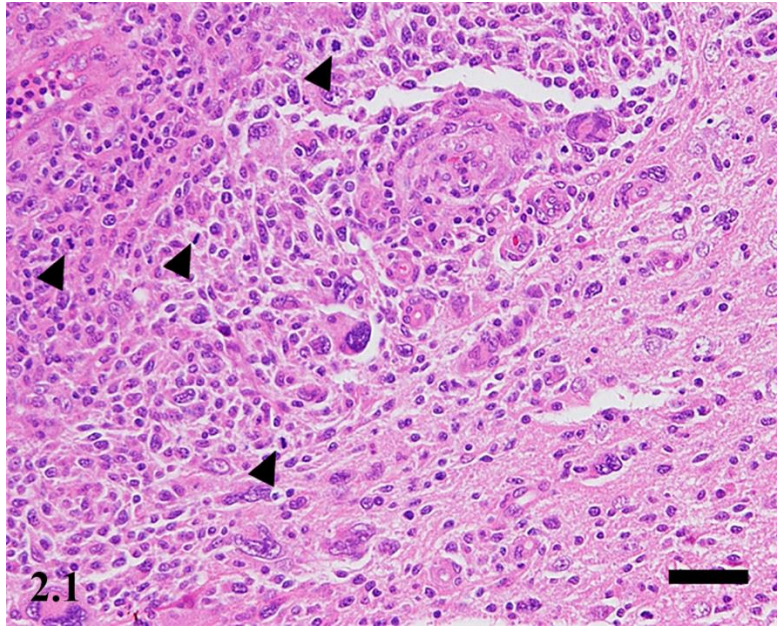
Figure 2.1 Histiocytic sarcoma. Cerebrum. Dog. Case No. 3. Numerous neoplastic histiocytes with severe cellular atypia invade to the neuropil. Atypical mitotic figures are commonly seen (arrowheads). HE. Scale bar = 50 μm.
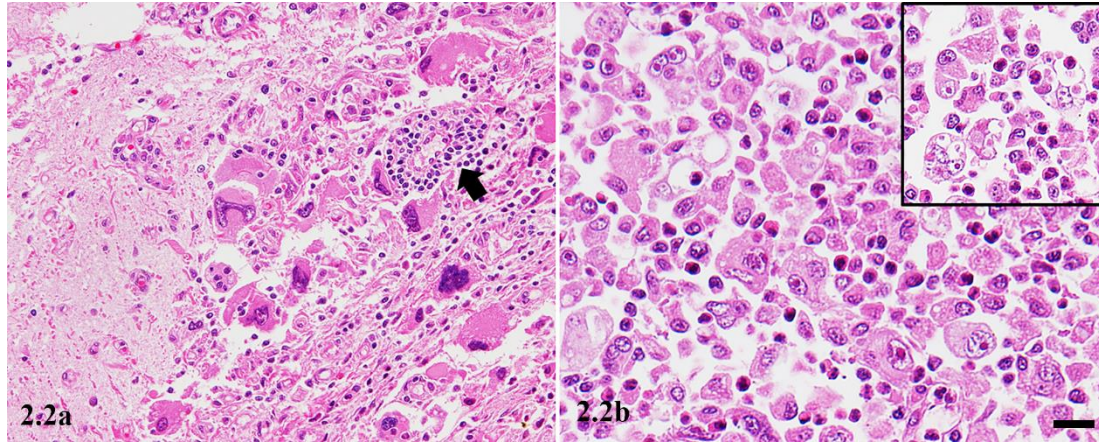
Figure 2.2 Histiocytic sarcoma. Cerebellum. Dog. Case No. 4. Neoplastic histiocytes invade to both molecular and granule cell layers (a). The infiltration of small lymphocytes is observed admixing with the tumor cell population, especially surrounding small arterioles (arrow). In higher magnification (b), these tumor cells are polygonal to pleomorphic and the nucleus has prominent nucleoli (1 − 2 nuclei/nucleus). Severe cellular atypia is notably observed. The hemophagocytosis is commonly found (inset). HE. Scale bar = 20 μm (including inset).
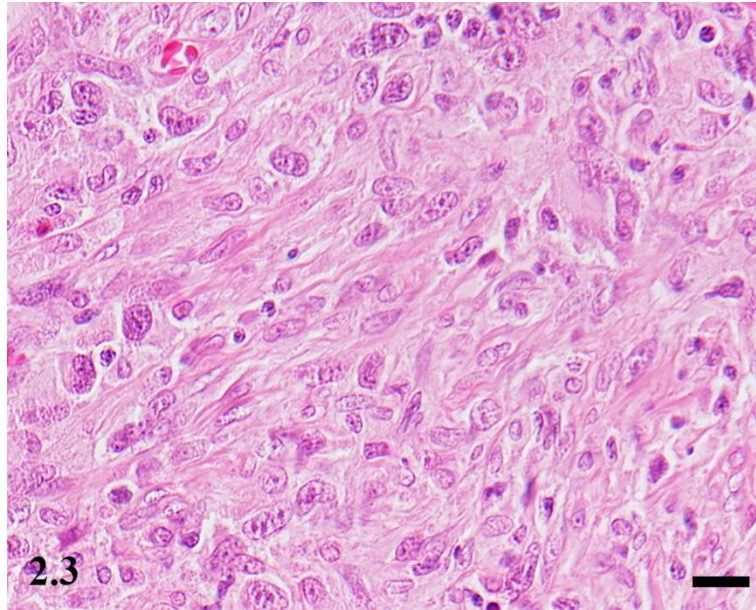
Figure 2.3 Histiocytic sarcoma. Cerebrum. Dog. Case No. 20. Most of the tumor cells are spindle-shaped. HE. Scale bar = 20 μm.
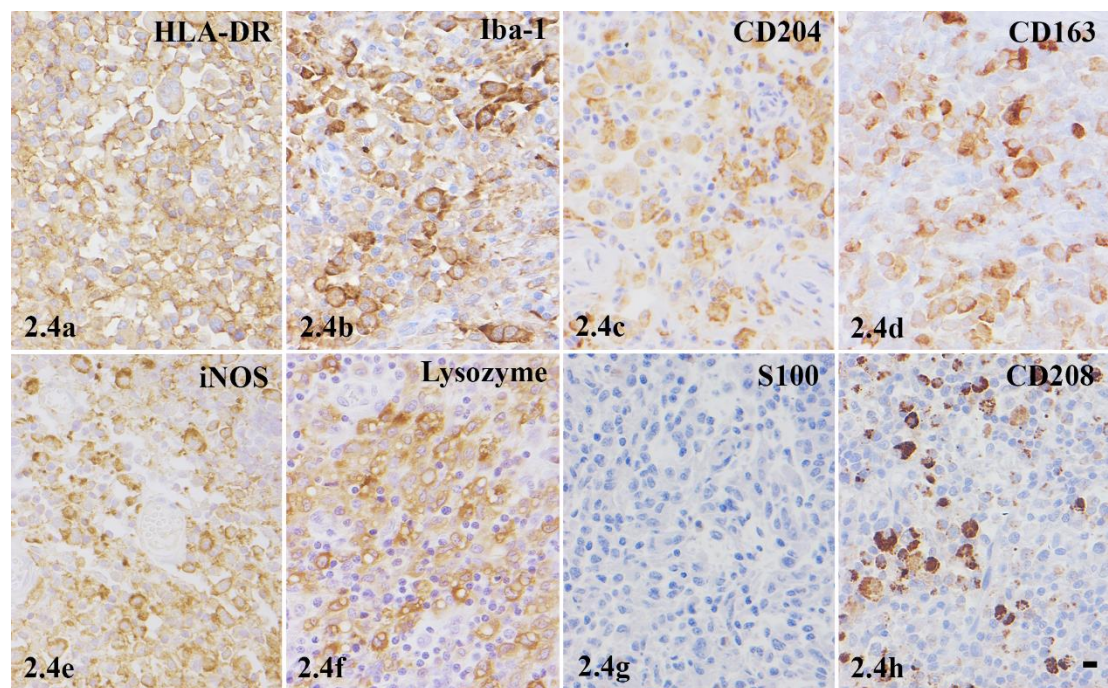
Figure 2.4 Histiocytic sarcoma. Cerebrum. Dog. Case No. 6. Neoplastic histiocytes are positive for HLA-DR (a), Iba-1 (b), CD204 (c), CD163 (d), iNOS (e), lysozyme (f) and CD208 (h), but negative for S100 (g). IHC. Hematoxylin counterstain. Scale bar = 10 μm.

CHAPTER 3

The establishment and characterization of canine

histiocytic sarcoma cell lines

INTRODUCTION

In Chapter 2, primary histiocytic sarcoma (HS) in the CNS may in part possess the features of both macrophage and DC. In addition, M1 and M2 types of the macrophage origin are relatively predominant compared to the DC phenotype. In order to verify cellular origins of canine HS arising in the CNS, I try to establish canine HS cell lines and examine their features in this chapter.

Over the last 5 decades, there have been only few literatures demonstrating the establishment of canine HS cell lines isolated from the bone marrow, skin mass and synovial mass [8, 78, 95]. In addition, to our knowledge, the establishment of those from neural tissue have not been described. Two new HS cell lines, designated as PWC-HS01 and FCR-HS02, obtaining from brain and synovial mass, respectively, are described. Cellular morphological and immunocytochemical characteristics, molecular features and biological behaviors of the lines are elucidated. In addition, the tumor xenotransplantation and metastasis assay are performed using immunodeficient mice in order to evaluate cellular and metastasis properties of these new cell lines.

MATERIALS AND METHODS

Animals

Tumor samples were obtained from 2 dogs, presented to the Veterinary Medical Center, the University of Tokyo. The tumors were histologically diagnosed as HS. Dog No.1 was an 11years and 5 months old female Pembroke Welsh Corgi with a history of right hemiplegia and convulsion. Magnetic resonance imaging (MRI) of the brain revealed a solitary multilobulated mass located in the left frontal bone. No evidence of

distant metastases was observed. Brain surgery requested by the owner was eventually performed. Dog No.2 was an 8 years and 6 months old male Flat coated retriever suffering from right forelimb stiffness and non-weight bearing. Computed tomography (CT) scan revealed a soft mass located around periarticular area of the right shoulder joint and proximal part of humerus with periosteal bone formation and lysis were detected. Limb amputation as well as lymphadenectomy of the regional lymph nodes were performed.

Cell cultivation

Fresh tumor samples were finely minced and washed twice with sterile phosphate buffered saline without Ca^{2+} and Mg^{2+} (PBS; pH 7.4) containing 1% penicillin-streptomycin solution. The samples were then suspended in Dulbecco's modified eagle medium (DMEM; GIBCO, Invitrogen, Tokyo, Japan) containing 0.25% crude trypsin and incubated in 4ºC for 16 to 18 hrs. All the samples were then agitated at 37ºC for 30 min and centrifuged at 1000 rpm, 4ºC for 5 min. The pellets were resuspended in new DMEM supplemented with 10% heat inactivated fetal bovine serum (FBS, GE Healthcare Life Sciences, UT, USA) and 1% penicillin-streptomycin (Wako Pure Chemical, Osaka, Japan). After filtration through a cell strainer (70μm nylon, Falcon, Tokyo, Japan), the suspended cells were seeded into 100-mm petri dishes (Thermo Scientific, Tokyo, Japan) and subsequently incubated at 37ºC in an atmosphere of 5% CO_2/95% air.

Three months after the initial cultivation, tumor cells were cloned by a serial dilution method. After cells had grown to cover the cell culture plate, cloned cells were removed and seeded into 60-mm petri dishes (Thermo Scientific, Tokyo, Japan) containing with two different media, i.e. DMEM and RPMI 1640 (GIBCO, Invitrogen,

54

Tokyo, Japan) supplemented with different concentrations of FBS (5%, 10%, 15% and 20%) in order to determine a suitable condition. Media were replaced every 4 days and cell passages were performed weekly. Population-doubling time (PDT) was determined using the procedure described previously [30, 78].

Morphological characterization of the canine HS cell lines

1×10^4 cells/ml of PWC-HS01 and FCR-HS02 cells was seeded into 2-well chamber slides (Nunc™ Lab-Tek™ II CC2™ chamber slide system, Thermo Scientific NY, USA). One week after cultivation, cells were stained with a Giemsa solution (Merck Millipore, Tokyo, Japan).

Ultrastructural observation was performed only for PWC-HS01 cell line. After trypsinization, suspended cells were washed twice with 0.1 M phosphate buffer (PB), pH 7.4, fixed with 2.5% glutaraldehyde (Wako Pure Chemical, Osaka, Japan) in PB at room temperature for 1 hr, and then postfixed with osmium tetroxide (2%; Nisshin EM, Tokyo, Japan) at 4°c for 1 hr. Samples were dehydrated with a graded series of alcohol and embedded in epoxy resin. Ultrathin sections (60 – 90 nm) were stained with uranyl acetate/lead citrate and then observed under a transmission electron microscope (New Bio-TEM H-7500, Hitachi High-Tech Science, Tokyo, Japan).

Immunophenotypic characterization of canine HS cell lines

PWC-HS01 and FCR-HS02 cells were spun at 1,000 rpm for 6 min using a cytocentrifuge (StatSpin® Cytofuge® 2 Cytocentrifuge, Japan), and the slides with the

cells on them were fixed with 4% paraformaldehyde at room temperature for 15 min. In cases of intracellular markers, a cell membrane permeabilization was performed by incubating tumor cells with 0.25% triton X-100 at room temperature for 10 min prior to the blocking step. After rinsing with PBS, all slides were treated with crude bovine serum albumin (BSA; Sigma-Aldrich, MO) in PBS with Tween®20 (PBST; final concentration = 1% BSA in PBST) at room temperature for 30 min in order to block non-specific reactions. Primary antibodies were then applied at 4°C overnight. Primary antibodies used are listed in **Table 3.1**. After rinsing with PBS, the slides were subsequently incubated with fluorochrome-labeled secondary antibodies including fluorescein horse anti-mouse IgG antibody, fluorescein goat anti-rabbit IgG antibody and fluorescein streptavidin (Vector laboratory, Tokyo, Japan) at room temperature for 1 hr and counterstained with DAPI (Vectashield®, Vector laboratory, Tokyo, Japan). All slides were observed under the Zeiss LSM 700 laser scanning confocal microscope (Carl Zeiss Meditec, Tokyo, Japan).

Proliferative index

In order to determine the proliferative index of the established cell lines, immunocytochemistry was performed. Briefly, 2 ml of PWC-HS01 and FCR-HS02 cells (1×10^4 cells/ml) were seeded into a 2-well chamber slide and allowed them to be an 80 to 90% confluence. The tumor cells were fixed with 4% paraformaldehyde at room temperature for 15 min and then permeabilized by incubating tumor cells with 0.25% triton X-100 at room temperature for 10 min. For blocking non-specific reactions, slides were immersed in 3% hydrogen peroxide (H_2O_2) at room temperature for 30 min and then

incubated in crude BSA in PBS (final concentration = 10% BSA in PBS) at room temperature for 1 hr. Anti-Ki67 antibody was applied at 4°C overnight (**Table 3.1**). After washing with PBS for 3 times, the slides were incubated with horseradish peroxidase (HRP)-labeled polymer reagent (Envision[+] system-HRP labeled polymer reagent, Dako, Tokyo, Japan) at room temperature for 30 min. After rinsing with PBS, all the slides were treated with a 3-3'-diaminobenzidine solution containing 0.03% H_2O_2, and being counterstained with hematoxylin. The proliferative index was determined as a count of Ki67-positive cells 1,000 tumor cells in the "hot spot" areas.

Western blot analysis

Extracted whole cell proteins were used in this experiment. Briefly, suspended tumor cells (1×10^6 cell/ml) were seeded to a wells of 100-mm Nunc Petri dish and allowed them to be 80 to 90% confluence. The adherent cells were washed twice with ice-cold PBS and subsequently RIPA buffer [50mM Tris-HCl, 150 mM NaCl, 1% Triton X-100, 0.5% Sodium deoxycholate, 0.1% Sodium dodecyl sulfate, 5mM EDTA, 2mM Na_3VO_4, 1mM Phenylmethysulfonyl fluoride, 10mM Sodium fluoride, and complete tablets, mini EDTA free, easypack (Roche Diagnostic, Mannheim, Germany)] were added. The tumor cells were gently removed by cell scraper (Jus-Tis, AS ONE, Tokyo, Japan) and transferred to new pre-cooled tubes. These lysed cells were then agitated at 4°C for 30 min and centrifuged at 12,000 rpm, at 4°C for 20 min. The supernatant was collected for Western blotting. Protein concentration was quantified by the SmartSpec™ Plus spectrophotometer (BIO-RAD, Tokyo, Japan). Protein samples were diluted (1:1) with a loading buffer (2x Laemmli sample buffer containing with β-mercaptoethanol) and then

heated at 99ºC for 5 min. Sample of equal protein concentration was loaded onto 15% polyacrylamide gel (e-PAGEL®, ATTO corporation, Tokyo, Japan) and electrophoresed for 90 min. The protein bands were transferred onto polyvinylidene fluoride (PVDF) membranes (Immibilon®-P transfer membrane, Millipore Corporation, MA) and then immersed with skim milk in Tris-buffered saline with Tween®20 (TBST; final concentration = 3.75% dry skim milk in PBST) at room temperature for 1 hr in order to block non-specific reactions. After that, all the membranes were incubated with the primary antibodies against CD204 (1:500, TransGenic, Kobe, Japan) and β-actin (1:2000, Cell Signaling Technology, Tokyo, Japan) and then agitated at 4ºC overnight. After washing with TBST, the membranes were incubated with horseradish-peroxidase (HRP)-conjugated anti-rabbit IgG or anti-mouse IgG (1:5000; GE Healthcare, Little Chalfont, UK) at room temperature for 1 hr. Chemiluminescence method was used for immunoblotting detection (Amersham™ ECL™ prime Western blotting detection reagent, GE Healthcare, Little Chalfont, UK).

Reverse transcription-polymerase chain reaction (RT-PCR)

Total RNA was isolated from PWC-HS01 and FCR-HS02 cells, and the frozen spleen from hemophagocytic HS using an RNA extraction kit (RNeasy Mini Kit, Qiagen, Tokyo, Japan) according to the manufacturer's protocol. RNA concentration was then quantified using the NanoDrop 2000 spectophotometer (Thermo scientific, Wilmington, DE, USA) with 260/280 nm absorbance ratio between 1.8 and 2.0. In reverse transcription process, cDNA was synthesized from RNA of each sample using an RT-PCR Kit (Prime

Scipt™, Takara Bio, Tokyo, Japan) according to the manufacturer's protocol. The cDNA products were stored at -20°C until used.

RT-PCR amplification for canine CD11b, CD11c and CD204 genes was performed. In addition, glyceraldehyde-3-phosphate dehydrogenase (GAPDH) was also used as an internal control. The primers were conducted the sequence appearing in the Primer 3Plus (www.bioinformatics.nl) or a previous report [97]. The sequences are detailed in **Table 3.2**. The amplification process was comprised of cDNA activation at 95°C for 3 min, 40 cycles of denaturation at 94°C for 30 s, annealing at 52 or 60°C for 1 min, and extension at 72°C for 30 s. The PCR products were mixed with GRRed DNA loading buffer (Excellgen, Rockville, MD) and then electrophoresed onto 2% agarose gel. OneSTEP DNA ladder 50 (Nippon Gene, Toyama, Japan) was used as a DNA marker. To visualize the results, a molecular imager, GelDoc™ XR plus system was used.

Chromosome analysis

Cultured HS cells were seeded into a 100-mm Nunc Petri dish and allowed to be 80 to 90% confluence. Cells were incubated with colcemid (KaryoMax®, Invitrogen, Tokyo, Japan) at the final concentration = 0.02 μg/ml) at 37°C for 2 hr, and subsequently treated with a pre-warmed hypotonic solution (0.075 M KCl) at 37°C for 30 min. After centrifugation (1,000 rpm) at 4°C for 4 min, the pellets were resuspended in a fixative solution (Methanol-Acetic acid; 1:1) on ice for 30 to 60 min and then washed twice with the fixation solution. Suspended cells were then dropped on a slide glass and subsequently stained with a Giemsa solution in 0.1 M Phosphate buffer (pH 6.8). The chromosome number was counted under a light microscope in an oil immersion filed (1,000X).

Phagocytosis assay

The cultured cells were seeded onto a 2-well chamber slide (1×10^5 cells/well) and then incubated at 37°C in an atmosphere of 5% CO_2/95% air overnight. Then, the medium was replaced by serum-free DMEM with zymosan A bioparticle® (Invitrogen, Tokyo, Japan), and then an incubation at 37°C for 2 hrs was done. After rinsing with cold PBS 4 times, the cells were fixed in 4% paraformaldehyde for 20 min and counterstained with DAPI (Vector laboratory, Tokyo, Japan). The phagocytic activity was observed under Zeiss LSM 700 laser scanning confocal microscope (Carl Zeiss Meditec, Tokyo, Japan).

Tumorigenicity and metastasis assays

Six 5-week-old female C.B-17/Icr-scid/scidJcl mice (SCID) (CLEA Japan, Tokyo, Japan) were randomly divided into 2 groups for PWC-HS01 and FCR-HS02 cell lines, respectively. Five to seven days prior to experiment, these mice were allowed to acclimatize and housed under a specific pathogen free condition. The experiments, particularly animal utilization was approved by the Animal Care and Use Committee of the Graduate School of Agricultural and Life Sciences, the University of Tokyo.

The established canine HS cells (3×10^6 cells/ml) suspended in 200 μl of Hanks' balanced salt solution (HBSS; GIBCO, Invitrogen, Tokyo, Japan) were subcutaneously injected into the lower flank of the immunodeficient mice. The tumor size was evaluated every 4 days and tumor volume was calculated using the following equation:

$$\text{Tumor volume (mm}^3) = (\text{Length x Width}^2)/2$$

One and a half to 2 months after tumor transplantation, SCID mice were euthanized and tumors and visceral organs including CNS tissues were collected. The samples were immediately fixed in a 10% neutral buffered formalin solution for pathological examination. Two to four-μm-thick paraffin sections were stained with HE. Immunohistochemical (IHC) examination was also performed. Primary antibodies used for IHC were listed in **Table 3.5**. IHC was performed in the same manner as described in Chapter 1.

The HS cells (5×10^5 cells/ml) suspended in 200 μl of HBSS were injected into the lateral tail vein of the SCID mice. Two months after injection, all the mice were euthanized and grossly examined for tumor development. Metastatic tumor masses and visceral organs including CNS tissues were immediately fixed in a 10% neutral buffered formalin solution for pathological examination mentioned above.

RESULTS

Growth characterization of canine HS cell lines in vitro

Histopathological features of the original tumor tissues in the brain and shoulder joint, respectively were indicated in **Figs 3.1 and 3.2**. Established cell line were designated as PWC-HS01 and FCR-HS02, respectively. Both cell lines have successfully grown in culture media of DMEM and RPMI 1640 with different FBS concentrations **(Table 3.3)**. I chose, therefore, the condition of DMEM supplementing with 10% FBS throughout the study. The PDT of PWC-HS01 and FCR-HS02 was approximately 64.8 and 56.5 hours, respectively **(Fig. 3.3)**.

Morphological characterization of canine HS cell lines

In both HS cell lines, most of cells were round- to polygonal-shaped with abundant cytoplasm. Their nuclei were eccentrically round with prominent single or multiple nucleoli. Atypical mitoses were commonly observed. Mild to moderate anisocytosis, anisokaryosis and anisonucleoliosis were also noted. Bizarre binucleated and multinucleated giant cells were occasionally found. PWC-HS01 cells proliferated in monolayer, whereas FCR-HS02 cells usually proliferated clumping in culture **(Figs. 3.4 – 3.5)**.

An ultrastructural study revealed that PWC-HS01 cells had abundant cellular processes and few organelles. Mitochondria were commonly observed. Vesicular membrane structures were occasionally seen. Birbeck granules were not detected. Lobulated heterochromatic nuclei were noted **(Fig. 3.6)**.

Immunocytochemical characterization of canine HS cell lines

Immunocytochemical examination revealed that both cell lines were consistently positive for HLA-DR, Iba-1, CD163, iNOS, lysozyme, S100, CD208, vimentin, CD34, CD4, CD1a, CD11b and CD273. Variable or weak membrane CD54 immunoreaction, was also observed. However, both the cells were negative for cytokeratin AE1/AE3. For PWC-HS01cells were positive for CD68 and CD204, but FCR-HS02 cells were negative **(Figs. 3.7 – 3.8 and Table 3.4)**. The ratio of Ki67 immunopositive cells were 91.78% and 49.79% in PWC-HS01 and FCR-HS02, respectively **(Figs. 3.9 – 3.10)**.

Western blot

Extracted proteins from both HS cell lines were examined for the expression of CD204. The result revealed that CD204 (72 kDa) was only detected in PWC-HS01 cells **(Fig. 3.11)**.

RT-PCR

CD11b mRNA was detected in both HS cells. Strong and moderate expression of CD11c mRNA was observed in PWC-HS01 and FCR-HS02 cells, respectively, whereas hemophagocytic HS tissue had low expression. FCR-HS02 cells and hemophagocytic HS tissue showed low expression of CD204 mRNA **(Fig. 3.12)**.

63

Chromosome analysis

The modal chromosome number of PWC-HS01 cell line was 63 – 88 (mode = 75, mean = 74.7), and that of FCR-HS02 was 42 – 49 (mode = 46, mean = 45.4) **(Figs. 3.13 – 3.14)**.

Phagocytosis assay

Both PWC-HS01 and FCR-HS02 cell lines had the capacity to engulf zymosan A bioparticle®, indicating that they had phagocytic ability resembling to normal histiocytes **(Figs. 3.15 – 3.16)**.

Tumorigenicity assay

Solitary subcutaneous masses were observed in all the SCID mice injected with both HS cells one month after tumor inoculation **(Fig. 3.17)**. Tumors from both groups showed the same features. Numerous round- to polygonal-shaped anaplastic cells arranged in sheet to solid pattern. Bizarre mononuclear tumor cells were commonly seen. The tumor cells had abundant eosinophilic cytoplasm. Their nuclei were mainly round- to pleomorphic-shaped with one or multiple prominent nucleoli. Moderate anisocytosis and anisokaryosis were noted. Mitotic figures were frequently observed (> 100 mitoses/10 hpf, 400x). Multinucleated giant cells observed in the original tumor were rarely detected in the xenotransplanted tumor. Moreover, necrosis was commonly detected in the center of the tumor tissues.

IHC examination revealed that both tumor cells were consistently positive for HLA-DR, CD204, CD163 and vimentin. Immunoreactivities to Iba-1 and lysozyme were variable. None or very few S100-positive tumor cells were observed (**Figs 3.18 – 3.19**). Furthermore, tumor cells were negative for CD208, unlike the original tumor. The IHC features are summarized in **Table 3.6**.

Metastasis assay

Metastatic lesions in the lung, hilar lymph nodes and abdominal cavity were grossly observed in 2 of 3 mice intravenously injected with PWC-HS01 cell line. The lesions were also detected in the brain, diaphragm, sternum and cardiac muscle microscopically. The tumor cells were round- to polygonal-shaped with indistinct borders. Most of the cells contained a lot of vacuoles of various sizes. The nuclei were round- to ovoid-shaped with 1 or 2 prominent nucleoli. Moderate atypia was observed. Atypical mitoses were notably found (>100 mitoses/10 hfp, 400X). Multinucleated giant cells were rare. Necrotic foci were scattered throughout the neoplastic tissues. Immunohistochemically, contrary to the original tumor, tumor cells at the metastatic lesions lacked the expression of S100, whereas immunoreactivities to HLA-DR, lysozyme and CD208 were variable. These metastatic tumors were consistently positive for Iba-1, CD204, CD163, lysozyme and vimentin as were the original tumor (**Fig. 3.20 and Table 3.6)**

On the other hand, metastatic masses in the skin were commonly observed in all the mice injected with FCR-HS02 cell. In addition, the lesions in the thoracic cavity as well as the abdominal cavity were detected. Histopathologically, the tumor cells were

round- to polygonal-shaped with light eosinophilic cytoplasm and indistinct borders. Most of the cells contained a lot of vacuoles. The nuclei were round- to ovoid-shaped with 1 or 2 prominent nucleoli. Marked anisocytosis and anisokarryosis were noted. Atypical mitoses were notably found (>100 mitoses/10 hfp, 400X). Bizarre mononuclear tumor cells were commonly found, whereas multinucleated giant tumor cells were rare. Multifocal necrosis were seen in all the mice. The tumor cells invading to the lung parenchyma as well as bone marrow were also observed in 1 mouse.

Contrary to the original tumors, all the metastatic tumors lacked the expression of S100 and CD208. The immunoreactivities to HLA-DR and lysozyme were variable. However, the metastatic tumors were positive for Iba-1, CD204 and CD163 (**Fig. 3.21 and Table 3.6**).

DISCUSSION

As mentioned before, there have been few publications demonstrating generated HS cell lines from dogs [8, 78, 95]. Herein, we report the establishment success of new HS cell lines, PWC-HS01 and FCR-HS02, which were derived from brain and synovial tumors, respectively. These cell lines can grow in both DMEM and RPMI1640 supplementing with different FBS concentrations. Cellular morphological and ultrastructural (only examined for PWC-HS01) characteristics of the cell lines were similar to those of normal histiocytes and other canine HS cell lines described previously [2, 8, 9, 38, 68, 95]. Cai *et al* [12] mentioned that during cell cultivation, morphological alteration (also known as cell dedifferentiation) are frequently observed. The cultured cells in the present study contained few organelles. Furthermore, the immunophenotypic changes may be found in case of long-term passage cultures [39].

The results of immunocytochemical examination revealed that PWC-HS01 cells were positive for HLA-DR, Iba-1 and CD204, similar to those of the original tumor, indicating histiocytic differentiation. Interestingly, the cells expressed both macrophage (CD204, CD163, iNOS, LZ, CD68 and CD11b) and DC (S100, CD1a, CD4, CD54 (weak), and CD273) markers. In addition, the RT-PCR results also showed the expression of both CD11b (macrophage marker) and CD11c (DC marker) mRNA [19, 32, 57, 60, 77, 88]. These findings may support the possibility that PWC-HS01 cells are the neural origin, and normally express both the macrophage and DC phenotypes that is aberrant in HS from other organ systems [57]. Moreover, the PWC-HS01 cells were intensely positive for iNOS and CD163, suggesting that primary HS with CNS involvement may in part possess the features of both the M1 and M2 macrophage differentiations in accordance with the results in Chapter 2. Unlike the PWC-HS01 cell line, FCR-HS02

cells were immunonegative for CD204 and CD68, whereas DC markers such as S100, CD208, CD1a, CD54, CD273 and CD4 were consistently positive. These observations may support that the extraneural FCR-HS02 cell line has the DC phenotype [46], which is consistent with the characteristics of HS derived from the extraneural organs described previously [32, 41, 51, 57]. However, FCR-HS02 cells also expressed lysozyme. This aberrant phenomenon indicates that cell dedifferentiation has occurred in the cell line, resulting in a variety of histiocytic molecular expression [39, 46]. No CD204 band was detected in FCR-HS02 cell lysates by Western blot analysis, which was associated with the very low expression of CD204 mRNA by RT-PCR. Moreover, the expression of CD11b (low intensity band) and CD11c (high intensity band) mRNA were also detected. These results strongly support the DC phenotype of the FCR-HS02 cell line [34].

Modal chromosome aberration was detected in the current study. Both of HS cell lines exhibited hypoploidy as reported in previous literatures [9, 35]. Based on cell-sized, number of organelles (by transmission electron microscope) and the expression patterns of markers for DC, macrophage, and hematopoietic stem and progenitor cells in both established cell lines, the term of cell dedifferentiation has been used. Interestingly, although these cells revert into the progenitors, high phagocytic capability was detected. In accordance with the phagocytosis ability, Golovkina *et al* [33] have illustrated that the presence of high FBS in the cell culture medium leads to low phagocytic activity of cells. Furthermore, high cell culture density also affects the phagocytosis of macrophages [93]. These observation suggests that a low cell density as well as serum-free medium used in the present study can stimulate the phagocytic activity of both PWC-HS1 and FCR-HS02 cell lines.

In the xenotransplanted mice, all the tumor masses were confined to the dermis and/or subcutaneous tissues. Spontaneous metastases to distant organs were not detected grossly and microscopically. These findings suggest that a certain surrounding microenvironment is relevant for tumor escape from the primary injected sites [73, 84]. To access the metastatic activity, suspended cells were intravenously introduced into immunodeficient mice. Gross as well as microscopic metastatic lesions were observed in the skin, lung, diaphragm, sternum, cardiac muscle, abdominal cavity, bone marrow and brain. However, other visceral organs such as the spleen and liver were not affected. These observations suggest that metastatic capacity of established HS cells may generate tumor in almost all organs of SCID mice.

Variable (negative to strongly positive) immunoreaction to HLA-DR, Iba-1, lysozyme, S100 and CD208 were observed in both xenotransplanted and metastatic tumor cells, whereas cultured PWC-HS01 and FCR-HS02 cells prior to injection exhibited all the markers used steadily. Interestingly, both established cell lines also expressed CD34, whereas those of *in vivo* were negative (data not shown). Moreover, despite all the HS cells of *in vivo* and original tumors were consistently express CD204, those of FCR-HS02 *in vitro* showed negative for this molecule. These observations strongly support that the original HS may revert into their progenitors (dedifferentiation) by the cell cultivation [12, 100]. Moreover, the cultured tumor cells may redifferentiate into another cell phenotype through *in vivo* proliferation.

Table 3.1 Primary antibodies used in immunocytochemical examination

Antibody [a]	Type [b]	Dilution [c]	Cellular expression	Source
HLA-DR	Mouse, mAb (TAL.1B5)	1:50	Cell membrane	Santa Cruz, CA, USA
Iba-1	Rabbit, pAb	1:250	Cytoplasm	Wako, Osaka, Japan
CD204	Mouse, mAb (SRA-E5)	1:50	Cell membrane	TransGenic, Kobe, Japan
CD163	Mouse, mAb (AM-3K)	1:50	Cell membrane	TransGenic, Kobe, Japan
iNOS	Rabbit, pAb	1:50	Cytoplasm/Nucleus	Abcam, Tokyo, Japan
Lysozyme	Rabbit, pAb	1:1000	Cytoplasm	Dako, Glostrup, Denmark
S100	Rabbit, pAb	1:1000	Cytoplasm/Nucleus	Dako, Tokyo, Japan
CD208 (DC-LAMP)	Rat, mAb (1010E1.01)	1:50	Cytoplasm	Dendritics, Lyon, France
Myeloid/Histiocyte antigen	Mouse, mAb (MAC387)	1:250	Cytoplasm	Dako, Glostrup, Denmark
CD1a	Mouse, mAb (010)	RTU	Cell membrane	Dako, Tokyo, Japan
CD11b	Mouse, mAb (M1/70.15)	1:50	Cell membrane	Cedarlane, NC, USA
CD54	Mouse, mAb (1A29)	1:25	Cell membrane	BD Pharmingen, CA, USA
CD68	Mouse, mAb (PG-M1)	RTU	Cell membrane	Dako, Tokyo, Japan
CD273	Rat, mAb (XX19)	1:25	Cell membrane	Santa Cruz, CA, USA
CD34	Goat, pAb (C-18)	1:80	Cell membrane	Santa Cruz, CA, USA
CD4	Mouse, mAb (10B5)	1:20	Cell membrane	GeneTex, CA, USA
Cytokeratin	Mouse, mAb (AE1/AE3)	RTU	Cytoplasm	Dako, Tokyo, Japan
Vimentin	Mouse, mAb (V9)	1:200	Cytoplasm	Dako, Tokyo, Japan
Ki67	Mouse, mAb (MIB-1)	RTU	Nucleus	Dako, Glostrup, Denmark

[a] HLA-DR = Human leukocyte antigen-DR; Iba-1 = Ionized calcium-binding adapter molecule-1; CD = Cluster of differentiation; iNOS = Inducible nitric oxide synthase; DC-LAMP = Dendritic cell lysosome-associated membrane glycoprotein.

[b] pAb = Polyclonal antibody; mAb = Monoclonal antibody. [c] RTU = Ready-to-use.

Table 3.2 Primer sequences

Target gene [a]	Sequence	Amplicon size (bp)	Tm (^{0}C) [b]	Genbank No.
CD11b	*Forward* 5'-GAGTCTGACGATTCCACTAATG-3'	60	60	XM843434
	Reverse 5'-GTTTATGCTGCAGCTGCTA-3'			
CD11c	*Forward* 5'-GTGCTGGATTTGGACACAGCGTG-3'	154	52	XM547049
	Reverse 5'-AAGGGGACCTGCAGTTGGATGG-3'			
CD204	*Forward* 5'-CAGGAAATCCTGGACCAAAA-3'	164	60	XP_005629987.1
	Reverse 5'-TTCCCAGTGGTCATCACAAA-3'			
GAPDH	*Forward* 5'-TGTCCCCACCCCCAATGTATC-3'	100	52	NM001003142
	Reverse 5'-CTCCGATGCCTGCTTCACTACCTT-3'			

[a] CD = Cluster of differentiation; GAPDH = Glyceraldehyde-3-phosphate dehydrogenase. [b] Tm = Melting temperature.

Table 3.3 The influence of culture conditions on the growth ability of PWC-HS01 and

FCR-HS02cell lines

Culture condition [a]	Growth ability [b]	
	PWC-HS01	FCR-HS02
DMEM + 5% FBS	+	+
DMEM + 10% FBS	+	+
DMEM + 15% FBS	+	+
DMEM + 20% FBS	+	+
RPMI 1640 + 5% FBS	+	+
RPMI 1640 + 10% FBS	+	+
RPMI 1640 + 15% FBS	+	+
RPMI 1640 + 20% FBS	+	+

[a] DMEM = Dulbecco's modified eagle medium; FBS = Fetal bovine serum; RPMI = Roswell Park Memorial Institute.
[b] + = The tumor cell can grow in this culture condition; - = The tumor cell cannot grow in this culture condition.

Table 3.4 Immunocytochemical and biological characteristics of HS cell lines

Parameter [a]	HS cell line [b]	
	PWC-HS01	FCR-HS02
Population doubling time (hours)	64.80	56.50
Marker		
HLA-DR	+	+
Iba-1	+	+
CD204	+	-
CD163	+	+
Lysozyme	+	+
S100	+	+
CD208 (DC-LAMP)	+	+
CD1a	+	+
CD11b	+	+w
CD54	+w	+
CD68	+	-
CD273	+	+
Myeloid/Histiocyte antigen	-	-
CD34	+	+
CD4	+	+
Cytokeratin	-	-
Vimentin	+	+
Ki67-proliferative index	91.78%	49.79%
Chromosomal number	63 – 88	42 – 49
Phagocytosis	Presence	Presence
Tumorigenicity	Presence	Presence
Metastasis	Presence	Presence

[a] HLA-DR = Human leukocyte antigen-DR; Iba-1 = Ionized calcium-binding adapter molecule-1; CD = Cluster of differentiation; DC-LAMP = Dendritic cell lysosome-associated membrane glycoprotein.

[b] + = Antibody immunoreactivity was presented by established HS cells;

  - = Antibody immunoreactivity was not presented by established HS cells; w = Weak immunoreaction.

Table 3.5 Primary antibodies used in immunohistochemical examination

Antibody [a]	Type [b]	Dilution [c]	Antigen retrieval for IHC [d]	Expression	Source
HLA-DR	Mouse, mAb (TAL.1B5)	1:50	Citrate buffer, pH 6.0 (HIER), 121°C, 10 min	Antigen presenting cell	Santa Cruz, CA, USA
Iba-1	Rabbit, pAb	1:250	Citrate buffer, pH 6.0 (HIER), 121°C, 10 min	Histiocyte, macrophage	Wako, Osaka, Japan
CD204	Mouse, mAb (SRA-E5)	1:100	Tris/EDTA buffer pH 9.0 (HIER), 121°C, 10 min	Monocyte, macrophage	TransGenic, Kobe, Japan
CD163	Mouse, mAb (AM-3K)	1:100	Citrate buffer, pH 2.0 (HIER), 121°C, 10 min	Histiocyte	TransGenic, Kobe, Japan
Lysozyme	Rabbit, pAb	1:100	Proteinase K (PIER), room temperature, 30 min	Monocyte, macrophage	Dako, Glostrup, Denmark
S100	Rabbit, pAb	1:1000	Citrate buffer, pH 6.0 (HIER), 121°C, 10 min	Dendritic cell	Dako, Tokyo, Japan
CD208 (DC-LAMP)	Rat, mAb (1010E1.01)	1:100	Citrate buffer, pH 6.0 (HIER), 121°C, 10 min	Dendritic cell	Dendritics, Lyon, France
Myeloid/Histiocyte antigen	Mouse, mAb (MAC387)	1:250	Proteinase K (PIER), room temperature, 30 min	Histiocyte, macrophage	Dako, Glostrup, Denmark
CD3	Rabbit, pAb	RTU	Tris/EDTA buffer pH 9.0 (HIER), 121°C, 10 min	T-lymphocyte	Dako, Tokyo, Japan
CD20	Rabbit, pAb	1:400	None	B-lymphocyte	Thermo scientific, CA, USA
Lambda light chain	Rabbit, pAb	1:50000	Citraconic anhydrate, Immunosaver® (HIER), 98°C, 45 min	Plasma cell	Dako, Glostrup, Denmark
Kappa light chain	Rabbit, pAb	1:10000	Citraconic anhydrate, Immunosaver® (HIER), 98°C, 45 min	Plasma cell	Dako, Glostrup, Denmark
Cytokeratin	Mouse, mAb (AE1/AE3)	RTU	Citrate buffer, pH 6.0 (HIER), 121°C, 10 min	Epithelial cell	Dako, Tokyo, Japan
Vimentin	Mouse, mAb (V9)	1:200	Citrate buffer, pH 6.0 (HIER), 121°C, 10 min	Mesenchymal cell	Dako, Tokyo, Japan

[a] HLA-DR = Human leukocyte antigen-DR; Iba-1 = Ionized calcium-binding adapter molecule-1; CD = Cluster of differentiation; DC-LAMP = Dendritic cell lysosome-associated membrane glycoprotein.
[b] pAb = Polyclonal antibody; mAb = Monoclonal antibody. [c] RTU = Ready-to-use. [d] HIER = Heat-induced epitope retrieval; PIER = Proteolytic-induced epitope retrieval.

Table 3.6 The comparison of immunohistochemical results of primary, xenotransplanted and metastatic tumors

Sample		IHC markers [a]													
		HLA-DR	Iba-1	CD204	CD163	LZ	S100	CD208	MAC387	CD3	CD20	λ	κ	CK	Vimentin
Original tumor	PWC-HS01	+	+	+	+	+	+	+	-	-	-	-	-	-	+
	FCR-HS02	+	+	+	+	+	+	+	-	-	-	-	-	-	+
Xenotransplanted tumor	PWC-HS01	+	+	+	+	+	- to +	-	-	-	-	-	-	-	+
	FCR-HS02	+	+	+w	+	- to +w	-	-	-	-	-	-	-	-	+
Metastatic tumor	PWC-HS01	+f	+	+	+	- to +w	-	- to +w	-	-	-	-	-	-	+
	FCR-HS02	+f	+f	+w	+	- to +w	-	-	-	-	-	-	-	-	+

[a] HLA-DR = Human leukocyte antigen-DR; Iba-1 = Ionized calcium-binding adapter molecule-1; CD = Cluster of differentiation; LZ = Lysozyme; λ = Lambda light chain; κ = Kappa light chain
CK = Cytokeratin AE1/AE3; Immunohistochemical scoring: - = Negative; + = Positive; f = Focal; w = Weak.
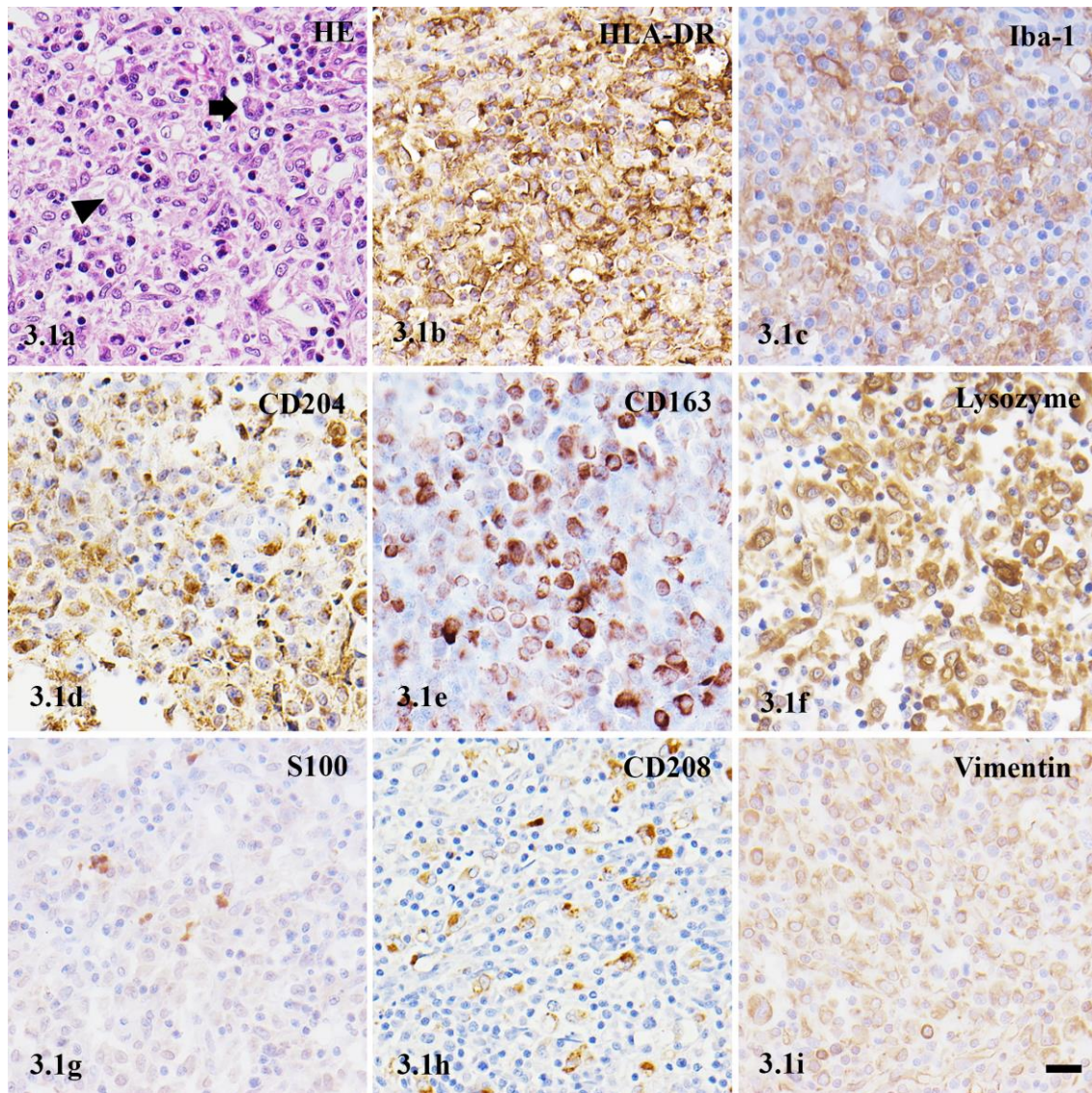
Figure 3.1. Histiocytic sarcoma. Cerebrum. Dog. PWC-HS01. The tumor contains numerous neoplastic histiocytes that are round- to polygonal-shaped with eosinophilic cytoplasm. Some of them contain large vacuole (arrowhead). Multinucleated tumor giant cells are occasionally observed (arrow). Moderate numbers of small lymphocytes admixing with tumor cell population are noted. HE (a). These cells are immunopositive for HLA-DR (b), Iba-1 (c), D204 (d), CD163 (e), lysozyme (f), S100 (g), CD208 (h) and vimentin (i). IHC. Hematoxylin counterstain. Scale bar = 20 μm.
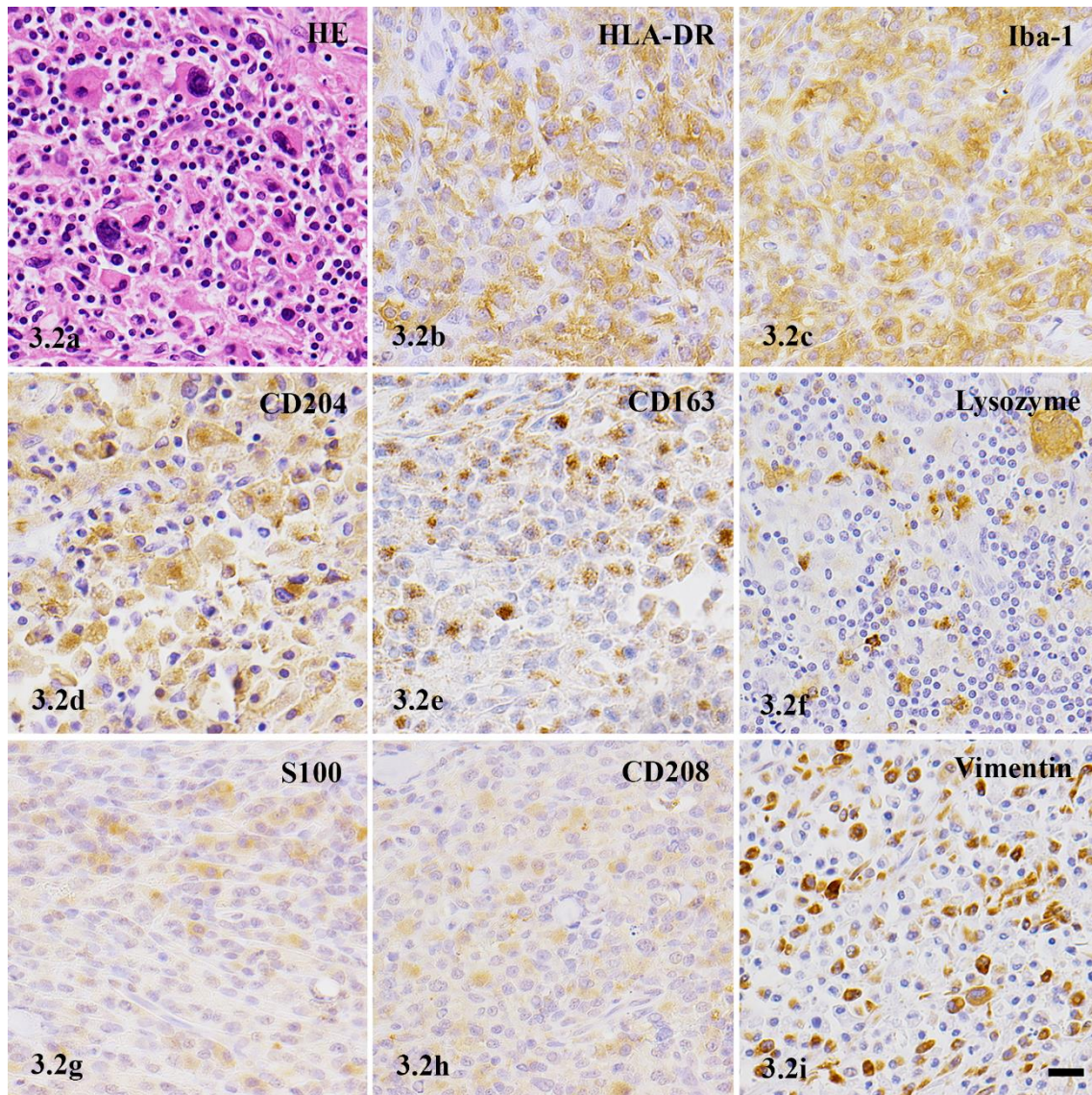
Figure 3.2. Histiocytic sarcoma. Right shoulder. Dog. FCR-HS02. The tumor cells are round- to polygonal-shaped with various sizes. Hemophagocytosis is occasionally observed. HE (a). These cells are immunopositive for HLA-DR (b), Iba-1 (c), CD204 (d), CD163 (e), S100 (g), CD208 (h) and vimentin (i). Variable immunoreaction for lysozyme is observed (f). IHC. Hematoxylin counterstain. Scale bar = 20 μm.

3.3
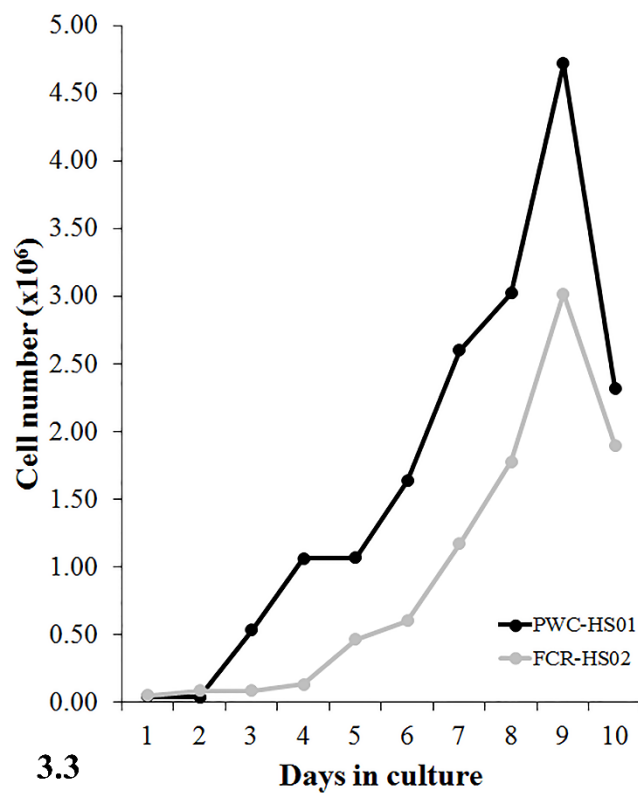
Figure 3.3. The growth curve of new canine histiocytic sarcoma cell lines in DMEM supplemented with 10%FBS. The population doubling time of PWC-HS01 and FCR-HS02 cell lines are approximately 64.8 and 56.5 hours, respectively.
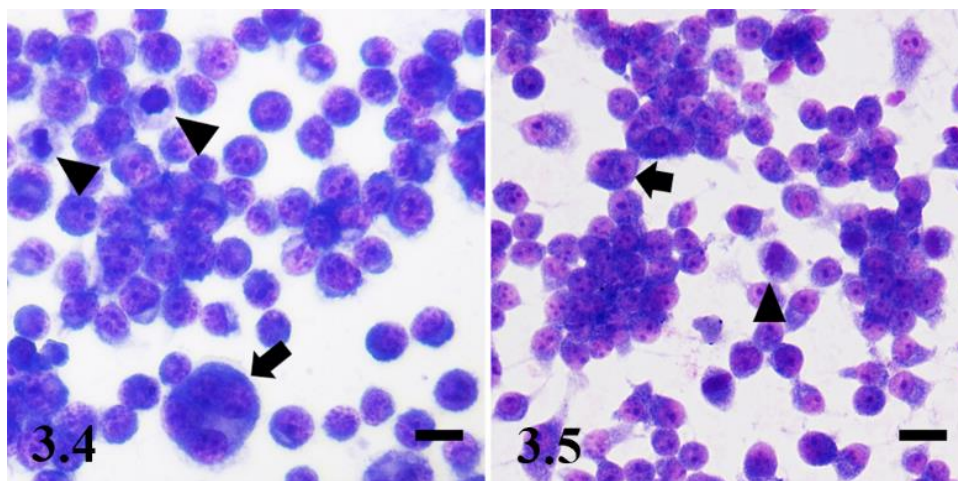
Figure 3.4. Histiocytic sarcoma. Dog. Morphological appearances of PWC-HS01 cells. The HS cell are round-shaped with various sizes. Atypical mitoses are observed (arrowheads). Furthermore, multinucleated cells are occasionally found (arrow). Giemsa stain. Scale bar = 20 μm.

Figure 3.5. Histiocytic sarcoma. Dog. Morphological appearances of FCR-HS02 cells. The cells usually proliferate clumping in culture. Most of the HS cells are round-shaped. Pseudopodia are commonly seen in this cell line. Atypical mitoses are observed (arrowhead). Furthermore, binucleated cells are occasionally found (arrow). Giemsa stain. Scale bar = 20 μm.
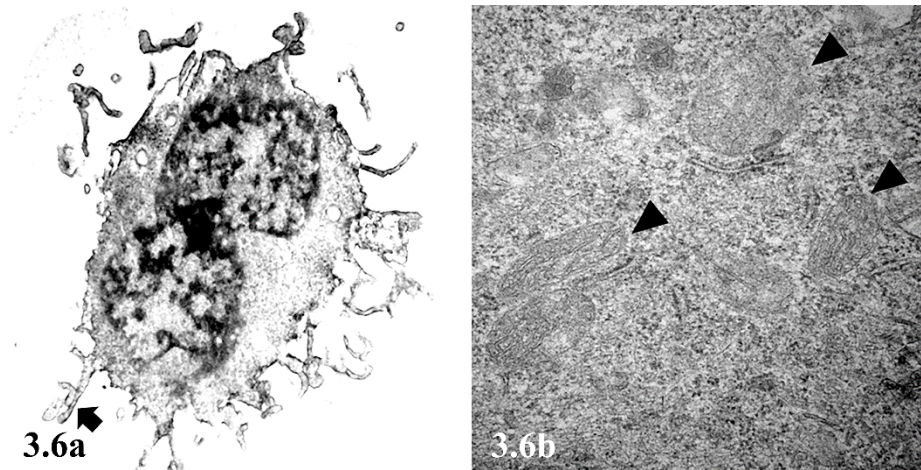
Figure 3.6. Histiocytic sarcoma. Dog. Ultrastructural morphology of PWC-HS01 cells. Cellular processes are commonly observed on the cell surface (arrows). The nucleus is lobulated. In high magnification (b), moderate numbers of mitochondria (arrowheads) are observed. Uranyl acetate/lead citrate. x15000 (a). x60000 (b). Transmission electron microscope.
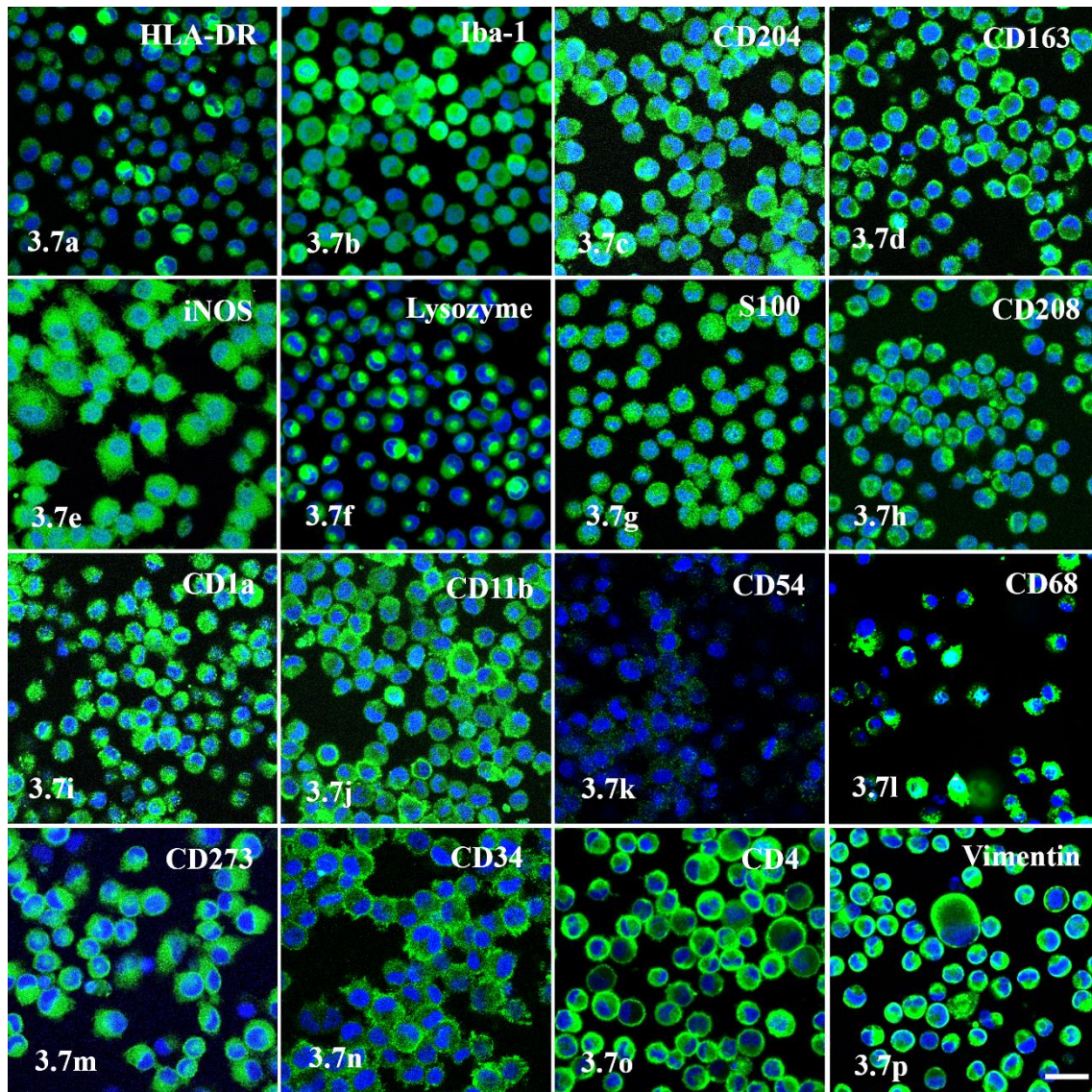
Figure 3.7. Histiocytic sarcoma. Dog. PWC-HS01 cell line. The tumor cells consistently express HLA-DR (a), Iba-1 (b), CD204 (c), CD163 (d), iNOS (e), lysozyme (f), S100 (g), CD208 (h), CD1a (i), CD11b (j), CD68 (l), CD273 (m), CD34 (n), CD4 (o) and vimentin (p). Variable and weak CD54 (k) expression is noted. Immunocytochemistry. DAPI counterstained. Scale bar = 20 μm.
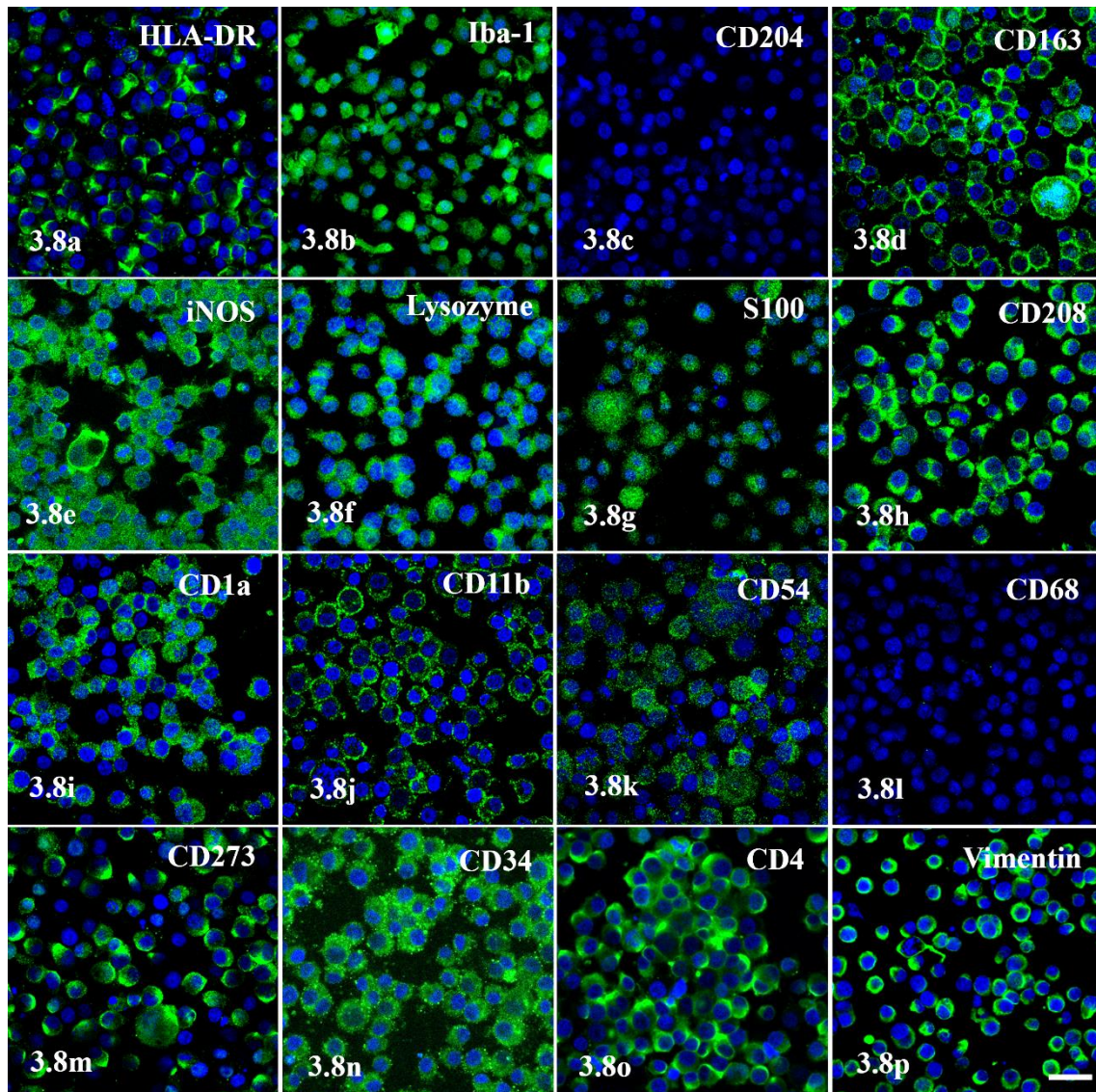
Figure 3.8. Histiocytic sarcoma. Dog. FCR-HS02 cell line. The tumor cells consistently express HLA-DR (a), Iba-1 (b), CD163 (d), iNOS (e), lysozyme (f), S100 (g), CD208 (h), CD1a (i), CD11b (j), CD54 (k), CD273 (m), CD34 (n), CD4 (o) and vimentin (p). These cells, conversely, are negative for CD204 (c) and CD68 (l). Immunocytochemistry. DAPI counterstained. Scale bar = 20 μm.
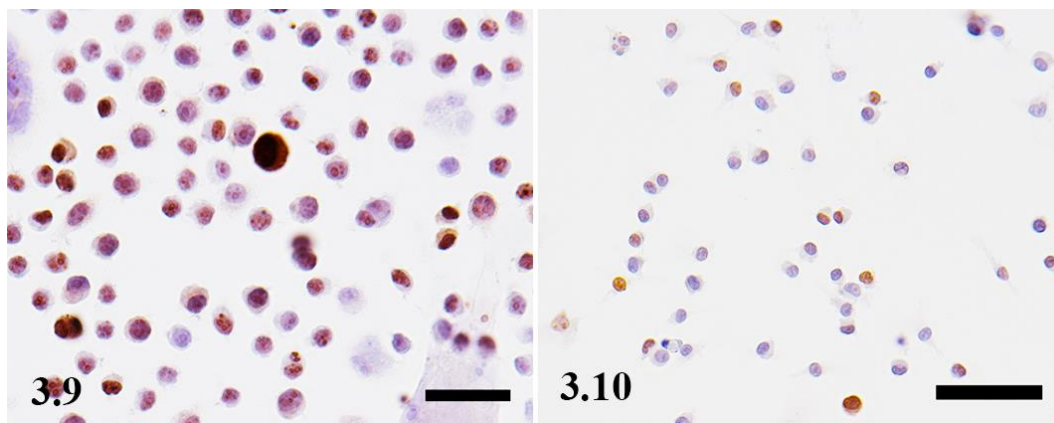
Figure 3.9. Histiocytic sarcoma. Dog. PWC-HS01 cell line. Ki67-proliferative index is 91.78%. Immunocytochemistry. Hematoxylin counterstain. Scale bar = 50 μm.

Figure 3.10. Histiocytic sarcoma. Dog. FCR-HS02 cell line. Ki67-proliferative index is 49.79%. Immunocytochemistry. Hematoxylin counterstain. Scale bar = 50 μm.
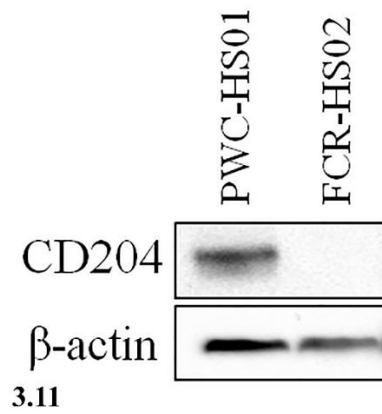
Figure 3.11. Protein expression of CD204 in PWC-HS01 and FCR-HS02 cells is analyzed by Western blot. β-actin is used a loading control. The western blot reveals CD204 band is only detected in PWC-HS01 cells.

3.12
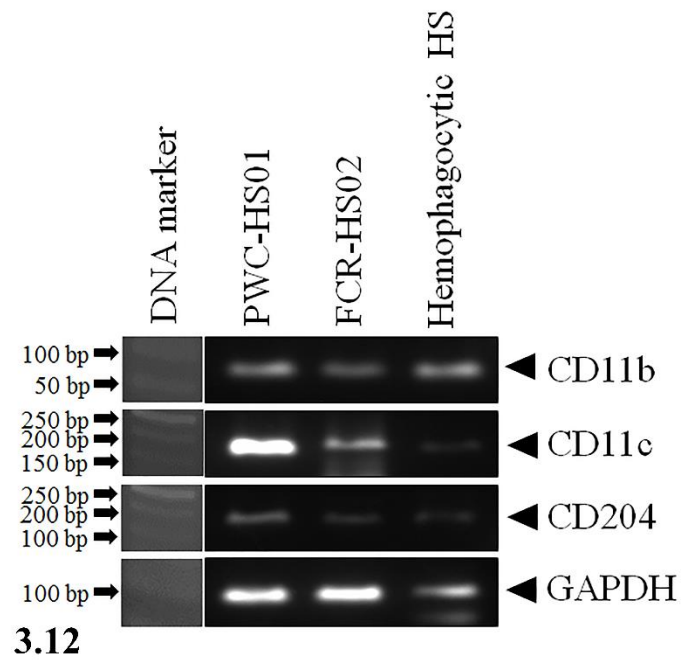
Figure 3.12. RT-PCR study demonstrates the presence of CD11b mRNA in both established HS cell lines. Strong and moderate expression of CD11c mRNA is detected in PWC-HS01 and FCR-HS02 cells, respectively. In addition, low expression of CD204 mRNA is observed in FCR-HS02 cell line and hemophagocytic HS tissue. GAPDH is used as the internal control.
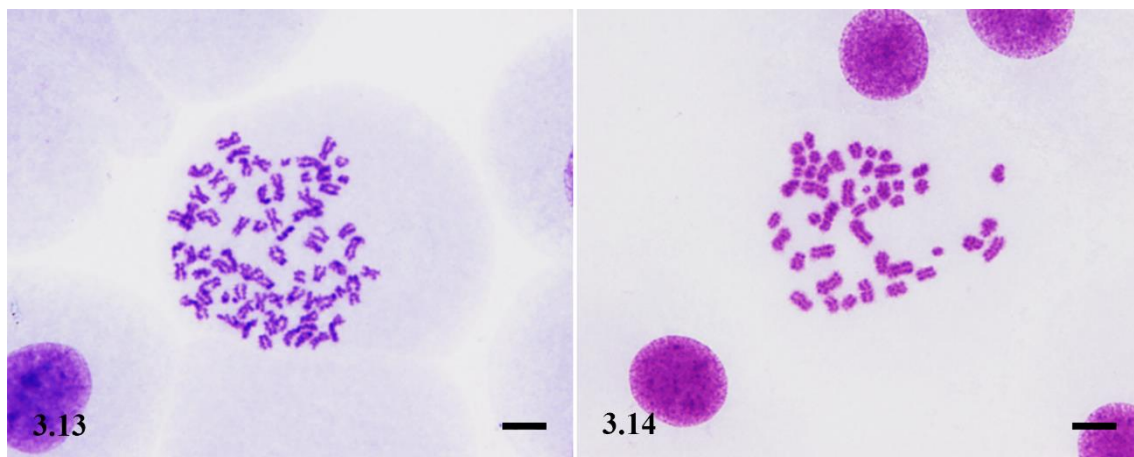
Figure 3.13. Histiocytic sarcoma. Dog. PWC-HS01 cells. Modal chromosome numbers of PWC-HS01 cells are 63 − 88. Chromosome analysis. Scale bar = 10 μm.

Figure 3.14. Histiocytic sarcoma. Dog. FCR-HS02 cells. Modal chromosome numbers of FCR-HS02 cells are 42 − 49. Chromosome analysis. Scale bar = 10 μm.
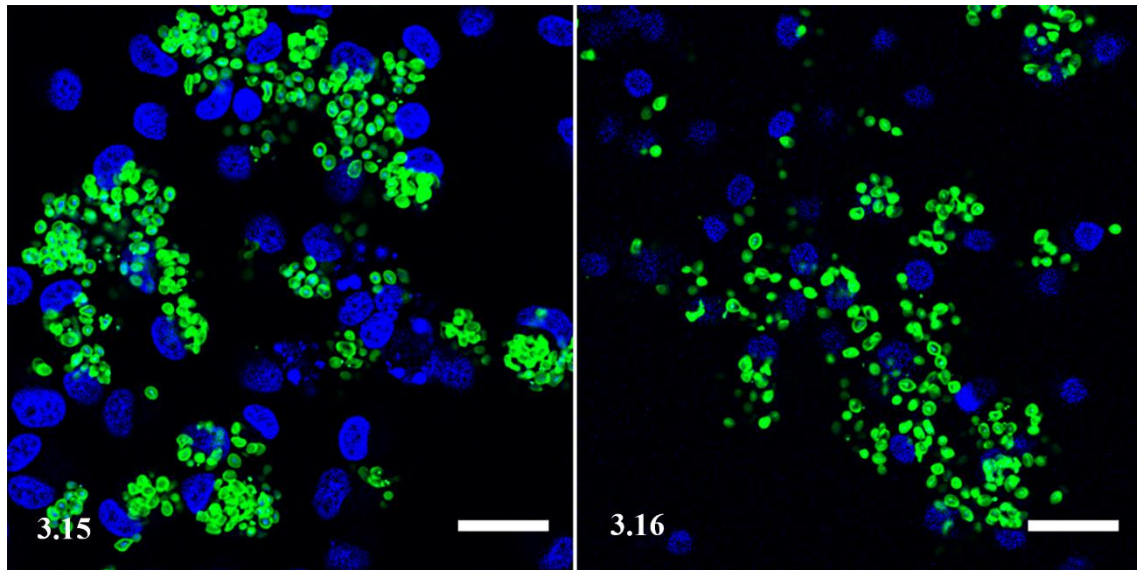
Figure 3.15. Histiocytic sarcoma. Dog. PWC-HS01 cells. Fluorescent particles are phagocytized by PWC-HS01 cells. Phagocytosis assay. DAPI counterstained. Scale bar = 20 μm.

Figure 3.16. Histiocytic sarcoma. Dog. FCR-HS02 cells. Fluorescent particles are phagocytized by FCR-HS02 cells. Phagocytosis assay. DAPI counterstained. Scale bar = 20 μm.
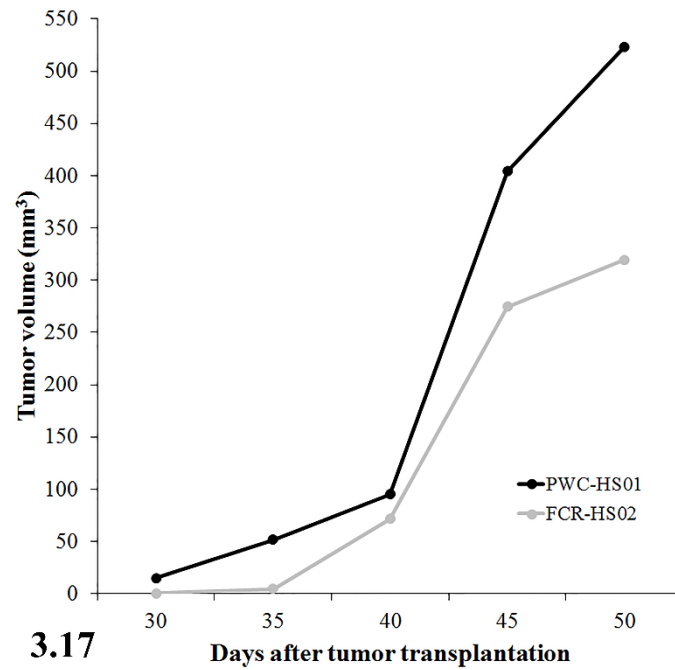
Figure 3.17. The tumor sized of xenotransplanted mice injected with PWC-HS01 and FCR-HS02 cells. One month after tumor inoculation, the masses are grossly observed in all mice. Tumorigenicity assay.
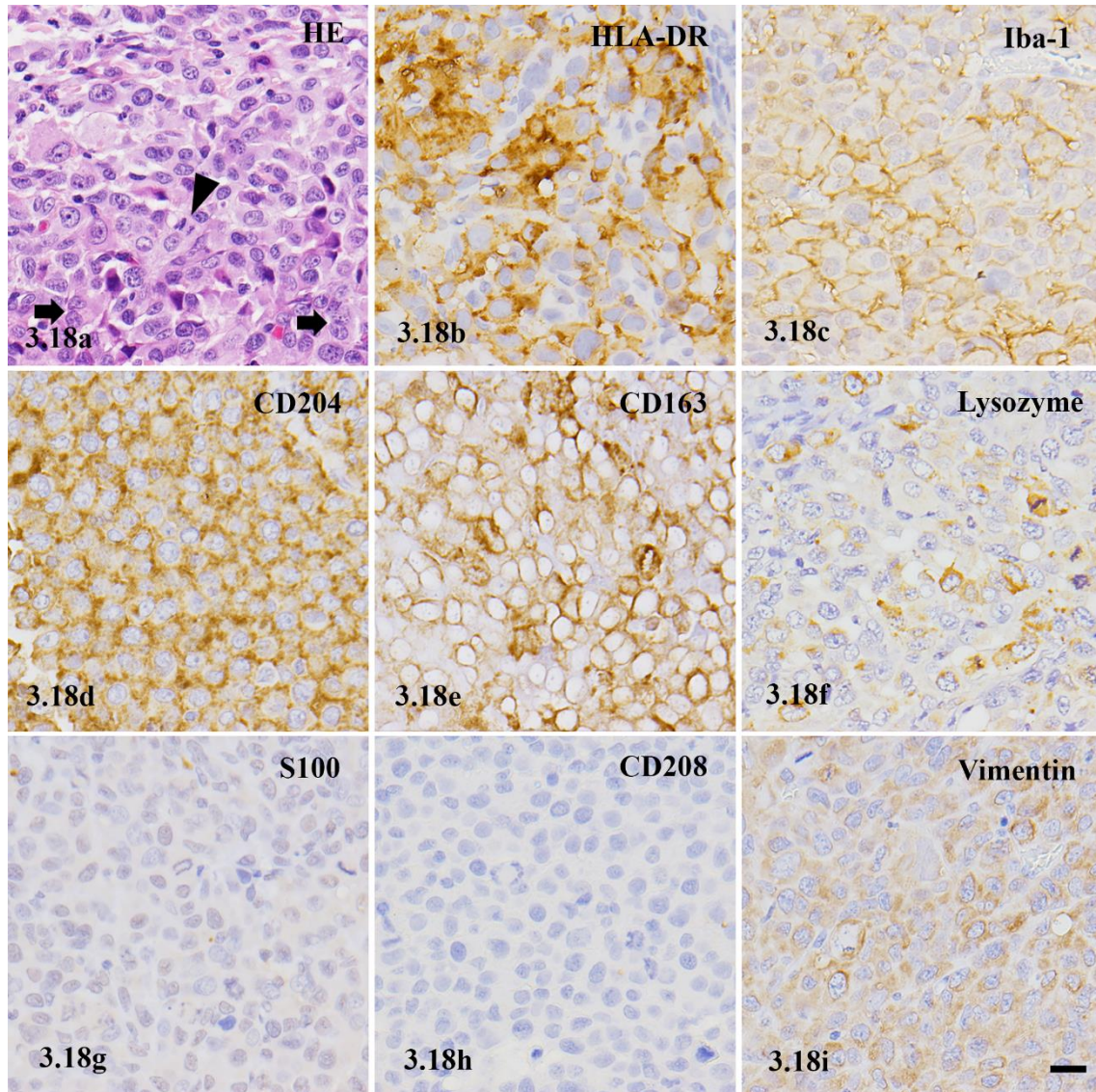
Figure 3.18. Xenotransplanted tumor (PWC-HS01). SCID mouse. Neoplastic histiocytes invade to the dermis and subcutis. These cells are round- to polygonal-shaped with light eosinophilic cytoplasm and various sizes. Binucleated tumor cells are occasionally observed (arrows). Mitotic figure is also found (arrowhead). The tumor cells are immunopositive for HLA-DR (b), Iba-1 (c), CD204 (d), CD163 (e), lysozyme (f), S100 (g) and vimentin (i), but negative for CD208 (h). HE (a). IHC (b – i). Hematoxylin counterstain. Scale bar = 20 μm.
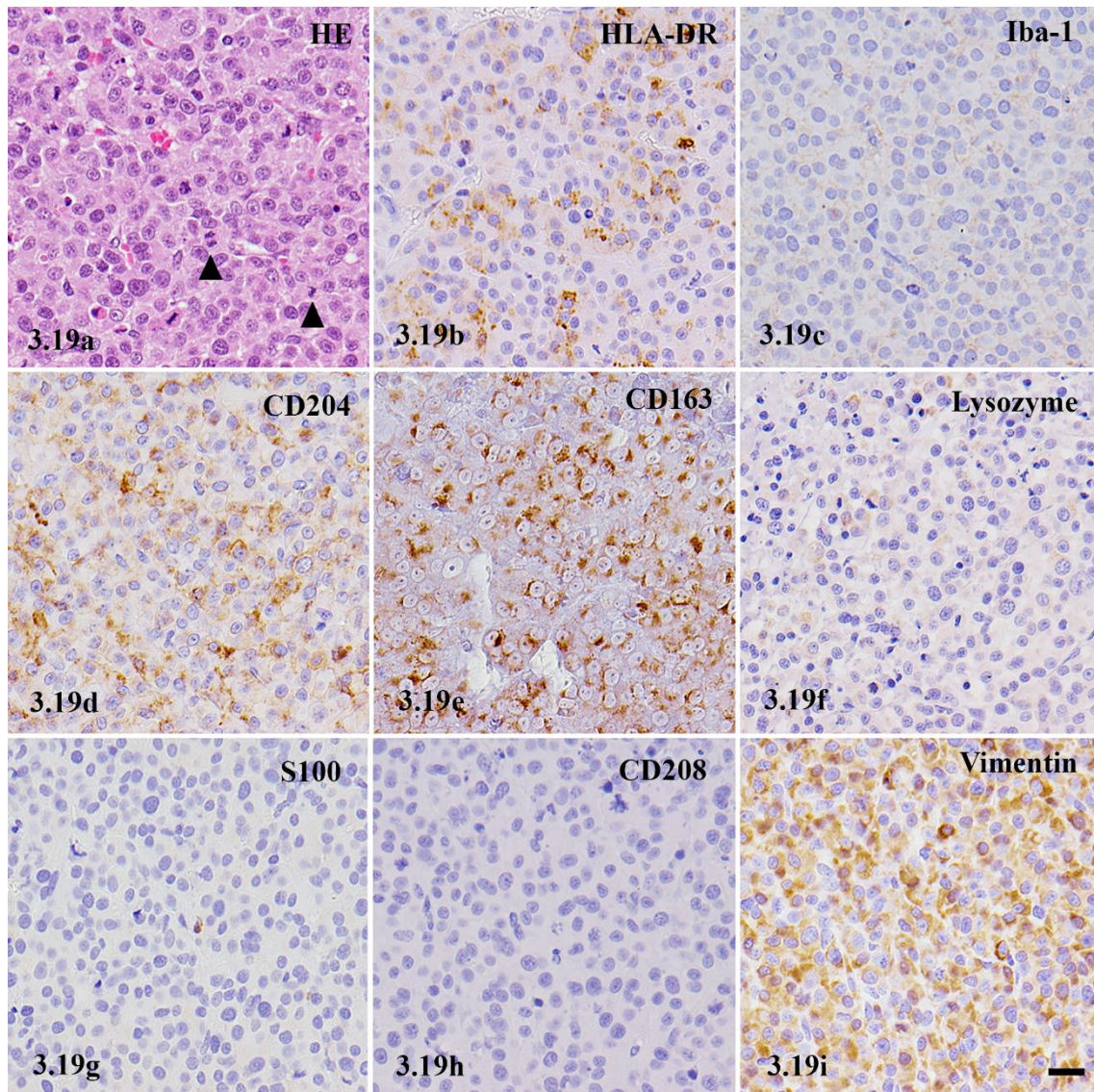
Figure 3.19. Xenotransplanted tumor (FCR-HS02). SCID mouse. Tumor cells are round-to polygonal-shaped with light eosinophilic cytoplasm. Cytoplasmic vacuolation was notably observed. Atypical mitoses are frequently found (arrowheads). HE (a). These cells are immunopositive for HLA-DR (b), CD204 (d), CD163 (e) and vimentin (i). Weakly immunostaining for Iba-1 (c) and lysozyme (f) are noted. However, the tumor cells lack the expression of S100 (g) and CD208 (h). IHC. Hematoxylin counterstain. Scale bar = 20 μm.
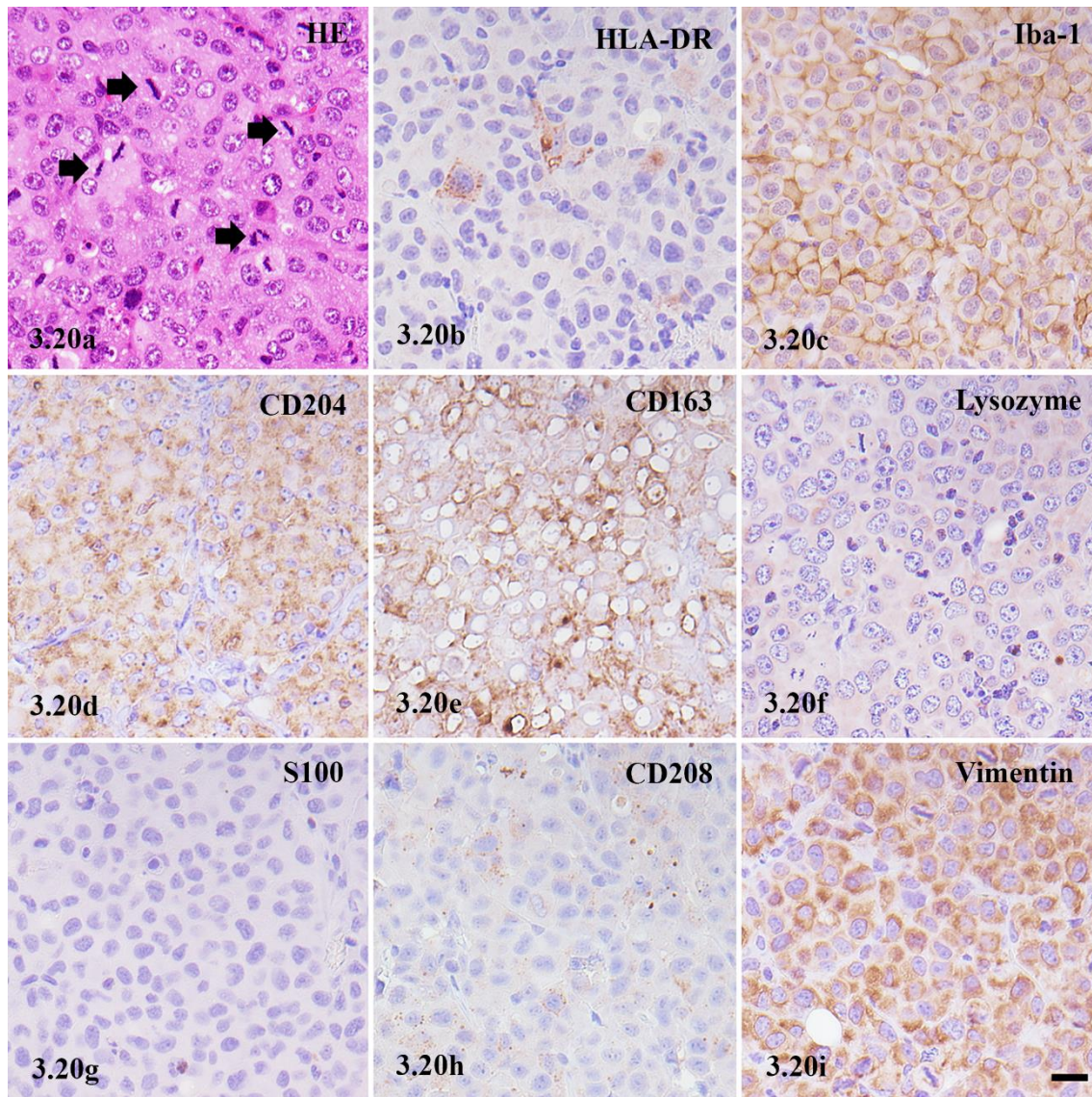
Figure 3.20. Metastatic lesions of SCID mouse injected with PWC-HS01 cells. Thoracic mass. The mass contained numerous neoplastic histiocytes. Atypical mitoses are notably observed (arrows). Cytoplasmic vacuolation is commonly found. HE (a). These cells are immunopositive for HLA-DR (b), Iba-1 (c), CD204 (d), CD163 (e), lysozyme (f), CD208 (h) and vimentin (i), but negative for S100 (g). IHC. Hematoxylin counterstain. Scale bar = 20 μm.
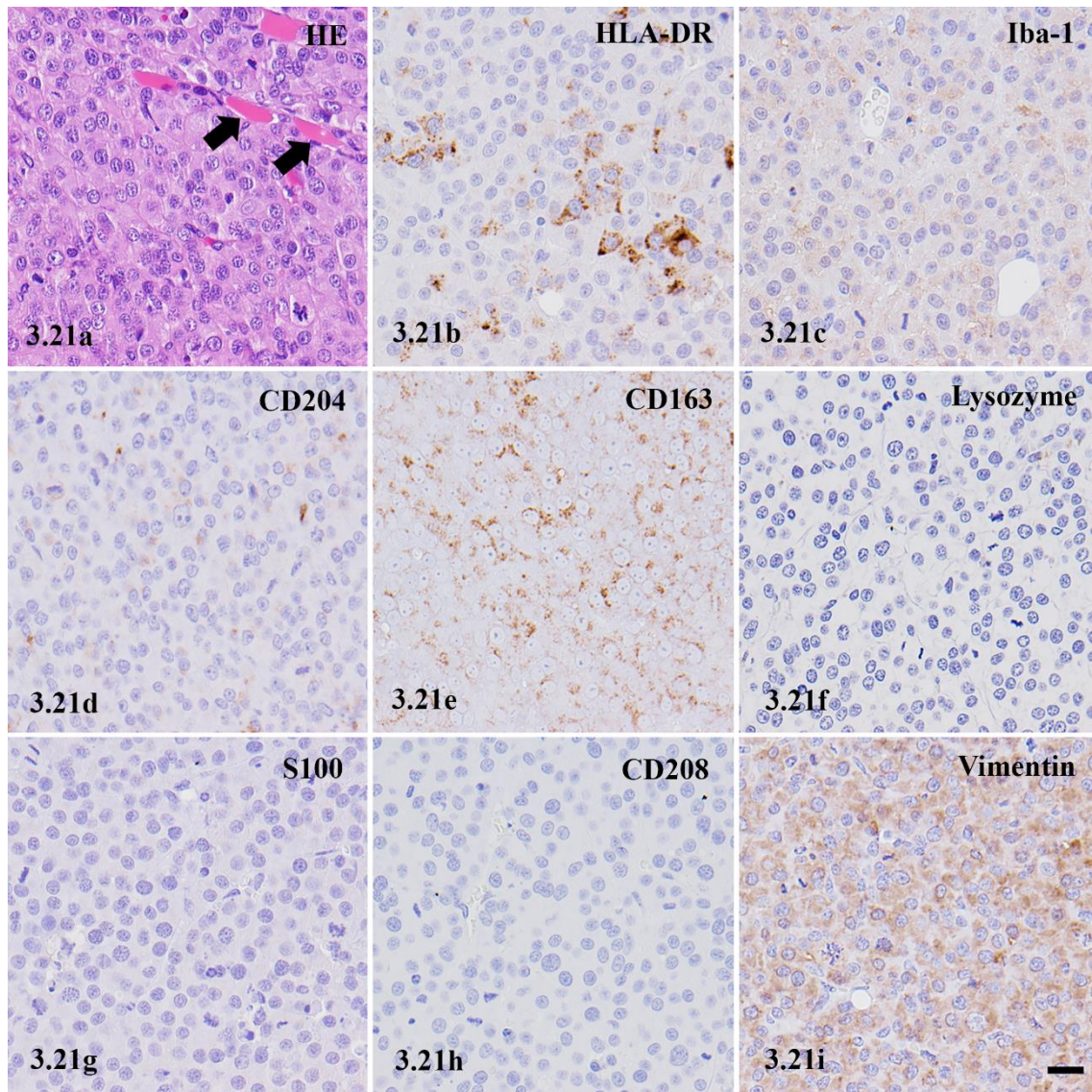
Figure 3.21. Metastatic lesions of SCID mouse injected with FCR-HS02 cells. Skin mass. SCID mouse. Neoplastic histiocytes invade to underlying muscular layer of skin. These cells arrange in solid pattern. Atypical mitoses are found. Muscular fiber degeneration (arrows) are noted within the lesion. HE (a). The tumor cells are immunopositive for HLA-DR (b), Iba-1 (c), CD204 (d), CD163 (e) and vimentin (i), but negative for lysozyme (f), S100 (g) and CD208 (h). IHC. Hematoxylin counterstain. Scale bar = 20 μm.

GENERAL CONCLUSIONS

Histiocytic sarcoma (HS) is a fatal aggressive hematopoietic tumor with a worse prognosis. This tumor is problematic not only in human, but also in various animal species, particularly in domestic animals. The pathological diagnosis of HS is often challenging due to its morphology closely resembling other hematopoietic tumors (i.e. anaplastic plasmacytoma and anaplastic large cell lymphoma), malignant melanoma and undifferentiated carcinoma. Immunohistochemical (IHC) confirmation, therefore, is necessary to identify cell origins.

In this thesis, conventional diagnostic markers, which are available for formalin-fixed, paraffin-embedded tissues were employed. In addition, the expression pattern of dendritic cell-lysozyme associated membrane protein (DC-LAMP or CD208) and inducible nitric oxide synthase (iNOS), the markers for DC and macrophage, respectively, were also examined. And the aims of this study are 1) to describe the comparative pathological features of canine HS derived from neural and extraneural origins, 2) to unveil histological and IHC characteristics of primary canine HS in the CNS, and 3) to comparatively elucidate biological, morphological and immunophenotypic features of 2 newly established HS cell lines isolated from brain and synovial tumors, respectively. Herein, *in vivo* model, tumorigenicity and metastasis assays, are also illustrated.

In Chapter 1, canine HS cases were categorized into HS deriving from neural and extraneural origins in order to compare morphological and IHC features between the two primary sites. Clinicopathological findings revealed the Pembroke Welsh corgi and Flat coated retriever were high risk breeds for HS with the central nervous system (CNS) and non-CNS involvement, respectively, suggesting that a genetic factor may contribute to the HS development in HS. The clinical signs varies depending upon types and the numbers of primary and/or distant organ involvement. Localized HS might be the main

distribution pattern of intracranial HS in the dog. This findings also reflects the possibility that the occurrence of distant metastasis on brain tumor is an unusual event. Considering the IHC expression patterns, the HS cells from the CNS tend to exhibit the macrophage phenotype, whereas those from other organ possesses dendritic cell differentiation. Although histopathological and IHC features were not different in the 2 primary organs, the mitotic index of HS in the CNS was significantly higher than that of the other. These observations support the fact that canine HS cases with CNS involved is relatively more aggressive than those of other organ involvement.

In Chapter 2, clinicopathological and pathological appearances of HS cases in the CNS were described in details. The cerebrum is a common primary site for HS in the brain, especially the frontal and temporal lobes. Seizure is the major clinical signs in almost all the affected dogs. The HS cell morphologies were histologically classified into 1) round/polygonal and 2) spindle cell types. Furthermore, hemophagocytosis was observed more frequently in the former than in the latter, and intracranial HS with round/polygonal cell type was more aggressive than the other. However, the difference of tumor morphology cannot be used alone for predicting the severity of HS with CNS involvement. Interestingly, the result of the IHC showed that HS cells exhibited both DC and macrophage phenotypes, and moreover, both macrophage subtypes (M1 and M2 phenotypes). These findings suggest that variable differentiation stage of the tumor cells.

In Chapter 3, two novel canine HS cell lines (PWC-HS01 and FCR-HS02) isolated from brain and synovial tumors, respectively, were established. The population doubling time of PWC-HS01 and FCR-HS02 was approximately 64.8 and 56.5 hours, respectively. Microscopically, both cultured HS cells were small round- to polygonal-shaped with the abundant cytoplasm. Their nuclei were eccentrically round with

prominent single or multiple nucleoli. Mild to moderate atypia with mitotic figures was commonly observed. Bizarre-shaped binucleated or multinucleated giant cells were occasionally found. Ultrastructural observation revealed the cultured tumor cells contained few organelles and lysosome-like structures, suggesting progenitor or stem cell dedifferentiation during cell cultivation. Although, these cultured HS cells had the identical morphology, the results of the immunocytochemistry and reverse transcription-polymerase chain reaction were relatively different. The PWC-HS01 cell line expressed both DC and macrophage markers, whereas a majority of FCR-HS02 cells expressed DC markers. These findings strongly support the fact that primary canine HS arising from neural tissue normally expresses both the DC and macrophage phenotypes, whilst the FCR-HS02 of extraneural origin had only the DC phenotype. Interestingly, the established cell lines were intensely positive for hematopoietic stem and progenitor cell markers. This finding may indicate that the cultured HS cells can revert into their progenitor or stem cells. Injected PWC-HS01 and FCR-HS02 cell lines can develop masses in an immunodeficient mouse model, but spontaneous metastases have not been detected. Interestingly, a panel of histiocytic markers in xenotransplanted and metastatic tumor cells were commonly detected. Furthermore, they were negative for CD34 as were the original tumors. These observations support the idea that dedifferentiated tumor cells can redifferentiated towards the DC and/or macrophage phenotype after the dedifferentiation.

In these series of experiments, it is now clearly understood that primary canine intracranial HS normally shares both DC and macrophage differentiation, unlike HS cases in extraneural organs, indicating that these cells display progenitor- or stem-like features. These observations reflect the biological behavior of primary HS in the CNS having a

tendency to be a poorly differentiated, comparing with HS from the other organ systems. As mentioned above, due to the aggressiveness and poor outcome of HS, precise diagnostic confirmation as well as early diagnosis is highly regarded.

ACKNOWLEDGEMENT

Firstly, I would like to express my sincere gratitude to my advisor, Professor Hiroyuki Nakayama, Professor of Department of Veterinary Pathology, Graduate School of Agricultural and Life Sciences, the University of Tokyo, for patient guidance, encouragement and support me throughout half a year (for research student) and 4 years (for doctoral course) in Japan.

In addition, my greatest gratitude goes to Associate Professor Kazuyuki Uchida, my co-advisor, and Assistant Professor James K. Chambers, Department of Veterinary Pathology, Graduate School of Agricultural and Life Sciences, the University of Tokyo, for their valuable advice and encouragement. I am thankful to them for carefully reading and providing insightful comments in the thesis and also academic articles.

I owe a great debt of gratitude to Dr. Yumiko Kagawa (North Lab, Hokkaido), Dr. Yasutsugu Miwa (Department of Veterinary Emergency Medicine, Graduate School of Agricultural and Life Sciences, the University of Tokyo), Dr. Masaya Tsuboi and Dr. Yousuke Murata (Department of Veterinary Pathology, Graduate School of Agricultural and Life Sciences, the University of Tokyo), and veterinarians from Veterinary Medical Center, the University of Tokyo and Private hospitals for providing information and specimens of histiocytic sarcoma.

Besides, I would also like to acknowledge Dr. Masumi Sato, Director of Pathological and Pathophysiology Research Division, National Institute of Animal Health, for her kindly teaching and technical advice of the transmissible electron microscope technique.

I would like to thank my fellow labmates (Dr. Makiko Ozawa and Dr. Meina Tei), my colleagues and Ms. Chiyo Doi for generous support and encouragement during my stay in Japan.

Unforgettably, I am indebted to the past members of Department of Veterinary Pathology, Graduate School of Agricultural and Life Sciences, the University of Tokyo, Dr. Eun-Sil Park, Dr. Sebastián Rodríguez, Dr. Satoshi Suzuki, Dr. Mizue Ogawa and Dr. Ken-ichi Watanabe for their technical guidance. I am also thankful to them for their kindly encouragement.

My sincerest thanks go to Chiang Mai University, Thailand for providing the financial support by Chiang Mai University's scholarship during my study period.

Finally, I must express my gratitude to my parent, brother, sister-in-law and niece for supporting and encouraging me throughout writing this thesis.

Thongtharb Atigan
トンターブ　アティガン

REFERENCES

1. Abadie, J., Hédan, B., Cadieu, E., De Briso, C., Devauchelle, P., Bourgain, C., Parker, H.G., Vaysse, A., Margaritte-Jeannin, P., Galibert, F., Ostrander, E.A. and André, C. 2009. Epidemiology, pathology, and genetics of histiocytic sarcoma in the Bernese Mountain dog breed. *J. Hered.* **100**: S19-S27.

2. Abraham, S., Indrasingh, I., Vettivel, S. and Chandi, G. 2000. Gross morphology and ultrastructure of dendritic cells in the normal human decidua. *Clin. Anat.* **13**: 177-180.

3. Affolter, V.K. and Moore, P.F. 2000. Canine cutaneous and systemic histiocytosis: reactive histiocytosis of dermal dendritic cells. *Am. J. Dermatopathol.* **22**: 40-48.

4. Affolter, V.K., Moore, P.F. 2002. Localized and disseminated histiocytic sarcoma of dendritic cell origin in dogs. *Vet. Pathol.* **39**: 74-83.

5. Alexie, B.A., Sailey, C.J., McClure, S.A., Ord, R.A., Zhao, X.F. and Papadimitriou, J.C. 2007. Primary histiocytic sarcoma arising in the head and neck with predominant spindle cell component. *Diagn. Pathol.* **2**: doi:10.1186/746-596-2-7.

6. Allen, C.E., Ladisch, S. and McClain, K.L. 2015. How I treat Langerhans cell histiocytosis. *Blood* **126**: 26-35.

7. Anjiki, T., Wada, Y., Honma, H., Niizeki, H., Shibahara, T. and Kadota, K. 2000. Malignant histiocytosis in cattle. *J. Vet. Med. Sci.* **62**: 1235-1240.

8. Azakami, D., Bonkobara, M., Washizu, T., Iida, A., Kondo, M., Kato, R., Niikura, Y., Iwaki, S., Tamahara, S., Matsuki, N. and Ono, K. 2006. Establishment and biological characterization of canine histiocytic sarcoma cell lines. *J. Vet. Med. Sci.* **68**: 1343-1346.

9. Barnes, A., Bee, A., Bell, S., Gilmore, W., Mee, A., Morris, R. and Carter, S.D. 2000. Immunological and inflammatory characterisation of three canine cell lines: K1, K6 and DH82. *Vet. Immunol. Immunopathol.* **75**: 9-25.

10. Bauchet, A.L., Fouque, M.C., Belluco, S., Château-Joubert, S., Elies, L., Maliver, P., Schorsch, F. and Fontaine, J.J. 2008. An atypical case of histiocytic sarcoma in a Wistar rat (*Rattus norvegicus*). *Exp. Toxicol. Pathol.* **59**: 385-390.

11. Beckstead, J.H., Wood, G.S. and Turner, R.R. 1984. Histiocytosis X cells and Langerhans cells: enzyme histochemical and immunologic similarities. *Hum. Pathol.* **15**: 826-833.

12. Cai, S., Fu, X. and Sheng, Z. 2007. Dedifferentation: a new approach in stem cell research. *Bioscience* **57**: 655-662.

13. Cao, M., Eshoa, C., Schultz, C., Black, J., Zu, Y. and Chang, C.C. 2007. Primary central nervous system histiocytic sarcoma with relapse to mediastinum - a case report and review of the iterature. *Arch. Pathol. Lab. Med.* **131**: 301-305.

14. Chandra, A.M.S. and Ginn, P.E. 1999. Primary malignant histiocytosis of the brain in a dog. *J. Comp. Pathol.* **121**: 77-82.

15. Chen, H.C., Slone, T.W. and Frith, C.H. 1992. Histiocytic sarcoma in an aging gerbil. *Toxicol. pathol*. **20**: 260-263.

16. Christgau, M., Caffess, R.G., Newland, R., Schmalz, G. and D'Souza, R.N. 1998. Characterization of immunocompetent cells in diseased canine periodontium. *J. Histochem. Cytochem*. **46**: 1443-1454.

17. Cline, M.J. 1994. Histiocytes and histiocytosis. *Blood* **84**: 2840-2853.

18. Constantino-Casas, F., Mayhew, D., Hoather, T.M. and Dobson, J.M. 2011. The clinical presentation and histopathologic-immunohistochemical classification of histiocytic sarcomas in the Flat Coated Retriever. *Vet. Pathol*. **48**: 764-771.

19. Coomer, A.R. and Liptak, J.M. 2008. Canine histiocytic siseases. *Compend. Contin. Educ. Vet*. **30**: 202-215.

20. Cornegliani, L., Gracis, M., Ferro, S., Vercelli, A. and Roccabianca, P. 2011. Sublingual reactive histiocytosis in a dog. *J. Vet. Dent*. **28**: 164-170.

21. Cumberbatch, M., Dearman, R.J., Griffths, C.E. and Kimber, I. 2000. Langerhans cell migration. *Clin. Exp. Dermatol*. **25**: 413-418.

22. Cunningham, A.L., Carbone, F. and Geijtenbeek, T.B.H. 2008. Langerhans cell and viral immunity. *Eur. J. Immunol*. **38**: 2377-2385.

23. de Saint-Vis, B., Vincent, J., Vandenabeele, S., Vanbervliet, B., Pin, J.J., Aït-Yahia, S., Patel, S., Mattei, M.G., Banchereau, J., Zurawski, S., Davoust, J., Caux, C. and Lebecque, S. 1998. A novel lysosome-associated membrane glycoprotein, DC-LAMP, induced upon DC maturation, is transiently expressed in MHC class II compartment. *Immunity* **9**: 325-336.

24. Delcour, N.M., Klopfleisch, R., Gruber, A.D. and Weiss, A.T.A. 2013. Canine cutaneous histiocytomas are clonal lesions as defined by X-linked clonality testing. *Vet. Comp. Path*. **149**: 192-198.

25. Denstedt, E. 2014. Suspected disseminated histiocytic sarcoma in a 3-year-old Perro de Presa Canario dog. *Can. Vet. J*. **55**: 181-184.

26. Edin, S., Wikberg, M.L., Dahlin, A.M., Rutegård, J., Öberg, Å., Oldenborg, P.A. and Palmqvist, R. 2012. The distribution of macrophages with a M1 or M2 phenotype in

relation to prognosis and the molecular characteristics of colorectal cancer. *PLoS One* **7**: e47045.

27. Fant, P., Caldin, M., Furlanello, T., De Lorenzi, D., Bertolini, G., Bettini, G., Morini, M. and Masserdotti, C. 2004. Primary gastric histiocytic sarcoma in a dog − A case report. *J. Vet. Med. A*. **51**: 358-362.

28. Favara, B.E., Feller, A.C., Pauli, M., Jaffe, E.S., Weiss, L.M., Arico, M., Bucsky, P., Egeler, R.M., Elinder, G., Gadner, H., Gresik, M., Henter, J.I., Imashuku, S., Janka-Schaub, G., Jaffe, R., Ladisch, S., Nezelof, C. and Pritchard, J. 1997. Contemporary classification of histiocytic disorders. *Med. Pediatr. Oncol*. **29**: 157-166.

29. Ferenbach, D. and Hughes, J. 2008. Macrophages and dendritic cells: what is the difference? *Kidney Int.* **74**: 5-7

30. Freshney, R.I. Culture of Animal Cells: A Manual of Basic Technique and Specialized Apllications. 6th ed. NJ, USA: John Wiley & Sons; 2010.

31. Friedrichs, K.R. and Young, K.M. 2008. Histiocytic sarcoma of macrophage origin in a cat: case report with a lirerrature review of feline histiocytic malignancies and comparison with canine hemophagocytic histiocytic sarcoma. *Vet. Clin. Pathol*. **37**: 121-128.

32. Fulmer, A.K. and Mauldin, G.E. 2007. Canine histiocytic neoplasia: An overview. *Can. Vet. J*. **48**: 1041-1050.

33. Golovkina, M.S., Skachkov, I.V., Metelev, M.V., Kuzevanov, A.V., Vishniakova, K.S., Kireev, I.I. and Dunina-Barkovskaya, A.Y. 2009. Serum-induced inhibition of the phagocytic activity of cultured macrophages IC-21. *Biochem. (Mosc) Suppl. Ser. A Membr. Cell Biol*. **3**: 417-424.

34. Guilliams, M., Ginhoux, F., Jakubzick, C., Naik, S.H., Onai, N., Schraml, B.U., Segura, E., Tussiwand, R. and Yona, S. 2014. Dendritic cells, monocytes and macrophages: a unified nomenclature based on ontogeny. *Nat. Rev. Immunol.* **14**: 571-578.

35. Gustavsson, I. 1964. The chromosomes of the dog. *Hereditas* **51**: 187-189.

36. Hage, C., Willman, C.L., Favara, B.E. and Isaacson, P.G. 1993. Langerhans' cell histiocytosis (Histiocytosis X): immunophenotype and growth fraction. *Hum, Pathol.* **24**: 840-845.

37. Hao, N.B., Lü, M.H., Fan, Y.H., Zhang, Z.R. and Yang, S.M. 2012. Macrophages in tumor microenvironments and the progression of tumors. *Clin. Dev. Immunol.* **2012**: 1-11.

38. Hayden, D.W., Waters, D.J., Burke, B.A. and Manivel, J.C. 1993. Disseminated malignant histiocytosis in a Golden Retriever: Clinicopathologic, ultrastructural, and immunohistochemical findings. *Vet. Pathol.* **30**: 256-264.

39. Heinrich, F., Contioso, V.B., Stein, V.M., Carlson, R., Tipold, A., Ulrich, R., Puff, C., Baumgärtner, W. and Spitzbarth, I. 2015. Passage-dependent morphological and phenotypical changes of a canine histiocytic sarcoma cell line (DH82 cells). *Vet. Immunol. Immunopathol.* **163**: 86-92.

40. Hélie, P., Kiupel, M. and Drolet, R. 2014. Congenital cutaneous histiocytosis in a piglet. *Vet. Pathol.* **51**: 812-815.

41. Hirako, A., Sugiyama, A., Sakurai, M., Ozaki, K., Sakai, H., Takeuchi, T., Morita, T. and Moore, P.F. 2015. Cutaneous histiocytic sarcoma with E-cadherin expression in a Pembroke Welsh Corgi dog. *J. Vet. Diagn. Invest.* **27**: 589-595.

42. Hure, M.C., Elco, C.P., Ward, D., Hutchinson, L., Meng, X., Dorfman, D.M. and Yu, H. 2012. Histiocytic sarcoma arising form clonally related mantle cell lymphoma. *J. Clin. Oncol*. **30**: e49-e53.

43. Ide, T., Uchida, K., Kagawa, Y., Suzuki, K. and Nakayama, H. 2011. Pathological and immunohistochemical features of subdural histiocytic sarcomas in 15 dogs. *J. Vet. Diagn. Invest*. **23**: 127-132.

44. Johnson, G.C., Coates, J.R. and Wininger, F. 2014. Diagnostic immunohistochemistry of canine and feline intracalvarial tumors in the age of brain biopsies. *Vet. Pathol*. **15**: 146-160.

45. Juvet, S.C., Hwang, D. and Downey, G.P. 2010. Rare lung diseases III: pulmonary langerhans' cell histiocytosis. *Can. Respir. J*. **17**: e55-e62.

46. Kato, Y., Murakami, M., Hoshino, Y., Mori, T., Maruo, K., Hirata, A., Nakagawa, T.L.D.R., Yanai, T. and Sakai, H. 2013. The class A macrophage scavenger receptor CD204 is a useful immunohistochemical marker of canine histiocytic sarcoma. *J. Comp. Pathol*. **148**: 188-196.

47. Lee, Y.J., Kang, S.Y., Jo, M.S., Suh, D.S., Kim, K.H. and Yoon, M.S. 2014. S100 expression in dendritic cells is inversely correlated with tumor grade in endometrial carcinoma. *Obstet. Gynecol*. **57**: 201-207.

48. Leissinger, M., Brandão, J., Wakamatsu, N., Le Roux, A., Rich, G. and Gaunt, S. 2013. Pulmonary histiocytic sarcoma in a rabbit. *Vet. Clin. Pathol*. **42**: 364-367.

49. Loftus, B., Loh, L.C., Curran, B., Henry, K. and Leader, M. 1991. Mac387: tis non-specific as a tumor marker or marker of histiocytes. *Histopathology* **19**: 251-255.

50. Margo, C.E. and Goldman, D.R. 2008. Langerhans cell histiocytosis. *Surv. Ophthalmol*. **53**: 332-358.

51. Mariani, C.L., Jennings, M.K., Olby, N.J., Borst, L.B., Brown, Jr J.C., Robertson, I.D., Seiler, G.S. and MacKillop, E. 2015. Histiocytic sarcoma with central nervous system involvement in dogs: 19 cases (2006 - 2012). *J. Vet. Intern. Med*. **29**: 607-613.

52. Mason, D.Y. and Taylor, C.R. 1975. The distribution of muramidase (lysozyme) in human tissues. *J. Clin. Pathol*. **28**: 124-132.

53. Mastrorilli, C., Spangler, E.A., Christopherson, P.W., Aubry, O.A., Newton, J.C., Smith, A.N., Kennis, R.A,, Weismann, J.L. and Moore, P.F. 2012. Multifocal cutaneous histiocytic sarcoma in a young dog and review of histiocytic cell immunophenotyping. *Vet. Clin. Pathol*. **41**: 412-418.

54. Matsuda, K., Nomoto, H., Kawamura, Y., Someya, Y., Koiwa, M. and Taniyama, H. 2010. Hemophagocytic histiocytic sarcoma in a Japanese black cow. *Vet. Pathol*. **47**: 339-342.

55. Mays, M.B. and Brgeron, J.A. 1986. Cutaneous histiocytosis in dogs. *J. Am. Vet. Med. Assoc*. **188**: 377-381.

56. McMenamin, P.G., Wealthall, R.J., Deverall, M., Cooper, S.J. and Griffin, B. 2003. Macrophages and dendritic cells in the rat meninges and choroid plexus: three-dimensional localisation by environmental scanning electron microscopy and confocal microscopy. *Cell. Tissue Res*. **313**: 259-269.

57. Moore, P.F. 2014. A review of histiocytic diseases of dogs and cats. *Vet. Pathol*. **51**: 167-184.

58. Moore, P.F. 1984. Systemic histiocytosis of Bernese mountain dogs. *Vet. Pathol*. **21**: 554-563.

59. Moore, P.F. 1986. Utilization of cytoplasmic lysozyme immunoreactivity as a histiocytic marker in canine histiocytic disorders. *Vet. Pathol*. **23**: 757-762.

60. Moore, P.F., Affolter, V.K. and Vernau, W. 2006. Canine hemophagocytic histiocytic sarcoma: A proliferative disorder of CD11d+ macrophages. *Vet. Pathol*. **43**: 632-645.

61. Moore, P.F., Schrenzel, M.D., Affolter, V.K., Olivry, T. and Naydan, D. 1996. Canine cutaneous histiocytoma is an epidermotropic Langerhans cell histiocytosis that expresses CD1 and specific f32-lntegrin molecules. *Am. J. Pathol*. **148**: 1699-1708.

62. Nagata, M., Hirata, M., Ishida, T., Hirata, S. and Nanko, H. 2000. Progressive Langerhans' cell histiocytosis in a puppy. *Vet. Dermatol*. **11**: 241-246.

63. Nielsen, L., Andreasen, S.N., Andersen, S.D. and Kristensen, A.T. 2010. Malignant histiocytosis and other causes of death in Bernese mountain dogs in Denmark. *Vet. Rec*. **166**: 199-202.

64. Paciello, O., Passantino, G., Costagliola, A., Papparella, S. and Perillo, A. 2013. Histiocytic sarcoma of the nasal cavity in a horse. *Res. Vet. Sci*. **94**: 648-650.

65. Palmeiro, B.S., Morris, D.O., Goldschmidt, M.H. and Mauldin, E.A. 2007. Cutaneous reactive histiocytosis in dogs: a retrospective evaluation of 32 cases. *Vet. Dermatol*. **18**: 332-340.

66. Paździor-Czapula, K., Rotkiewicz, T., Otrocka-Domagała, I., Gesek, M. and Śmiech, A. 2015. Morphology and immunophenotype of canine cutaneous histiocytic tumours with particular emphasis on diagnostic application. *Vet. Res. Commun*. **39**: 7-17.

67. Perez, L., Shurin, M.R., Collins, B., Kogan, D., Tourkova, I.L. and Shurin, G.V. 2005. Comparative analysis of CD1a, S-100, CD83, and CD11c human dendritic cells in normal, premalignant, and malignant tissues. *Histol. Histopathol*. **20**: 1165-1172.

68. Perrotta, I., Carito, V., Russo, E., Tripepi, S., Aquila, S. and Donato, G. 2011. Macrophage autophagy and oxidative stress: An ultrastructural and immunoelectron microscopical study. *Oxid. Med. Cell. Longev*. **2011**: 1-8.

69. Pierezan, F., Mansell, J., Ambrus, A. and Hoffmann, A.D. 2014. Immunohistochemical expression of ionized calcim binding adapter molecule 1 in cutaneous hisitocytic proliferativve, neoplastic andd inflammatory disorders of dogs and cats. *J. Comp. Pathol*. **151**: 347-351.

70. Pileri, S.A., Grogan, T.M., Harris, N.L., Banks, P., Campo, E., Chan, J.C.K., Favera, R.D., Delsol, G., De Wolf-Peeters, C., Falini, B., Gascoyne, R.D., Gaulard, P., Gatter, K.C., Isaacson, P.G., Jaffe, E.S., Kluin, P., Knowles, D.M., Mason, D.Y., Mori, S., Müller-Hermelink, H.K., Piris, M.A., Ralfkiaer, E., Stein, H., Su, I.J., Warnke, R.A. and Weiss, L.M. 2002. Tumors of histiocytes and accessory dendritic cells: an immunohistochemical approach to classification from the international lymphoma study group based on 61 cases. *Histopathology* **41**: 1-29.

71. Puff, C., Risha, E. and Baumgärtner, W. 2013. Regression of canine cutaneous histiocytoma is associated with an orchestrated expression of matrix metalloproteinases. *J. Comp. Pathol*. **149**: 208-215.

72. Pumphrey, S.A., Pizzirani, S., Pirie, C.G., Sato, A.F. and Buckley, F.I. 2013. Reactive histiocytosis of the orbit and posterior segment in a dog. *Vet. Ophthalmol*. **16**: 229-233.

73. Quail, D.F. and Joyce, J.A. 2013. Microenvironmental regulation of tumor progression and metastasis. *Nat. Med*. **19**: 1423-1437.

74. Randolph, G.J. 2002. Is maturation required for Langerhans cell migration? *J. Exp. Med*. **196**: 413-416.

75. Reed, N., Begara-McGorum, I.M., Else, R.W. and Gunn-Moore, D.A. 2006. Unusual hisiocytic disease in a Somali cat. *J. Feline Med. Surg*. **8**: 129-134.

76. Romero-Palomo, F., Risalde, M.A., Molina, V., Sánchez-Cordón, P.J., Pedrera, M. and Gómez-Villamandos, J.C. 2013. Immunohistochemical detection of dendritic cell markers in cattle. *Vet. Pathol*. **50**: 1099-1108.

77. Rossi, S., Gelain, M.E. and Comazzi, S. 2009. Disseminated histiocytic sarcoma with peripheral blood involvement in a Bernese Mountain dog. *Vet. Clin. Pathol*. **38**: 126-130.

78. Sakai, H., Nakano, H., Yamaguchi, R., Yonemaru, K., Yanai, T. and Masegi, T. 2003. Establishment of a new canine cell line (CCT) originated from malignant histiocytosis. *J. Vet. Med. Sci*. **65**: 731-735.

79. Salaun, B., de Saint-Vis, B., Pacheco, N., Pacheco, Y., Riesler, A., Isaac, S., Leroux, C., Clair-Moninot, V., Pin, J.J., Griffith, J., Treilleux, I., Goddard, S., Davoust, J., Kleijmeer, M. and Lebecque, S. 2004. CD208/Dendritic cell-lysosomal associated membrane protein is a marker of normal and transformed type II pneumocytes. *Am. J. Pathol*. **164**: 861-871.

80. Schultz, R.M., Puchalski, S.M., Kent, M. and Moore, P.F. 2007. Skeletal lesionss of histiocytic sarcoma in nineteen dogs. *Vet. Radiol. Ultrasound* **48**: 539-543.

81. Soare, T., Noble, P.J., Hetzel, U., Fonfara, S. and Kipar, A. 2012. Paraneoplastic syndrome in haemophagocytic histiocytic sarcoma in a dog. *J. Comp. Pathol*. **146**: 168-174.

82. Solinas, G., Germano, G., Mantovani, A. and Allavena, P. 2009. Tumor-associated macrophages (TAM) as major players of the cancer-related inflammation. *J. Leukoc. Biol*. **86**: 1065-1073.

83. Soulas, C., Conerly, C., Kim, W.K., Burdo, T.H., Alvarez, X., Lackner, A.A. and Williams, K.C. 2011. Recently infiltrating MAC387^{+} monocyte/macrohpages. *Am. J. Pathol*. **178**: 2121-2135.

84. Spano, D. and Zollo, M. 2012. Tumor microenvironment: a main actor in the metastasis process. *Clin. Exp. Metastasis* **29**: 381-395.

85. Suzuki, M., Uchida, K., Morozumi, M., Yanai, T., Nakayama, H., Yamaguchi, R. and Tateyama, S. 2003. A comparative pathological study on granulomatous meningoencephalomyelitis and central malignant histiocytosis in dogs. *J. Vet. Med. Sci*. **65**: 1319-1324.

86. Tamura, S., Tamura, Y., Nakamoto, Y., Ozawa, T. and Uchida, K. 2009. MR imaging of histiocytic sarcoma of the canine brain. *Vet. Radiol. Ultrasound* **50**: 178-181.

87. Thio, T., Hilbe, M., Grest, P. and Pospischil, A. 2006. Malignant histiocytosis of the brain in three dogs. *J. Comp. Pathol*. **134**: 241-244.

88. Tzipory, L., Vernau, K.M., Sturges, B.K., Zabka, T.S., Highland, M.A., Petersen, S.A., Wisner, E.R., Moore, P.F. and Vernau, W. 2009. Antemortem diagnosis of localized central nervous system histiocytic sarcoma in 2 dogs. *J. Vet. Intern. Med.* **23**: 369-374.

89. Uchida, K., Morozumi, M., Yamaguchi, R. and Tateyama, S. 2001. Diffuse leptomeningeal malignant histiocytosis in the brain and spinal cord of a Tibetan Terrier. *Vet. Pathol*. **38**: 219-222.

90. Villablanca, E.J. and Mora, J.R. 2008. A two-step model for Langerhans cell migration to skin-draining LN. *Eur. J. Immunol*. **38**: 2975-2980.

91. Villalta, S.A., Nguyen, H.X., Deng, B., Gotoh, T. and Tidball, J.G. 2009. Shifts in macrophage phenotypes and macrophage competition for arginine metabolism affect the severity of muscle pathology in muscular dystrophy. *Hum. Mol. Gnet*. **18**: 482-496.

92. Villiers, E., Baines, S., Law, A.M. and Mallows, V. 2006. Identification of acute myeloid leukemia in dogs using flow cytometry with myeloperoxidase, MAC387, and a canine neutrophil-specific antibody. *Vet. Clin. Pathol*. **35**: 55-71.

93. Vishniakova, K.S., Kireev, I.I. and Dunina-Barkovskaya, A.Y. 2011. Effects of cell culture density on phagocytosis parameters in IC-21 macrophages. *Biochem. (Mosc) Suppl. Ser. A Membr. Cell Biol*. **5**: 355-363.

94. Weiss, T., Wever, L., Scharffetter-Kochanek, K. and Weiss, J.M. 2005. Solitary cutaneous dendritic cell tumor in a child: role of dendritic cell markers for the diagnosis of skin Langerhans cell histiocytosis. *J. Am. Acad. Dermatol*. **53**: 838-844.

95. Wellman, M.L., Krakowka, S., Jacobs, R.M. and Kociba, G.J. 1988. A macropahge-monocyte cell line from a dog with malignant histiocytosis. *In Vitro Cell Dev. Biol*. **24**: 223-229.

96. Wong, V.M., Snyman, H.N., Ackerley, C. and Bienzle, D. 2012. Primary nasal histiocytic sarcoma of macrophage-myeloid cell type in a cat. *J. Comp. Pathol*. **147**: 209-213.

97. Yamazaki, H., Takagi, S., Oh, N., Hoshino, Y., Hosoya, K. and Okumura, M. 2014. Comparative analysis of mRNA expression of surface antigens between histiocytic and nonhistiocytic sarcoma in dogs. *J. Vet. Intern. Med*. **28**: 204-210.

98. Yang, G.C.H., Besanceney, C.E. and Tam, W. 2010. Histiocytic sarcoma with interdigitating dendritic cell differentiation: A case report with fine needle aspiration cytology and review of literature. *Diagn. Cytopathol*. **38**: 351-356.

99. Zhang, M., He, Y., Sun, X., Li, Q., Wang, W., Zhao, A. and Di, W. 2014. A high M1/M2 ratio of tumor-associated macrophages is associated with extended survival in ovarian cancer patients. *J. Ovarian Res*. **7**: 1-16.

100. Zhang, Y., Li, T.S., Lee, S.T., Wawrowsky, K.A., Cheng, K., Galang, G., Malliaras, K., Abraham, M.R., Wang, C. and Marbán, E. 2010. Dedifferentiation and proliferation of mammalian cardiomyocytes. *PLoS One* **5**: e12559.

101. Zimmerman, K., Almy, F., Carter, L., Higgins, M., Rossmeisl, J., Inzana, K. and Duncan, R. 2006. Cerebrospinal fluid from a 10-year-old dog with a single seizure episode. *Vet. Clin. Pathol*. **35**: 127-131.

REFERENCE ARTICLE

Histological and immunohistochemical features

of histiocytic sarcoma in domestic ferret

(*Mustela putorius furo*): The comparative study

INTRODUCTION

The domestic ferret (*Mustela putorius furo*) has been extensively used for many purposes such as pharmacology, toxicology and virology in the medical research field over the last decade. Genetically modified ferrets are also used as models for human diseases [9, 11, 51]. Currently, the ferret has become a popular companion animal worldwide. Hence, neoplastic diseases in ferrets have been increasingly studied. And endocrine tumors (i.e., pancreatic islet cell tumor and adrenal cortical carcinoma) and lymphomas are most common in this species [4, 6, 17, 18, 32, 33, 44, 49].

Histiocytic sarcoma (HS) is a fatal, aggressive malignant hematopoietic tumor of histiocytes. Other than human, this tumor has also been well described in animals, especially in dogs and cats [3, 18, 19, 25, 27, 36, 38]. Moreover, cases in horse [42], cattle [7, 34], a rabbit [31], mice [41, 55], a rat [10] and a gerbil [13] have also been reported. According to a previous study [35], the occurrence of HS in ferrets was <0.1% (only 1 HS case in 945 tumor cases) and the tumor was involved in the integumentary system. To our knowledge, characteristics of HS in this species have never been studied.

In the reference article, therefore, morphological and immunohistochemical features of HS in 4 domestic ferrets are elucidated. In addition, the occurrence and immunohistochemical features of histiocytic proliferative disorders in animals are compared.

MATERIALS AND METHODS

Animals

Four tumor samples were obtained from 3 surgical biopsy cases and 1 autopsy case of the domestic ferret, which were submitted to the Department of Veterinary Pathology, the University of Tokyo, Japan, for pathological examination between 2010 and 2015. The clinical presentations, tumor distribution and treatment history are summarized in **Table 1**.

Histological examination

Samples, including the spleen, stomach, adrenal glands, liver, epigastric and mesenteric lymph nodes and a free-moving abdominal mass were fixed in 10% neutral-buffered formalin solution and subsequently processed for paraffin embedding. The sections (2 to 4 µm-thick) were stained with hematoxylin and eosin (HE). To evaluate the mitotic index, the total number of mitosis per 10 high power fields (hpf, 400×) was counted under a light microscope.

Immunohistochemical examination

In order to identify the cellular origin of tumor cells, immunohistochemical examination was performed. The IHC procedure and IHC scoring system were performed in the same manner as described in Chapter 1. Primary antibodies used are detailed in **Table 2**. In addition, normal ferret tissues, including the spleen, liver and lymph nodes,

were also used as positive controls, whereas negative control reactions were performed through applying with TBS instead of the primary antibodies.

RESULTS

Clinical features and gross lesions

Four domestic ferrets examined were 3 males and 1 female with the median age of 4.6 years (2 years 6 months to 6 years). Clinical feature of the ferrets were summarized in **Table 1**. Grossly, major lesions were found in the abdominal cavity in all the ferret cases, which included splenomegaly and white to gray, non-circumscribed masses scattered throughout the splenic parenchyma **(Fig. 1)**. Marked splenic necrosis was found in cases No. 2 and 3. Furthermore, solitary or multiple masses in the regional lymph nodes (cases No. 2, 3 and 4; **Fig. 2**), left adrenal gland (case No. 2), stomach (case No. 2), and liver (case No. 4) were also noted. A free-moving abdominal mass with ascites was present in case No. 4.

Histological lesions

Tumor masses in the spleen of all the cases comprised numerous round to pleomorphic cells of various sizes, often arranged in a loose sheet pattern. Tumor cells had abundant pale eosinophilic cytoplasm, some of which were coarsely vacuolated, and contained round to ovoid nuclei with fine to coarsely stippled chromatin patterns. One to 3 prominent nucleoli were observed. Atypical mitotic figures with a highly variable mitotic index were also noted **(Table 1)**. In addition, interspersing of bizarre, binucleated tumor cells and multinucleated giant tumor cells were commonly found among mononuclear tumor cells. A few tumor cells engulfed red blood cells and granulocytes **(Fig. 3)**. Marked necrosis and moderate lymphocytic infiltration were also noted. Moderate to marked extramedullary hematopoiesis were observed **(Fig. 4)**. Likewise,

117

tumor cells in other organs (stomach, adrenal glands, liver, and free-moving abdominal mass) were morphologically identical to those in the spleen. However, hemophagocytic activity was rarely observed **(Fig. 5)**. Tumor cell invasion into blood vessels in the organs was occasionally seen in case No. 2, 3 and 4. Furthermore, metastases perigastric and mesenteric nodes, were found in cases No. 2, 3 and 4 **(Fig. 6)**.

Immunohistochemistry

Immunohistochemical examination revealed that the cytoplasm of the tumor cells was strongly immunopositive for vimentin and human leukocyte antigen-DR (HLA-DR; all cases). Cytoplasmic expression of ionized calcium-binding adapter molecule-1 (Iba-1) and lysozyme was also observed in almost all tumor cells (all cases). Granular cytoplasmic and membrane immunoreactivities to CD163 were variably distributed in cases No. 1, 3 and 4. In addition, cases No. 3 and 4 had a patchy dot-like cytoplasmic immunoreactivity to CD208 (**Fig. 7 and Table 3**). However, tumor cells were negative for S100, MAC386, cytokeratin, CD3, CD20, lambda and kappa light chains, and von Willebrand factor in all the cases. Normal ferret tissues were negative for CD204, indicating that this marker is not suitable to be used in this species.

DISCUSSION

According to histological and immunohistochemical results, tumor cells in the present cases possessed characteristics of histiocytic differentiation. Therefore, the diagnosis of HS was made for all the 4 cases.

Histiocytic proliferative disorders have been well documented in domestic animals, particularly in dogs. Canine histiocytic sarcoma is generally categorized into 3 types (canine cutaneous histiocytoma, canine reactive histiocytosis and HS), according to clinical and pathological features [19]. HS in dogs, which is recognized as a malignant form of histiocytic tumors, can be subgrouped into localized and disseminated forms based on the number of primary organs and/or the evidence of distant metastases [3, 19, 36]. In ferrets, this tumor can be speculatively categorized into localized (case No. 1 and 3) and disseminated (case No. 2 and 4) forms, as well.

As mentioned previously, histiocytic tumor in ferrets was first described in the integumentary system [35]. However, in 3 of the 4 present cases, the tumor lesions were confined to the abdominal cavity, especially to the spleen (cases No. 1, 3, and 4), and only 1 case (case No. 2) exhibited extra-abdominal lesions (adrenal gland).

Splenomegaly observed in middle-aged or older ferrets is generally associated with extramedullary hematopoiesis [20]. Moreover, such splenic tumors as lymphoma and hemangiosarcoma are also mentioned as causes of splenic enlargement in this species. As cytopathological and histological characteristics of histiocytic sarcoma and other undifferentiated large cell tumors, such as lymphoma, metastatic malignant melanoma, and undifferentiated carcinoma, are often similar, further immunohistochemical examinations are recommended in order to confirm the diagnosis.

Tumor cells of all the present ferret cases exhibited immunoreactivities to histiocytic markers, such as HLA-DR, Iba-1 and lysozyme, similar to those in other species mentioned previously **(Table 3)**. However, the lack of CD163 or CD208 expression was found in cases No. 1 and 2 **(Table 4)**. In general, CD163 or monocyte and/or macrophage-restricted membrane protein is expressed exclusively in the monocyte/macrophage lineage, particularly in the M2 macrophage phenotype [29, 30]. This marker is also used for confirming the diagnosis of HS in human and canine cases. Most of the canine HS cases originate from the dendritic cell lineage, whereas some dominantly exhibit the monocyte/macrophage phenotype and are called hemophagocytic HS [36, 38]. Histological features of hemophagocytic HS include a marked erythrophagocytosis by neoplastic histiocytes interspersing among the areas of extramedullary hematopoiesis. Tumor cells in the 3 present ferret cases (cases No. 1, 3, and 4) had immunoreactivity to CD163, which supports the monocyte/macrophage phenotype, though very few tumor cells showed erythrophagocytosis.

CD208 or dendritic cell lysosome-associated membrane glycoprotein (DC-LAMP) is generally expressed in human dendritic cells and is closely associated with the maturation and activation of the cells [16]. In our present study, tumor cells in cases No. 3 and 4 were positive for CD208, suggesting that the tumor cells originated from dendritic cells. Moreover, neoplastic histiocytes of ferrets are also positive for other macrophage markers, like in dogs [36]. Conversely, tumor cells in case No. 2 were negative for CD163 and CD208 reported to be positive markers in human HS cases [16, 29]. This indicates that the expression levels of these 2 markers may associate with cell differentiation and maturation of the neoplastic histiocytes. Because the survival time of the ferrets with HS

after treatment was very short (9 days to 5 months; **Table 1**), prognosis of histiocytic

sarcoma in this species is very poor.

Table 1 Four cases of histiocytic sarcoma in the domestic ferret

No.	Sex [a]	Age [b]	Clinical presentation	Tumor distribution	MI [c]	Treatments	Survival time after initial diagnosis
1	M, castrated	4Y11M	Chronic diarrhea; Splenic mass with mesenteric lymphadenopathy; Hypoalbuminemia; Leukocytosis	Localized	41	Surgical excision; Vincristine 0.025 mg/kg	9 days
2	M, castrated	5Y1M	Mild splenomegaly; Multiple nodules in the spleen, stomach, abdominal lymph nodes, and left adrenal gland; Perigastric lymphadenopathy	Disseminated	28	Surgical excision; Prednisolone 2 mg/kg	2 months
3	M, castrated	2Y6M	Fever; Marked splenomegaly; Abdominal lymphadenopathy	Localized	14	Surgical excision; Prednisolone 2 mg/kg	2 months
4	F, OVH	6Y	Multiple nodules in the spleen, abdominal lymph nodes and liver, and a free-moving abdominal mass; Ascites; Hypoglycemia	Disseminated	10	Surgical excision; L-asparanigase 400 IU/kg; Cyclophosphamide 10mg/kg	5 months

[a] M = Male; F = Female; OVH = Ovariohysterectomy. [b] Y = Year (s); M = Month (s). [c] MI = Mitotic index: Total number of mitotic figures per 10 high power fields (hpf: 400X)

Table 2 Primary antibodies used in immunohistochemical examination

Antibody to [a]	Type [b]	Dilution [c]	Antigen retrieval for IHC [d]	Expression	Source
HLA-DR	Mouse, mAb (TAL.1B5)	1:50	Citrate buffer, pH 6.0 (HIER), 121°C, 10 min	Antigen presenting cell	Santa Cruz, CA, USA
Iba-1	Rabbit, pAb	1:250	Citrate buffer, pH 6.0 (HIER), 121°C, 10 min	Histiocyte, macrophage	Wako, Osaka, Japan
CD204	Mouse, mAb (SRA-E5)	1:100	Tris/EDTA buffer pH 9.0 (HIER), 121°C, 10 min	Monocyte, macrophage	TransGenic, Kobe, Japan
CD163	Mouse, mAb (AM-3K)	1:100	Citrate buffer, pH 2.0 (HIER), 121°C, 10 min	Histiocyte	TransGenic, Kobe, Japan
Lysozyme	Rabbit, pAb	1:100	Proteinase K (PIER), room temperature, 30 min	Monocyte, macrophage	Dako, Glostrup, Denmark
S100	Rabbit, pAb	1:1000	Citrate buffer, pH 6.0 (HIER), 121°C, 10 min	Dendritic cell	Dako, Tokyo, Japan
CD208 (DC-LAMP)	Rat, mAb (1010E1.01)	1:100	Citrate buffer, pH 6.0 (HIER), 121°C, 10 min	Dendritic cell	Dendritics, Lyon, France
Myeloid/Histiocyte antigen	Mouse, mAb (MAC387)	1:250	Proteinase K (PIER), room temperature, 30 min	Histiocyte, macrophage, granulocyte	Dako, Glostrup, Denmark
CD3	Rabbit, pAb	RTU	Tris/EDTA buffer pH 9.0 (HIER), 121°C, 10 min	T-lymphocyte	Dako, Tokyo, Japan
CD20	Rabbit, pAb	1:400	None	B-lymphocyte	Thermo scientific, CA, USA
Lambda light chain	Rabbit, pAb	1:50000	Citraconic anhydrate, Immunosaver® (HIER), 98°C, 45 min	Plasma cell	Dako, Glostrup, Denmark
Kappa light chain	Rabbit, pAb	1:10000	Citraconic anhydrate, Immunosaver® (HIER), 98°C, 45 min	Plasma cell	Dako, Glostrup, Denmark
vWF	Rabbit, pAb	1:500	Proteinase K (PIER), room temperature, 30 min	Endothelial cell, megakaryocyte	Dako, Tokyo, Japan
Cytokeratin	Mouse, mAb (AE1/AE3)	RTU	Citrate buffer, pH 6.0 (HIER), 121°C, 10 min	Epithelial cell	Dako, Tokyo, Japan
Vimentin	Mouse, mAb (V9)	1:200	Citrate buffer, pH 6.0 (HIER), 121°C, 10 min	Mesenchymal cell	Dako, Tokyo, Japan

[a] HLA-DR = Human leukocyte antigen-DR; Iba-1 = Ionized calcium-binding adapter molecule-1; CD = Cluster of differentiation; DC-LAMP = Dendritic cell lysosome-associated membrane glycoprotein; vWF = von Willebrand factor.

[b] pAb = Polyclonal antibody; mAb = Monoclonal antibody.

[c] RTU = Ready-to-use.

[d] HIER = Heat-induced epitope retrieval; PIER = Proteolytic-induced epitope retrieval.

Table 3 Occurrence of histiocytic proliferative disorders in animals

Species	Tumor location	IHC markers [a] Positive	IHC markers [a] Negative	Diagnosis	Authors and year
Domestic ferret	Spleen, liver and lymph node	CD163, CD208, HLA-DR, Iba-1, lysozyme and vimentin	CD3, CD20, Cytokeratin AE1/AE3, kappa light chain, lambda light chain, MAC387, S100, vWF	Histiocytic sarcoma	*The present study*
Cat	Skin, spleen, brain, extremity, mediastinum, spinal cord, nasal cavity	Alpha-1 antichymotryypsin, Alpha-naphthybutyrate, BLA36[*], CD1a, CD1c, CD11b, CD11d[***], CD18, HLA-DR, Iba-1, leukointergrin β-subunit, MHCII, Mac 387[**]and vimentin	BLA36, CD1a[***], CD1b[***], CD3, CD5, CD8, CD11c[***], CD18[***], CD21, CD79a, cytokeratin, GFAP, IgG (H and L), lysozyme, Leu7, Mac387, neurofilament and S100	Histiocytic sarcoma Feline progressive histiocytosis [***]Histiocytic sarcoma (Macrophage origin)	Affolter et al [2], Friedrichs et al [18], Ide et al [25], Ide et al [27], Pinard et al [45], [**]Reed et al [47], [*]Smoliga et al [50], Teshima et al [52], [***] Wong et al [56]
Cat	Lung	CD18, E-cadherin and vimentin	CD3, CD20, CD45R, CD79a and cytokeratin	Pulmonary Langerhans cell histiocytosis	Buch et al [12]
Cat	Skin	MHCII	CD3,CD79a	Cutaneous histiocytoma	Day et al [15]
Cow	Spleen, thoracic vertebrae, lymph node and liver	CD18, CD68, HAM56, lysozyme, MAC387[*] and MHC-II	CD3, CD79a, cytokeratin, MAC387, S100, SMA	Histiocytic sarcoma	[*]Anjiki et al [7], Matsuda et al [34]
Dog	Spleen, liver, lymph node, extremity, skin/subcutis, lung, bone/joint, brain, eye, gastrointestinal tract and urinary system	Cathepsin B, CD1, CD4, CD11b, CD11c, CD11d, CD18, CD45, CD163, CD204, E-cadherin[*], HLA-DR, Iba-1, lysozyme, MHCII, UCHL-1 and vimentin	CD3, CD20, CD68, CD79a, cytokeratin, E-cadherin, MAC387, S100, SMA	Histiocytic sarcoma	Amores-Fuster et al [5], Coomer et al [14], Fulmer et al [19], Hayden et al [22], [*]Hirako et al [24], Ide et al [26], Moore [36], Naranjo et al [40], Rossi et al [48], Thio et al [53], Uchida et al [54]
Dog	Skin	Alpha-naphthyl acetate esterase, CD1 (a, b, c), CD11a, CD11c, CD44, E-cadherin, ICAM-1, MHC class II and VLA-4	Thy-1, CD3, CD8, CD21, CD79a	Cutaneous histiocytoma Langerhans cell histiocytosis	Baines et al [8], Glick et al [21], Kipar et al [28], Moore et al [39]
Dog	Skin, eye, lymph node, spleen, bone marrow, lung, liver, pancreas, testis, kidney	CD1, CD4, CD11c, MHC II and Thy-1	CD3, CD8, TCRαβ	Reactive histiocytosis (Cutaneous and systemic)	Affolter et al [1], Moore [37], Palmeiro et al [43], Pumphrey et al [46]
Horse	Nasal cavity	α1-antitrypsin, lysozyme, MAC387 and vimentin	CD3, CD79a, pancytokeratin	Histiocytic sarcoma	Paciello et al [42]

Table 3 Occurrence of histiocytic proliferative disorders in animals (continued)

Species	Tumor location	IHC markers [a]		Diagnosis	Authors and year
		Positive	**Negative**		
Mongolian gerbil	Spleen, liver and bone marrow	n/d	n/d	Histiocytic sarcoma	Chen *et al* [13]
Mouse	Liver, spleen, lung kidney, lymph node, uterus/vagina	CD68,CD204, F4/80, lysozyme, Ly-6C and MAC-2	CD5, CD45R, desmin, SMA, vWF	Histiocytic sarcoma	Ohnishi *et al* [41], Ward *et al* [55]
Pig	Skin	CD163, CD204, lysozyme and vimentin	α1-antitrypsin, E-cadherin, MAC387, S100 and SMA	Cutaneous histiocytosis	Hélie *et al* [23]
Rabbit	Lung	Vimentin	CD3, CD18, CD79a, cytokeratin	Histiocytic sarcoma	Leissinger *et al* [31]
Rat	Liver, spleen, pancreas	Vimentin	CD68, Lysozyme	Histiocytic sarcoma	Bauchet *et al* [10]

[a] n/d = No data.

Table 4 Immunohistochemical characteristics of histiocytic sarcoma in domestic ferret

No.	IHC results [a]													
	HLA-DR	Iba-1	CD163	Lysozyme	S100	CD208	MAC387	CD3	CD20	λ	κ	vWF	CK	Vimentin
1	+++	+++	++	+	-	-	-	-	-	-	-	-	-	+++
2	+++	+++	-	++	-	-	-	-	-	-	-	-	-	+++
3	+++	+++	+++	+	-	+++	-	-	-	-	-	-	-	+++
4	+++	+++	+	++	-	++	-	-	-	-	-	-	-	+++

[a] HLA-DR = Human leukocyte antigen-DR; Iba-1 = Ionized calcium-binding adapter molecule-1; CD = Cluster of differentiation; λ = Lambda light chain; κ = Kappa light chain; vWF = von Willebrand factor; CK = Cytokeratin AE1/AE3; Immunohistochemical scoring: - (Negative) = Negative labeled cells; + (Weakly positive) = 1 − 25% labeled cells; ++ (Moderately positive) = 26 − 50% labeled cells; +++ (Strongly positive) = > 50% labeled cells.
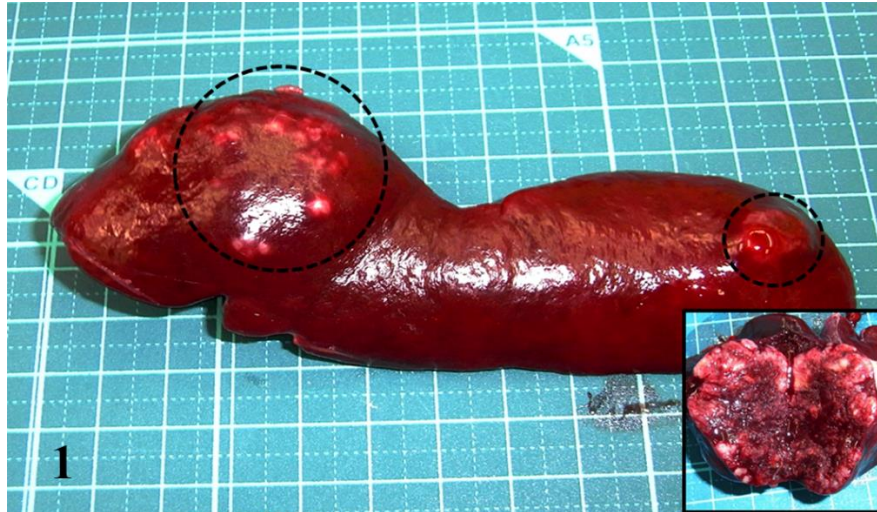
Figure 1. Histiocytic sarcoma. Spleen. Ferret. Case No. 2. Splenomegaly with poorly demarcated nodules (dotted circles). The cut surface of the nodule is whitish to red in color, indicating hemorrhage and necrosis (inset).
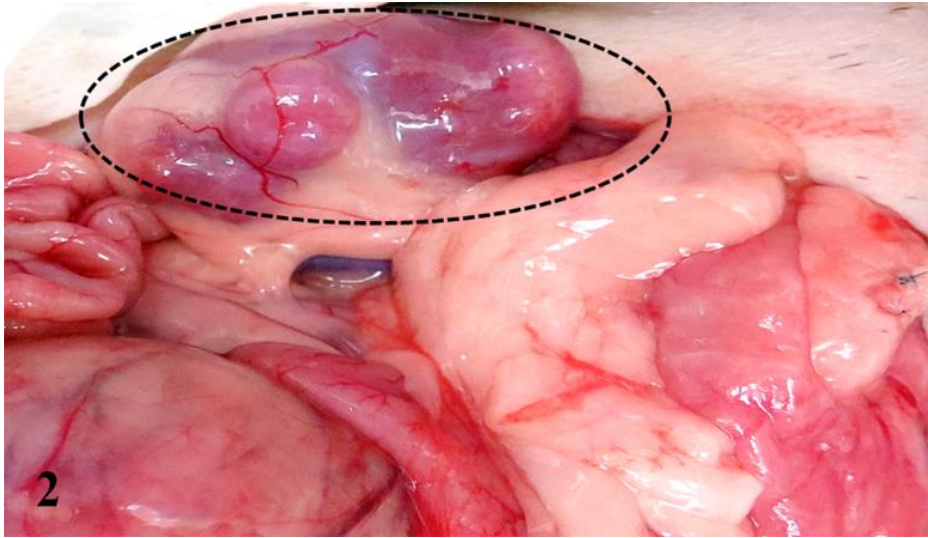
Figure 2. Histiocytic sarcoma. Abdominal viscera. Ferret. Case No. 3. Enlargement of mesenteric lymph nodes (dotted circle).
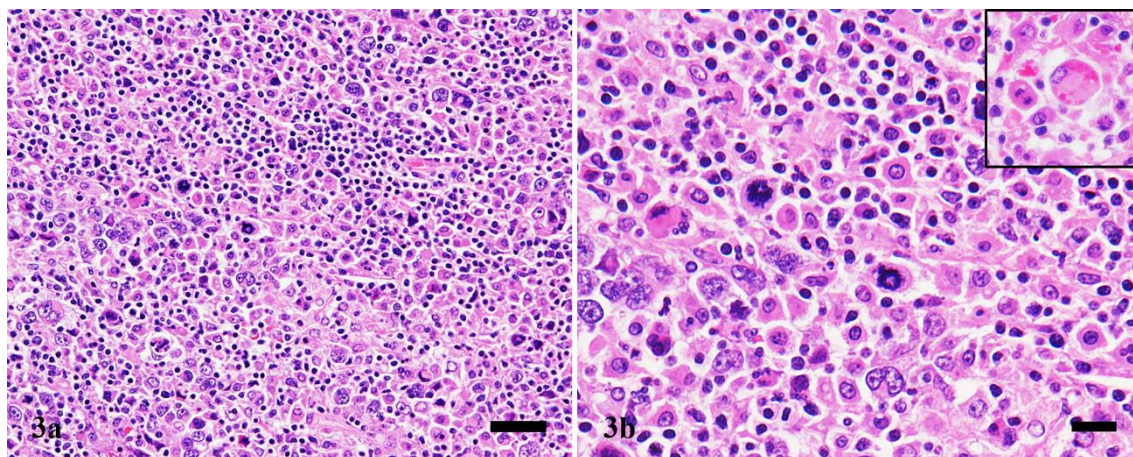
Figure 3. Histiocytic sarcoma. Spleen. Ferret. Case No. 2. Numerous neoplastic histiocytes expand into the splenic red pulp (a). In a high magnification photo (b), tumor cells were polygonal with eosinophilic cytoplasm. Bizarre binucleated and multinucleated neoplastic giant cells are commonly observed. Atypical mitoses are also noted. Few tumor cells show erythrophagocytosis (inset). HE. Scale bar = 50 *μ*m (a), 20 *μ*m (b).
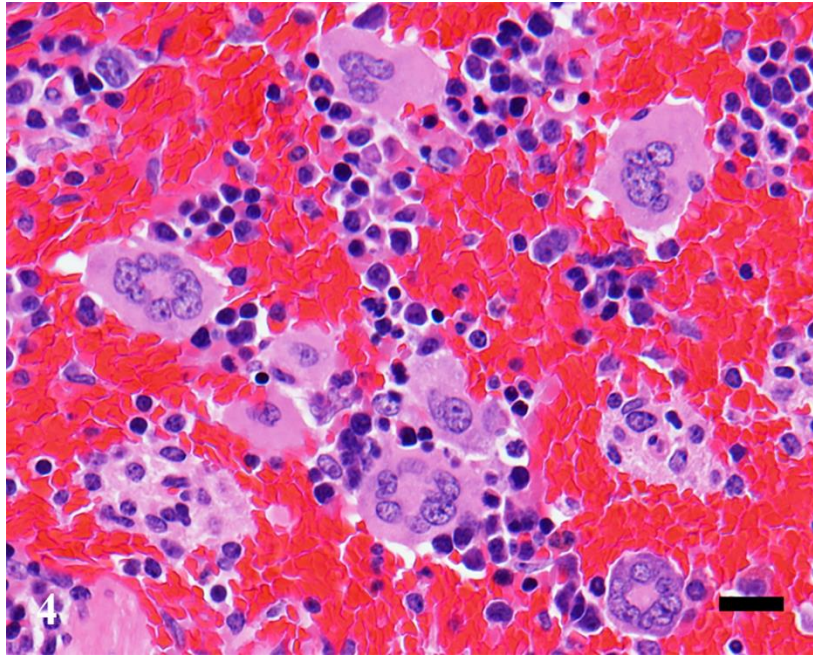
Figure 4. Histiocytic sarcoma. Spleen. Ferret. Case No. 2. Marked extramedullary hematopoiesis is observe. Multinucleated giant cells are megakaryocytes. HE. Scale bar = 20 μm.
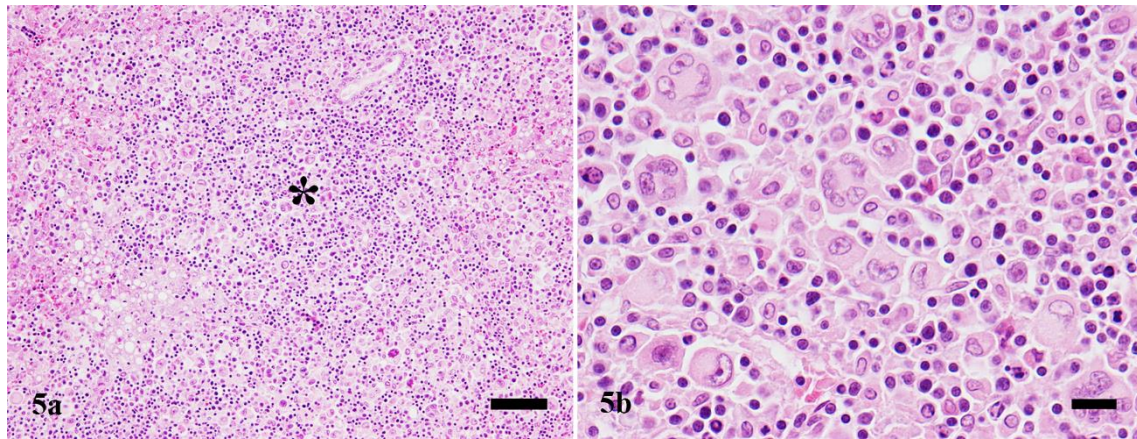
Figure 5. Histiocytic sarcoma. Liver. Ferret. Case No. 4. Numerous neoplastic histiocytes and small lymphocytes expand into the portal triad (a; asterisk). In high magnification (b), bizarre mononuclear and multinucleated neoplastic giant cells are commonly observed. HE. Scale bar = 100 μm (a), 20 μm (b).
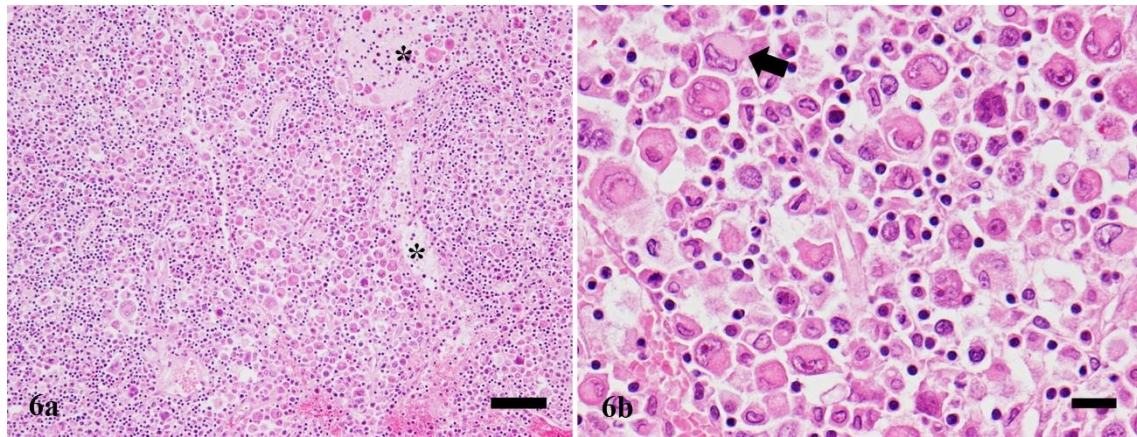
Figure 6. Histiocytic sarcoma. Perigastric lymph node. Ferret. Case No. 4. Numerous neoplastic histiocytes expand into the entire parts of lymph node (a). The tumor cells invading into the medullary sinus is observed (asterisks). In the high magnification photo (b), morphological characteristics of neoplastic histiocytes are similar to those in the liver. Some of them contain a large vacuole (arrow). HE. Scale bar = 100 μm (a), 20 μm (b).
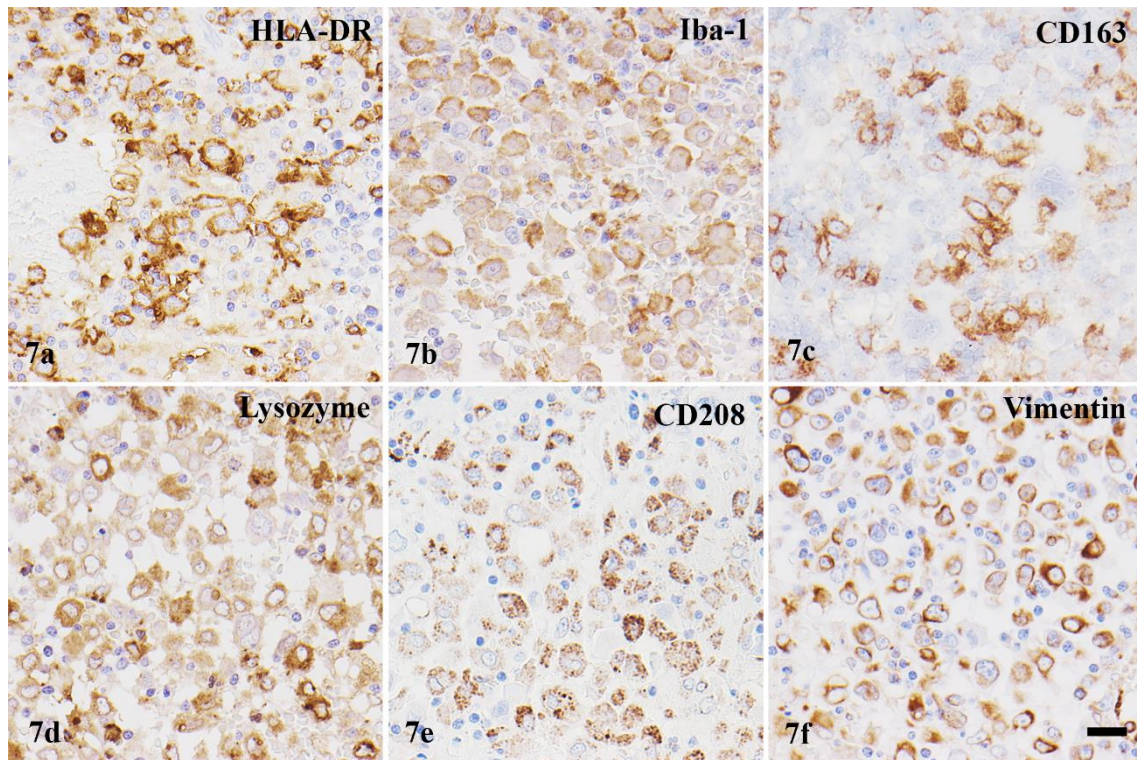
Figure 7. Histiocytic sarcoma. Perigastric lymph node. Ferret. Case No. 3. Tumor cells are positive for HLA-DR (a), Iba-1 (b), CD163 (c), lysozyme (d), CD208 (e) and vimentin (f). IHC. Hematoxylin counterstain. Scale bar = 20 μm.

REFERENCES

1. Affolter, V.K. and Moore, P.F. 2000. Canine cutaneous and systemic histiocytosis: reactive histiocytosis of dermal dendritic cells. *Am. J. Dermatopathol*. **22**: 40-48.

2. Affolter, V.K. and Moore, P.F. 2006. Feline progressive histiocytosis. *Vet. Pathol*. **43**: 646-655.

3. Affolter, V.K. and Moore, P.F. 2002. Localized and disseminated histiocytic sarcoma of dendritic cell origin in dogs. *Vet. Pathol*. **39**: 74-83.

4. Ammerbach, M., Delay, J., Caswell, J.L., Smith, D.A., Taylor, W.M. and Bienzle, D. 2008. Laboratory findings, histopathology, and immunophenotype of lymphoma in domestic ferrets. *Vet. Pathol*. **45**: 663-673.

5. Amores-Fuster, I., Elliott, J.W., Freeman, A.I. and Blackwood, L. 2011. Histiocytic sarcoma of the urinary bladder in a dog. *J. Small Anim. Pract*. **52**: 665.

6. Andrews, G.A., Myers, III N.C. and Chard-Bergstrom, C. 1997. Immunohistochemistry of pancreatic islet cell tumors in the ferret (*Mustela putorus furo*). *Vet. Pathol*. **34**: 387-393.

7. Anjiki, T., Wada, Y., Honma, H., Niizeki, H., Shibahara, T. and Kadota, K. 2000. Malignant histiocytosis in cattle. *J. Vet. Med. Sci*. **62**: 1235-1240.

8. Baines, S.J., McInnes, E.F. and McConnell, I. 2008. E-cadherin expression in canine cutaneous histiocytomas. *Vet. Rec*. **162**: 509-513.

9. Ball, R.S. 2006. Issues to consider for preparing ferrets as research subjects in the laboratory. *ILAR. J*. **47**: 348-357.

10. Bauchet, A.L., Fouque, M.C., Belluco, S., Château-Joubert, S., Elies, L., Maliver, P., Schorsch, F. and Fontaine, J.J. 2008. An atypical case of histiocytic sarcoma in a Wistar rat (*Rattus norvegicus*). *Exp. Toxicol. Pathol*. **59**: 385-390.

11. Belser, J.A., Katz, J.M. and Tumpey, T.M. 2011. The ferret as a model organism to study influenza A virus infection. *Dis. Model. Mech*. **4**: 575-579.

12. Buch, M.D.M., Reilly, C.M., Luff, J.A. and Moore, P.F. 2008. Feline pulmonary Langerhans cell histiocytosis with multiorgan involvement. *Vet. Pathol*. **45**: 816-824.

13. Chen, H.C., Slone, T.W. and Frith, C.H. 1992. Histiocytic sarcoma in an aging gerbil. *Toxicol. pathol*. **20**: 260-263.

14. Coomer, A.R. and Liptak, J.M. 2008. Canine histiocytic siseases. *Compend. Contin. Educ. Vet*. **30**: 202-215.

15. Day, M.J., Lopatkin, I., Lucke, V.M. and Whitbread, T.J. 2000. Multiple cutaneous histiocytomas in a cat. *Vet. Dermatol*. **11**: 305-310.

16. de Saint-Vis, B., Vincent, J., Vandenabeele, S., Vanbervliet, B., Pin, J.J., Aït-Yahia, S., Patel, S., Mattei, M.G., Banchereau, J., Zurawski, S., Davoust, J., Caux, C. and Lebecque, S. 1998. A novel lysosome-associated membrane glycoprotein, DC-LAMP, induced upon DC maturation, is transiently expressed in MHC class II compartment. *Immunity* **9**: 325-336.

17. Fix, A.S. and Harms, C.A. 1990. Immunocytochemistry of pancreatic endocrine tumors in three domestic ferrets (*Mustela putorius furo*). *Vet. Pathol*. **27**: 199-201.

18. Friedrichs, K.R. and Young, K.M. 2008. Histiocytic sarcoma of macrophage origin in a cat: case report with a literature review of feline histiocytic malignancies and comparison with canine hemophagocytic histiocytic sarcoma. *Vet. Clin. Pathol*. **37/1**: 121-128.

19. Fulmer, A.K. and Mauldin, G.E. 2007. Canine histiocytic neoplasia: An overview. *Can. Vet. J*. **48**: 1041-1050.

20. Garner, M.M., Ramsell, K., Schoemaker, N.J., Sidor, I.F., Hordhausen, R.W., Bolin, S., Evermann, J.F. and Kiupel, M. 2007. Myofasciitis in the domestic ferret. *Vet. Pathol*. **44**: 25-38.

21. Glick, A.D., Holscher, M. and Campbell, G.R. 1976. Canine cutaneous histiocytoma: ultrastructural and cytochemical observations. *Vet. Pathol*. **13**: 374-380.

22. Hayden, D.W., Waters, D.J., Burke, B.A. and Manivel, J.C. 1993. Disseminated malignant histiocytosis in a Golden Retriever: Clinicopathologic, ultrastructural, and immunohistochemical findings. *Vet. Pathol*. **30**: 256-264.

23. Hélie, P., Kiupel, M. and Drolet, R. 2014. Congenital cutaneous histiocytosis in a piglet. *Vet. Pathol*. **51**: 812-815.

24. Hirako, A., Sugiyama, A., Sakurai, M., Ozaki, K., Sakai, H., Takeuchi, T., Morita, T. and Moore, P.F. 2015. Cutaneous histiocytic sarcoma with E-cadherin expression in a Pembroke Welsh Corgi dog. *J. Vet. Diagn. Invest*. **27**: 589-595.

25. Ide, K., Setoguchi-Mukai, A., Nakagawa, Y., Uetsuka, K., Nakayama, H., Fujino, Y., Ohno, K. and Tsujimoto, H. 2009. Disseminated histiocytic sarcoma with excessive hemophagocytosis in a cat. *J. Vet. Med. Sci*. **71**: 817-820.

26. Ide, T., Uchida, K., Kagawa, Y., Suzuki, K. and Nakayama, H. 2011. Pathological and immunohistochemical features of subdural histiocytic sarcomas in 15 dogs. *J. Vet. Diagn. Invest*. **23**: 127-132.

27. Ide, T., Uchida, K., Tamura, S. and Nakayama, H. 2010. Histiocytic sarcoma in the brain of a cat. *J. Vet. Med. Sci*. **72**: 99-102.

28. Kipar, A., Baumgärtner, W., Kremmer, E., Frese, K. and Weiss, E. 1998. Expression of major histocompatibility complex class II antigen in neoplastic cells of canine cutaneous histiocytoma. *Vet. Immunol. Immunopathol*. **62**: 1-13.

29. Komohara, Y., Hirahara, J., Horikawa, T., Kawamura, K., Kiyota, E., Sakashita, N., Araki, N. and Takeya, M. 2006. AM-3K, an anti-macrophage antibody, recognizes CD163, a molecule associated with an anti-inflammatory macrophage phenotype. *J. Histochem. Cytochem*. **54**: 763-771.

30. Lau, S.K., Chu, P.G. and Weiss, L.M. 2004. CD163 a specific marker of macrophages in paraffin-embedded tissue samples. *Am. J. Clin. Pathol*. **122**: 794-801.

31. Leissinger, M., Brandão, J., Wakamatsu, N., Le Roux, A., Rich, G. and Gaunt, S. 2013. Pulmonary histiocytic sarcoma in a rabbit. *Vet. Clin. Pathol*. **42**: 364-367.

32. Li, X., Fox, J.G., Erdman, S.E. and Aspros, D.G. 1995. Cutaneous lymphoma in a ferret (*Mustela putorius furo*). *Vet. Pathol*. **32**: 55-56.

33. Lloyd, C.G. and Lewis, W.G.V. 2004. Two cases of pancreatic neoplasia in British ferrets (*Mustela putorius furo*). *J. Small Anim. Pract*. **45**: 558-562.

34. Matsuda, K., Nomoto, H., Kawamura, Y., Someya, Y., Koiwa, M. and Taniyama, H. 2010. Hemophagocytic histiocytic sarcoma in a Japanese black cow. *Vet. Pathol*. **47**: 339-342.

35. Miwa, Y., Kurosawa, A., Ogawa, H., Nakayama, H., Sasai, H. and Sasaki, N. 2009. Neoplasitic disease in ferrets in Japan: a questionnaire study for 2000 to 2005. *J. Vet. Med. Sci*. **71**: 397-402.

36. Moore, P.F. 2014. A review of histiocytic diseases of dogs and cats. *Vet. Pathol*. **51**: 167-184.

37. Moore, P.F. 1984. Systemic histiocytosis of Bernese mountain dogs. *Vet. Pathol*. **21**: 554-563.

38. Moore, P.F., Affolter, V.K. and Vernau, W. 2006. Canine hemophagocytic histiocytic sarcoma: A proliferative disorder of CD11d+ macrophages. *Vet. Pathol*. **43**: 632-645.

39. Moore, P.F., Schrenzel, M.D., Affolter, V.K., Olivry, T. and Naydan, D. 1996. Canine cutaneous histiocytoma is an epidermotropic Langerhans cell histiocytosis that expresses CD1 and specific f32-lntegrin molecules. *Am. J. Pathol*. **148**: 1699-1708.

40. Naranjo, C., Dubielzig, R.R. and Friedrichs, K.R. 2007. Canine ocular histiocytic sarcoma. *Vet. Ophthalmol*. **10**: 179-185.

41. Ohnishi, K., Tanaka, S., Oghiso, Y. and Takeya, M. 2012. Immunohistochemical detection of possible cellular origin of hepatic histiocytic sarcoma in mice. *J. Clin. Exp. Hematopathol*. **52**: 171-177.

42. Paciello, O., Passantino, G., Costagliola, A., Papparella, S. and Perillo, A. 2013. Histiocytic sarcoma of the nasal cavity in a horse. *Res. Vet. Sci*. **94**: 648-650.

43. Palmeiro, B.S., Morris, D.O., Goldschmidt, M.H. and Mauldin, E.A. 2007. Cutaneous reactive histiocytosis in dogs: a retrospective evaluation of 32 cases. *Vet. Dermatol*. **18**: 332-340.

44. Peterson, R.A., Kiupel, M. and Capen, C.C. 2003. Adrenal Cortical Carcinomas with Myxoid Differentiation in the Domestic Ferret (*Mustela putorius furo*). *Vet. Pathol*. **40**: 136-142.

45. Pinard, J., Wagg, C.R., Girard, C., Kiupel, M. and Bédard, C. 2006. Histiocytic sarcoma in the tarsus of a cat. *Vet. Pathol*. **43**: 1014-1017.

46. Pumphrey, S.A., Pizzirani, S., Pirie, C.G., Sato, A.F. and Buckley, F.I. 2013. Reactive histiocytosis of the orbit and posterior segment in a dog. *Vet. Ophthalmol*. **16**: 229-233.

47. Reed, N., Begara-McGorum, I.M., Else, R.W. and Gunn-Moore, D.A. 2006. Unusual hisiocytic disease in a Somali cat. *J. Feline Med. Surg*. **8**: 129-134.

48. Rossi, S., Gelain, M.E. and Comazzi, S. 2009. Disseminated histiocytic sarcoma with peripheral blood involvement in a Bernese Mountain dog. *Vet. Clin. Pathol*. **38**: 126-130.

49. Smith, M., and Schulman, F.Y. 2007. Subcutaneous neoplasms of the ventral abdomen with features of adrenocortical tumors in two ferrets. *Vet. Pathol*. **44**: 951-955.

50. Smoliga, J., Schatzbereg, S., Peters, J., McDonough, S. and deLahunta, A. 2005. Myelopathy caused by a histiocytic sarcoma in a cat. *J. Small Anim. Pract*. **46**: 34-38.

51. Sun, X., Sui, H., Fisher, J.T., Yan, Z., Liu, X., Cho, H., Joo, N.S., Zhang, Y., Zhou, W., Yi, Y., Kinyon, J.M., Lei-Butters, D.C., Griffin, M.A., Naumann, P., Luo, M., Ascher, J., Wang, K., Frana, T., Wine, J.J., Meyerholz, D.K. and Engelhardt, J.F. 2010. Disease phenotype of a ferret *CFTR*-knockout model of cystic fibrosis. *J. Clin. Invest*. **120**: 3149-3160.

52. Teshima, T., Hata, T., Nezu, Y., Michishita, M., Matsumoto, H., Mizutani, H., Takahashi, K. and Koyama, H. 2012. Amputation for histiocytic sarcoma in a cat. *J. Feline Med. Surg*. **14**: 147-150.

53. Thio, T., Hilbe, M., Grest, P. and Pospischil, A. 2006. Malignant histiocytosis of the brain in three dogs. *J. Comp. Pathol*. **134**: 241-244.

54. Uchida, K., Morozumi, M., Yamaguchi, R. and Tateyama, S. 2001. Diffuse leptomeningeal malignant histiocytosis in the brain and spinal cord of a Tibetan Terrier. *Vet. Pathol*. **38**: 219-222.

55. Ward, J.M. and Sheldon, W. 1993. Expression of mononuclear phagocyte antigens in histiocytic sarcoma of mice. *Vet. Pathol*. **30**: 560-565.

56. Wong, V.M., Snyman, H.N., Ackerley, C., Bienzle, D. 2012. Primary nasal histiocytic sarcoma of macrophage-myeloid cell type in a cat. *J. Comp. Pathol.* **147**: 209-213.